The Messenger

No. 170 – December 2017

Astronomy in Australia
First light for GRAVITY
MUSE observes gas stripping in galaxies
Unveiling accretion in a protobinary system

ESO

DOI: 10.18727/0722-6691/5047

Astronomy in Australia

Fred Watson[1]
Warrick Couch[1]

[1] Australian Astronomical Observatory, Sydney, Australia

Australians have watched the sky for tens of thousands of years. The nineteenth century saw the foundation of government observatories in capital cities such as Sydney and Melbourne. While early twentieth-century astronomy focused largely on solar physics, the advent of radio astronomy at the end of the Second World War enabled Australia to take a leading role in the new science, with particular emphasis on low-frequency studies. Today, the radio quietness of its outback interior provides an excellent location for the Australian core of the Square Kilometre Array. Australian optical astronomy has flourished since the 1960s, with the 3.9-metre Anglo-Australian Telescope becoming the principal national facility in 1974. Access to ESO's facilities at the La Silla Paranal Observatory is warmly welcomed by all Australian astronomers.

It is no idle boast that Australia has the world's oldest continuing culture. Recent research at a rock shelter in Kakadu, near Jabiru in Australia's Northern Territory, used optically-stimulated luminescence to date human settlement there back to a staggering 65 000 years. Stone tools and buried ochre pigments suggest the inhabitants were both technologically and culturally adept, with observations of the sky likely being an important part of their daily rituals.

Australian Aboriginal people trace their cultural heritage back to the Dreamtime — an ancient era of creation, rich in legends linking human and animal life with the country in which they lived. Dreamtime stories differ from one Aboriginal nation to another, but are full of allusions to the sky, with the Sun, Moon, planets and stars all playing significant roles. The Milky Way is also important, with "negative constellations" being identified in its dust lanes. The most notable of these, which is common to many different Aboriginal peoples, is the Emu, whose head, neck and body are the Coalsack Nebula and the dust clouds of Circinus, Norma and Scorpius.

Conventional "join-the-dots" constellations also abound, but vary widely from one Aboriginal culture to another. Orion, for example, is seen as Njiru (the hunter) in the Central Desert Region, but the Yolngu people of Northern Australia see the constellation as a canoe, with three brothers sitting abreast in the centre (Orion's Belt) and a forbidden fish in the canoe represented by the Orion Nebula. Virtually all Dreamtime stories characterise the Moon as male and the Sun as female, with a tacit understanding that the covering of the Sun by the Moon during an eclipse represents the consummation of the relationship. Likewise, planets figure in Dreamtime astronomy, with Venus, for example, taking on a personage known as Barnumbir in Arnhem Land. Barnumbir is a woman held firmly on a rope extending from the eastern horizon (morning star) or western horizon (evening star), a neat explanation for the planet's limited excursions from the Sun.

Besides the creation myths, the stories told in Aboriginal astronomy served a practical purpose. The orientation of the Emu would indicate when it was time for the Central Desert people to begin collecting emu eggs. Likewise, the Boorong people in north-western Victoria used the constellation of Lyra to tell them when to gather malleefowl eggs. Dreamtime astronomy was also used to establish a moral framework among the younger members of the community, instilling values that had a demonstrable connection to their ancestor spirits in the sky.

Colonial astronomy

The arrival of the First Fleet in January 1788 brought up to 1500 British settlers to Port Jackson in Sydney. Over the next century, the effect of continuing settlement on the indigenous population was devastating. Meanwhile, the new colony flourished. The settlers included convicts, free settlers and military personnel, and its first noteworthy astronomical figure was William Dawes (1762–1836), a lieutenant in the Royal Marines. Besides his official position as engineer and surveyor to the new settlement, Dawes was also a botanist and a keen astronomer who built a small observatory at what is now called Dawes Point, close to the southern pylon of the Sydney Harbour Bridge. He is also notable as the first compiler of an Aboriginal language dictionary through his association with Petyegarang (Grey Kangaroo), a woman of the Eora Nation.

Of more lasting significance to astronomy is a piece of Australian-Scottish heritage centring around Sir Thomas Makdougall Brisbane (1773–1860), a conservation-minded soldier, statesman and scientist. Brisbane was the sixth governor of New South Wales (NSW), and an examination of his career prior to this suggests that astronomy was the principal driving force of his life.

The main reason for his keenness to become governor of NSW may have been to establish an observatory in Parramatta in 1822, which he wanted to become "the Greenwich of the Southern Hemisphere". The Parramatta Observatory has a precursor in Largs, Scotland (1808) that still exists, albeit in a highly dilapidated and unstable condition. This elegant stone building was lost to history until the early 1980s, standing on a hillside in the middle of what is now a cow pasture and almost overgrown by vegetation.

Brisbane's Parramatta Observatory (1822–1847) was essentially a copy of his Largs building, but in wood rather than stone, and equipped with positional instruments brought from Scotland. In turn, the Parramatta Observatory became the forerunner of the Sydney Observatory (1858), which inherited Parramatta's telescopes. The wooden observatory at Parramatta is long gone, but the stone supports for a later transit telescope remain in Parramatta Park. Brisbane himself left Australia in 1825 after visiting a new penal settlement near Moreton Bay, which now bears his name as the capital city of Queensland.

The first NSW Government Astronomer was William Scott, appointed in 1856, two years before the opening of the Sydney Observatory. Erected on the highest point of the new colony close to Dawes Point, the stylish sandstone

CSIRO

Figure 1. Seen here at the time of its role in the Apollo lunar landings, the 64-metre Parkes Telescope is still a workhorse of Australian radio astronomy.

building is today dwarfed by the skyscrapers around it. Its principal function in the early years was to provide a time-keeping service for the community, complete with a time ball to allow mariners in the harbour to set their chronometers.

Astronomical research significantly advanced during the 35-year custodianship of the third Government Astronomer, Henry Chamberlain Russell, who was appointed in 1870. Highlights include the procurement of a 29-centimetre Schröder refractor in 1874, which is still operational; a major campaign to observe the 1874 transit of Venus; and the incorporation of the Sydney Observatory into the Astrographic Catalogue project in 1887. Russell also incorporated meteorology into the functions of the observatory.

Russell's efforts were criticised by a prominent amateur Australian astronomer, John Tebbutt (1834–1916), who is himself best known for discovering the spectacular comets of 1861 and 1881, and was honoured in 1914 by a visit from the Astronomer Royal Frank Watson Dyson. By then, Australia had attained nationhood in the wake of the Federation of 1901. Tebbutt's work was celebrated on the Australian $100 note from 1984 to 1996. The Sydney Observatory itself ceased astronomical research in 1982, reopening four years later as a public observatory under the auspices of Sydney's Museum of Applied Arts and Sciences.

The Great Melbourne Telescope

Another noteworthy observatory was built in the colony of Victoria as a direct result of wealth accumulated during the 1850s gold rush. June 1863 saw the foundation of a government-funded observatory in the capital city, Melbourne. The newfound riches of the Victorian government enabled the Royal Society to construct a large Southern Hemisphere reflector. The remarkable 1.2-metre Great Melbourne Telescope, then the world's largest working equatorial reflector, entered service in August 1869.

The Government Astronomer, Robert Ellery (1827–1908), expressed confidence in its capabilities as a premier research instrument. Sadly, this optimism was never fulfilled. The Great Melbourne's Cassegrain layout amplified the primary mirror's focal ratio to f/42, rendering the new technique of photography useless for all but the brightest objects. The mirror itself was made of speculum metal instead of with the newer technology of silver-on-glass. As a result, the mirror tarnished rapidly, requiring frequent risky re-polishing to restore its reflectivity. After many valiant efforts by Ellery, the Great Melbourne Telescope went into a long, slow decline and was eventually closed down in March 1944.

The telescope was then sold to the Commonwealth Solar Observatory at Mount Stromlo, on the outskirts of Canberra. Although it changed hands at scrap value (£500) it subsequently underwent a series of metamorphoses, culminating in the installation of a new 1.3-metre Pyrex mirror in 1959. The institution itself also metamorphosed into the Mount Stromlo Observatory of the Australian National University (ANU), which remains one of the nation's premier research centres.

In the early 1990s, the Great Melbourne Telescope, by then well over a century old, was reincarnated yet again to perform a specific scientific task — hunting for non-luminous objects in the galactic halo that might make up the mysterious "dark matter" known to permeate the Universe. This programme, called the MAssive Compact Halo Object (MACHO) experiment, was successful in effectively ruling out that possibility, and plans were well advanced in 2002 for the installation of a new camera that would be used in an ambitious survey for Kuiper belt objects — but then disaster struck.

On 18 January 2003, at the height of the bushfire season, a colossal firestorm in Canberra's south-western suburbs claimed the lives of four people and left more than 500 families homeless. Mount Stromlo Observatory lost all its heritage buildings, including the domes of the Great Melbourne plus five other historically-significant telescopes. For six years, the twisted remains of the Great Melbourne Telescope lay rusting in the rains that followed the end of the once-in-a-hundred-year drought. In 2009, those remains were taken to the city of Melbourne to be restored and re-erected on the original site as a fully-operational public observing facility. That remarkable work is still ongoing.

The beginnings of Australian radio astronomy

Radio astronomy had its genesis in the work of Karl Guthe Jansky (1905–1950) of the Bell Telephone Laboratories in Holmdel, New Jersey. In 1932, he discovered radio interference at a wavelength of 14.5 metres coming from the Milky Way; this was largely ignored by the scientific community. Jansky's antenna, a crude structure of wood and brass rotating on wheels purloined from a Model T Ford, was the first radio telescope.

It was followed in 1937 by the first steerable-dish type instrument, a 10-metre diameter reflecting radio telescope that was built not by Jansky but by another American, Grote Reber (1911–2002). Reber was the world's sole radio astronomer for almost a decade, observing not just the Milky Way but also a range of radio sources. In 1954, he moved to Australia's southernmost state, Tasmania, which was then largely radio quiet.

Radio astronomy in Australia had its origins in radar research carried out in the Second World War at what was known as the Radiophysics Laboratory, located at Sydney University. Following the end of hostilities, the renamed Commonwealth Scientific and Industrial Research Organisation (CSIRO) Division of Radiophysics fragmented into a number of peacetime research groups; one such group was led by Joseph Pawsey (1908–1962) and was charged with investigating radio noise from extraterrestrial sources. At first, Pawsey's group concentrated on solar radio emissions, near the South Head of Sydney Harbour. By 1947, this Dover Heights installation was being used to measure cosmic radio sources — most notably Cygnus A and the Crab Nebula in work led by John Bolton (1922–1993).

Other Australian astronomy pioneers include Wilbur Norman "Chris" Christiansen (1913–2007) and Bernard Mills (1920–2011), who both built radio array interferometers in the Sydney area. Mills adopted a cruciform configuration for his Mills Cross, and carried out all-sky surveys at 85.5 MHz (3.5 m). Christiansen adopted this configuration for the later "Chris Cross", which was used in the mid-1950s for solar research.

The availability of war-time radar equipment precipitated the rapid development of radio astronomy. At first, the purveyors of this new science were engineers, who were regarded with deep suspicion by their optical counterparts. For example, Richard Woolley, then Director of the Commonwealth Observatory (today's Mount Stromlo Observatory), was asked in 1947 where he thought radio astronomy would be in ten years' time. "Forgotten," was his acerbic reply.

Eventually, though, the two wavebands were seen as complementary, each providing different views of the Universe. Centres of excellence were established in Australia, the Netherlands and the United Kingdom, and instruments such as the 76-metre dish at Jodrell Bank (completed in 1957) and the 64-metre dish at Parkes in central western NSW (inaugurated in 1961; Figure 1) quickly became icons of the new science.

Australian radio astronomy had come of age by the time the Parkes Observatory was built, and the facility became well-known under the Directorship of John Bolton. It was instrumental in early studies of quasars and other extragalactic radio sources, pulsars, the Milky Way, and the interstellar medium. It also made history for its role in NASA's Apollo program, as well as its ongoing contribution to the NASA Deep Space Network.

In its early days, Parkes was complemented by the Culgoora Radio Heliograph, built at Narrabri in north-western NSW under the leadership of Paul Wild (1923–2008). The instrument consisted of 96 dishes (each 13.7 metres in diameter), arranged around the circumference of a circle three kilometres in diameter. From 1967 to 1984, the Radio Heliograph operated first at 80 and then later at 160 MHz, imaging the Sun at these wavelengths once per second.

The Culgoora site was also home to a pioneering optical interferometer that borrowed more from radio astronomy technology than optical interferometry. This was the Narrabri Stellar Intensity Interferometer, the brainchild of radio astronomer Robert Hanbury Brown (1916–2002). It consisted of a pair of f/1.64 hexagonally-segmented collecting mirrors (6.7 metres in diameter) mounted on a circular track around which each mirror could move independently. The instrument was completed in 1963, and measured the angular diameters of 32 stars before it retired in 1974.

The Stellar Intensity Interferometer was operated by the University of Sydney. A more conventional optical interferometer was also built and opened in April 1991. This was the Sydney University Stellar Interferometer (SUSI), which was a Michelson interferometer with a variable baseline variable of 5–640 metres, fed by a dozen 0.2-metre siderostats operating in pairs. While SUSI achieved an excellent track record in high-resolution optical astronomy, it eventually closed in the face of competition from ESO's Very Large Telescope Interferometer (VLTI) and other facilities.

B. Norris

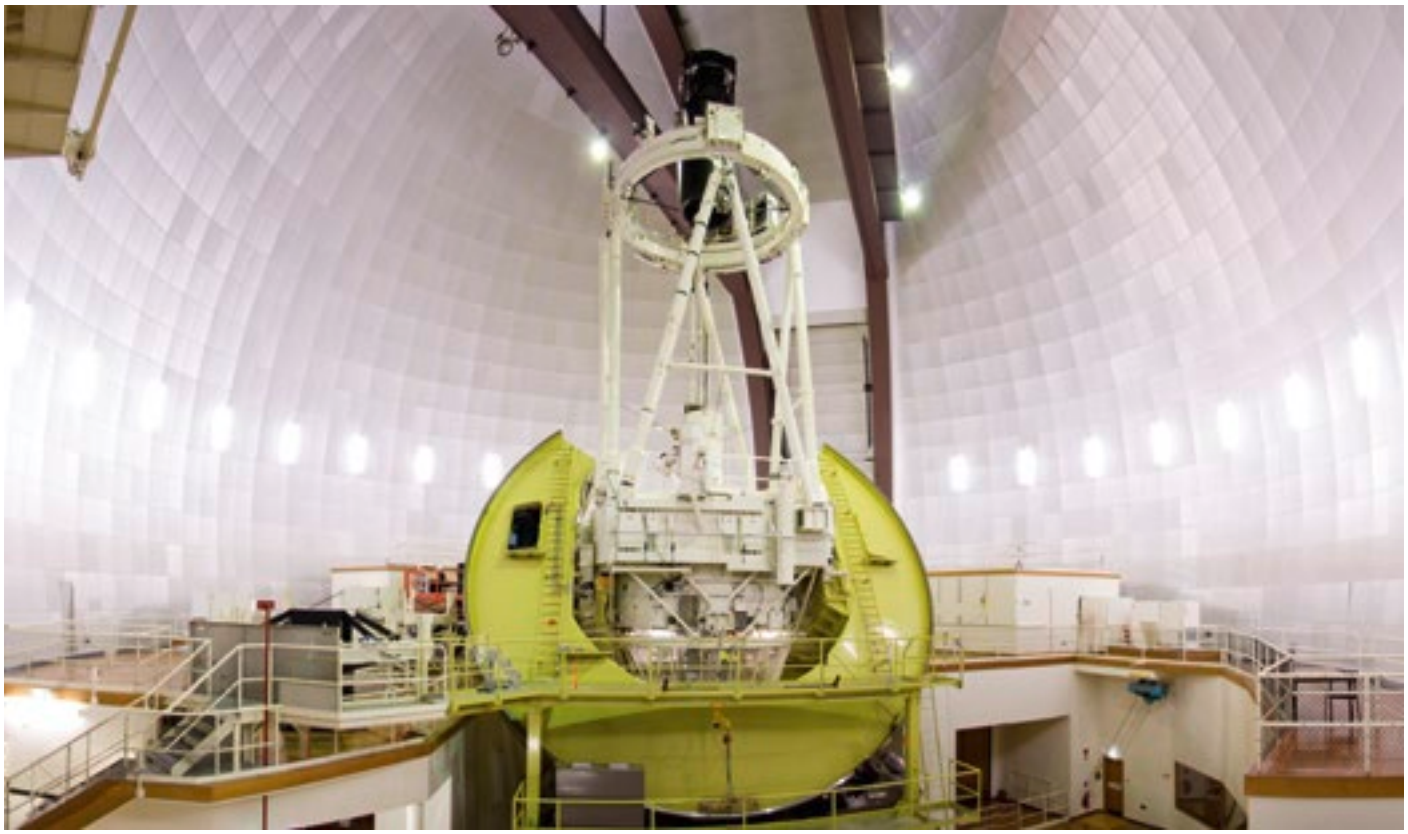

Figure 2. The 3.9-metre Anglo-Australian Telescope, opened in 1974, and became operational the following year.

Since 1988, Culgoora has been the location of CSIRO's Australia Telescope Compact Array, a group of six 22-metre radio dishes movable on a linear track, giving a maximum separation of six kilometres. The Compact Array is part of the Australia Telescope National Facility, which includes the 64-metre Parkes dish.

Siding Spring observatory

By 1960, the optical telescopes at Mount Stromlo Observatory were facing increasing light pollution from the encroaching suburbs of Canberra. The then-Director, Bart Bok (1906–1983), initiated the quest for a new dark sky site for the Australian National University's facilities, and selected Siding Spring Mountain. This 1200-metre high ridge in the Warrumbungle Range of north-western NSW was found to experience spectroscopic conditions for 65 % of the time, and photometric conditions for 35–50 % of the time, together with atmospheric turbulence as low as any other mountain site in Australia. The deciding factor in the selection was the small country town of Coonabarabran approximately 30 km away, which could provide infrastructure and accommodation for the supporting staff.

The first telescope was opened at Siding Spring in 1964, a 1-metre Boller and Chivens reflector quickly made famous by Bok and his wife, Priscilla Fairfield Bok, through their studies of the Milky Way. It was followed by two smaller ANU telescopes and, crucially, by infrastructure such as observer accommodation, power, water and a paved road to Coonabarabran.

The paucity of observing facilities for Australian and British optical astronomers led to the next major development. During the early 1960s British optical astronomers had access to a few small telescopes (up to 0.9 m), together with the 1.9-metre Radcliffe Telescope at Pretoria, South Africa, while their colleagues who worked at longer wavelengths had access to the impressive 76-metre dish at Jodrell Bank. Australian optical astronomers were similarly challenged, as their facilities at Siding Spring were dwarfed by the new Parkes Telescope.

When the British and Australian governments looked jointly at possible sites for a new 4-metre class telescope during the late 1960s, Siding Spring was considered to be the best location in Australia. This instrument eventually materialised as the 3.9-metre Anglo-Australian Telescope (AAT; Figure 2), which became operational in 1975. Observing time on the instrument was allocated equally between the two countries, an eminently successful arrangement.

The telescope itself was also extraordinarily successful from the beginning, partly as a result of its high level of computer control, the first for any instrument of this size. It was designed with versatility in mind, with a set of three interchangeable 4-tonne top-ends for the telescope providing a range of focal ratios from f/3.3 to f/36 at prime, Cassegrain and coudé focal stations. An auxiliary

suite of more than a dozen instruments was built to take advantage of this and satisfy the wide-ranging scientific interests of Australian and British astronomers. The AAT was an early pioneer of electronic detectors, including the Image Photon Counting System (IPCS) developed at University College London by Alec Boksenberg.When used with a spectrograph, the IPCS rendered the AAT at least as powerful as any other telescope in the world, providing astronomers with a unique tool for investigating the detailed properties of every kind of celestial object.

Two other circumstances conspired to increase the AAT's potency as a discovery machine. Firstly, the southern sky was essentially unexplored by large telescopes. Even obvious targets such as the Galactic Centre and the Magellanic Clouds had been observed only at low elevations by northern-hemisphere instruments. Secondly, the British decided to construct a wide-field photographic survey instrument in 1970: the 1.2-metre UK Schmidt Telescope (UKST).

The UKST opened at Siding Spring on 17 August 1973. Its initial task was to photograph the whole of the southern sky not covered by its near-twin, which conducted a survey on Palomar Mountain (USA) during the 1950s; the UKST took the better part of a decade for this task. In June 1988, the symbiotic relationship between the two telescopes was formalised, when the UKST became part of the Anglo-Australian Observatory (AAO) instead of an outstation of the Royal Observatory, Edinburgh. In 2010, the AAO itself transformed into the Australian Astronomical Observatory, when the original bi-national agreement was terminated and funding was taken over by the Australian Government.

Siding Spring has continued to attract astronomical infrastructure (Figure 3), at least partly due to its dark skies and legislative protection against light pollution. The ANU's 2.3-metre Advanced Technology Telescope was inaugurated in 1988, and the privately-funded 2-metre Faulkes Telescope South (now the Las Cumbres Observatory 2-metre telescope) followed in 2004. The ANU's 1.3-metre SkyMapper telescope and the 1.6-metre Korean

ANU

Figure 3. Siding Spring Observatory from the air, with the dome of the 3.9-metre Anglo-Australian Telescope in the centre, the 1.3-m ANU SkyMapper Telescope on the extreme left, and the 1.2-metre UK Schmidt Telescope and 2-metre Las Cumbres Observatory Telescope on the right.

Microlensing Telescope are more recent additions. In January 2013, all Siding Spring's facilities were under threat from a devastating bushfire that started almost exactly a decade after the Mount Stromlo fire. In the event, the only casualty was the old observer accommodation, which has been replaced by a multi-purpose Lodge.

Advanced radio instrumentation in Australia

A hallmark of Australian astronomy, both in universities and at national facilities, has been the development of innovative instrumentation. Radio astronomy leads the way in nationally-significant infrastructure. Scientists at CSIRO and elsewhere have built on the successes of the 20th century, leading international collaborations that are now developing major new facilities. The Murchison Widefield Array (MWA), which exploits Australia's expertise in low-frequency astronomy, is a joint project between approximately 15 institutions from Australia and abroad. Built between 2007 and 2012, the facility is located at the Murchison Radio-astronomy Observatory (MRO) at Boolardy in outback Western Australia. The radio quietness of this area is comparable to the pristine dark skies of Siding Spring, and the MWA's 128 phased dipole antennas give the telescope an extraordinary 30-degree field of view. Its scientific objectives include the detection of neutral hydrogen in the epoch of reionisation, together with heliospheric, ionospheric and interstellar medium research.

Boolardy is also home to CSIRO's Australian Square Kilometre Array Pathfinder (ASKAP; Figure 4), a radio telescope under construction since 2009. When completed, ASKAP will have 36 parabolic antennas, each 12 metres in diameter and equipped with advanced phased array feeds with a 6-degree field of view. ASKAP is a survey telescope, with cosmology and early galaxy evolution among its principal scientific objectives. The 12 antennae currently operating generate 5.2 terabytes of data per second — approximately 15 % of the entire internet's data rate. During initial commissioning in January 2017, several fast radio bursts were detected from an as yet unknown source. ASKAP is likely to detect a fast radio burst every few days once it is fully operational, with good prospects for unravelling the nature of these enigmatic phenomena.

As its name suggests, ASKAP demonstrates the technology of the Square Kilometre Array itself, a multi-national facility

CSIRO

Figure 4. 12-metre antennae of the Australian Square Kilometre Array Pathfinder in Western Australia.

that will be the world's largest telescope when completed in the late 2020s. The SKA will consist of widely-dispersed radio arrays in Southern Africa, New Zealand and Australia; due to its radio quietness, the MRO will be one of its core sites. The primary science objectives are centred on fundamental cosmology and extragalactic astronomy, with an emphasis on black holes, large-scale structure, and the Universe's "Dark Ages".

Astrobiology will also feature among SKA's scientific programmes, with prebiotic chemistry, protoplanetary discs, and the search for extraterrestrial intelligence being of interest. The Parkes Observatory is already working on pathfinders of the latter area of research; 25 % of its observing time is currently devoted to the "Breakthrough Listen" initiative.

Optical instrumentation and the AAO

Advanced instrumentation is also flourishing in Australian optical astronomy. The ANU's Research School of Astronomy and Astrophysics (RSAA) at Mount Stromlo, for example, has a fine track record of developing hybrid imaging detectors. It has completed two instruments for the 8-metre telescopes of the Gemini Observatory: the Near-infrared Integral-Field Spectrometer (NIFS) and Gemini South Adaptive Optics Imager (GSAOI). The Advanced Instrumentation Technology Centre (AITC) at Mount Stromlo also provides excellent facilities for instrumentation scientists and engineers at RSAA.

The AAO's scientists and engineers have honed their skills developing novel instruments for use with the AAT. In 1979, observations at infrared wavelengths with the Infrared Photometer-Spectrometer (IRPS) enabled the AAT to see through dust clouds and study the earliest stages of star formation. The infrared instrumentation that followed, the InfraRed Imaging Spectrometer (IRIS) and later IRIS2, also produced spectacular results, including imaging the 1994 impacts of Comet Shoemaker-Levy 9 fragments with Jupiter, as well as detailed observations of galactic and extragalactic targets.

However, it was the early use of optical fibres that set the AAO on its current course. While multi-fibre spectroscopy was not invented at the AAO, it was transformed from an interesting novelty to a highly productive technique during the early 1980s at the AAT and UKST. After pilot surveys, the AAO unveiled 2dF (Two Degree Field) in the mid-1990s, which allowed the spectra of 400 objects to be obtained simultaneously using robotically-positioned fibres.

The 2dF Galaxy Redshift Survey measured 221 000 galaxies and quickly became one of the most productive projects at the AAO in terms of both publications and citations. It helped establish the "missing link" between temperature fluctuations in the cosmic microwave background radiation and today's distribution of galaxies. Building on this success, the AAO produced a series of stationary spectrographs to be fed by 2dF. This included both the intermediate-dispersion AAOmega instrument in 2006, which remains one of the world's most powerful spectroscopic survey instruments, and HERMES in 2014, a high-dispersion spectrograph designed for galactic archaeology.

In 2001, the UKST also began a new role as a dedicated spectroscopic survey telescope using a robotic instrument called 6dF, originally a prototype for the OzPos fibre positioner delivered to Unit Telescope 2 of the VLT in 2003. Its first major project was the 6-degree Field Galaxy Survey (6dFGS). UKST also conducted the RAdial Velocity Experiment (RAVE) survey, a multi-national project that measured the radial velocities and physical parameters of half a million stars. Two new UKST surveys, Taipan and FunnelWeb, will use a novel fibre positioner in which each of the 300 fibres is positioned by its own micro-robot rather than a pick-place machine (Figure 5). This "Starbugs" technology was developed by the AAO as a demonstrator for the proposed Many Instrument Fiber System (MANIFEST), on the 25-metre Giant Magellan Telescope.

Another recent innovative instrument on the AAT is the Sydney-AAO Multi-object Integral field spectrograph (SAMI), which deploys 13 integral field units (IFUs) over a one-degree field of view and is being used to conduct the first major IFU survey of nearby galaxies. AAT instruments currently in development include HECTOR (a more powerful version of SAMI) and Veloce, a stabilised high-resolution (R ~ 80 000) echelle spectrograph for stellar spectroscopy.

Other AAO instrument projects include the Australian–European Southern Observatory Positioner (AESOP), a 2400-fibre tilting-spine positioner for ESO's

Kyler Kuehn, AAO

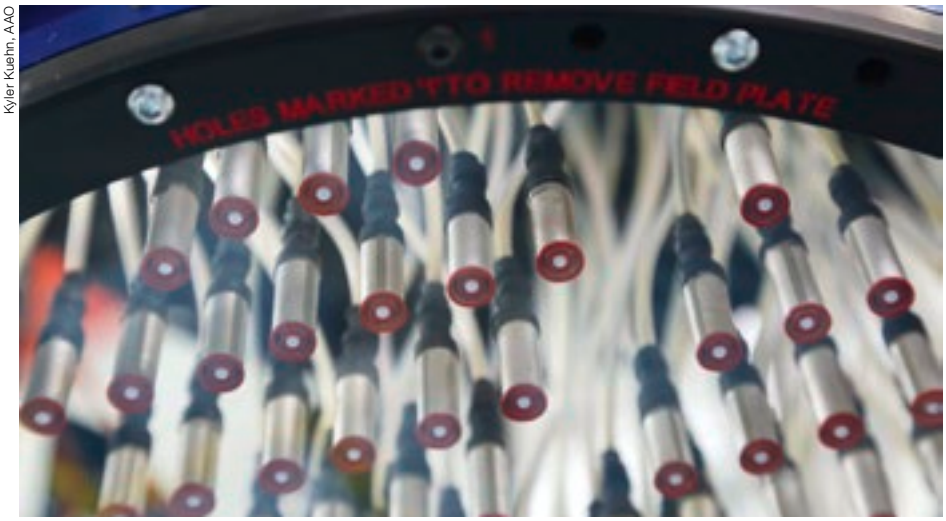

Figure 5. "StarBugs" on the glass focal plate of the 1.2-metre UK Schmidt Telescope. Each Bug is eight millimetres in diameter and contains an autonomous positioning robot, three metrology fibres and a science-fibre payload.

4-metre Visible and Infrared Survey Telescope for Astronomy (VISTA), and the Gemini High-Resolution Optical SpecTrograph (GHOST) for the Gemini South telescope in collaboration with the Herzberg Institute for Astrophysics in Canada and the Australian National University. More fundamental instrumentation research is also being carried out, particularly in astrophotonics. In collaboration with the University of Sydney, Macquarie University and the University of Western Australia, the AAO has tested OH-suppression devices based on fibre Bragg gratings, as well as slab-waveguide photonic spectrographs and photonic-comb calibration cells. The work on these devices is expected to radically change the way in which astronomical instruments are built, plus add entirely new capabilities.

Following the recent launch of Australia's ten-year strategic partnership with ESO, the AAO will split into two separate entities as of 1 July 2018. Operation of the AAT and UKST will be passed over to a consortium of Australian universities led by the ANU, which owns the Siding Spring site. The AAO's instrumentation and astronomy groups will be handed over to the research sector. The exact details of these new arrangements are yet to be defined; however the AAO brand name will be retained to ensure the pedigree of future astronomical instrumentation is not in doubt. A new era of instrument-building awaits the engineers and scientists of AAO, and it is expected that ESO will be one of its principal benefactors.

As well as the high-profile work outlined here, there are numerous university research endeavours in a range of fields including cosmic ray astronomy, gravitational wave astronomy, and space physics. Major facilities can also eclipse important activities in smaller observatories; for example, the research conducted by the University of Southern Queensland's Mount Kent Observatory and public outreach at the former Government Observatory in Perth, Western Australia.

Australia and ESO

Australian astronomers have long coveted the idea of an affiliation with ESO. They warmly applauded on 11 July 2017 at an event at the Astronomical Society of Australia's Annual Scientific Meeting in Canberra, when Arthur Sinodinos (Minister for Industry, Innovation and Science) and Tim de Zeeuw (ESO Director General) exchanged signatures to inaugurate the strategic partnership.

What exactly does this arrangement involve? While current fiscal realities prohibit full Australian membership of ESO, the ten-year strategic partnership that Australia formally entered on 11 July 2017 provides long-term access to the facilities at La Silla and Paranal. Access to the four 8.2-metre Unit Telescopes of ESO's VLT at Paranal is an important prize for Australian astronomers, whose critical need for time on telescopes in this class has been highlighted in successive Decadal Plans for Australian Astronomy, including the current one (2016–2025). Short-term financial arrangements with other 8-metre class facilities provide little opportunity to contribute to the design and procurement of advanced instrumentation for the telescopes, an area in which Australia has particular expertise. The new partnership with ESO explicitly aims to capitalise on that know-how, with promised benefits not only for technologically-adept institutions such as the AAO, but for partners in Australian universities and industry.

However, technology is only one of the reasons ESO welcomes Australian involvement. Another — also highlighted in successive Decadal Plans — is the high-impact science carried out by Australian astronomers. It has often been stated that Australian astronomical research "punches well above its weight", and Australia's scientific clout can only be increased by access to ESO's facilities. Australian astronomers became eligible in Period 101 to compete for time alongside astronomers based in ESO Member States, and no fewer than 55 Australian-led proposals were submitted.

Excluded from the new partnership is the Atacama Large Millimeter/submillimeter Array (ALMA), since access to this 5100-metre high submillimetre facility has lower priority for Australian astronomers than access to 8-metre class optical telescopes. Likewise the Extremely Large Telescope is excluded due to Australia's established participation in the proposed 25-metre Giant Magellan Telescope, also in northern Chile. Eventually, Australia will have the opportunity to enter into full ESO membership with access to ALMA and the ELT. While it is difficult to chart the financial landscape over the course of the current decade-long partnership, there is optimism that this is a real possibility.

Roland Bacon

The four laser guide stars of the Adaptive Optics Facility being deployed during MUSE observations on Unit Telescope 4.

DOI: 10.18727/0722-6691/5048

First Light for GRAVITY: A New Era for Optical Interferometry

GRAVITY Collaboration:
Roberto Abuter[8], Matteo Accardo[8], António Amorim[6], Narsireddy Anugu[7], Gerardo Ávila[8], Myriam Benisty[5], Jean-Philippe Berger[5], Nicolas Blind[9], Henri Bonnet[8], Pierre Bourget[8], Wolfgang Brandner[3], Roland Brast[8], Alexander Buron[1], Frédéric Cassaing[10], Frédéric Chapron[2], Élodie Choquet[2], Yann Clénet[2], Claude Collin[2], Vincent Coudé du Forestol[2], Willem-Jan de Wit[8], Tim de Zeeuw[8,14], Casey Deen[1], Françoise Delplancke-Ströbele[8], Roderick Dembet[8], Frédéric Derie[8], Jason Dexter[1], Gilles Duvert[5], Monica Ebert[3], Andreas Eckart[4,13], Frank Eisenhauer[1], Michael Esselborn[8], Pierre Fédou[2], Gert Finger[8], Paulo Garcia[7], Cesar Enrique Garcia Dabo[8], Rebeca Garcia Lopez[3], Feng Gao[1], Éric Gendron[2], Reinhard Genzel[1,15], Stefan Gillessen[1], Frédéric Gonté[8], Paulo Gordo[6], Marion Grould[2], Ulrich Grözinger[3], Sylvain Guieu[5,8], Pierre Haguenauer[8], Oliver Hans[1], Xavier Haubois[8], Marcus Haug[1,8], Frank Haußmann[1], Thomas Henning[3], Stefan Hippler[3], Matthew Horrobin[4], Armin Huber[3], Zoltan Hubert[2], Norbert Hubin[8], Christian A. Hummel[8], Gerd Jakob[8], Lieselotte Jochum[8], Laurent Jocou[5], Martina Karl[1], Andreas Kaufer[8], Stefan Kellner[1,13], Sarah Kendrew[3,11], Lothar Kern[8], Pierre Kervella[2,12], Mario Kiekebusch[8], Ralf Klein[3], Johan Kolb[8], Martin Kulas[3], Sylvestre Lacour[2], Vincent Lapeyrère[2], Bernard Lazareff[5], Jean-Baptiste Le Bouquin[5], Pierre Léna[2], Rainer Lenzen[3], Samuel Lévêque[8], Magdalena Lippa[1], Yves Magnard[5], Leander Mehrgan[8], Marcus Mellein[3], Antoine Mérand[8], Javier Moreno-Ventas[3], Thibaut Moulin[5], Eric Müller[3,8], Friedrich Müller[3], Udo Neumann[3], Sylvain Oberti[8], Thomas Ott[1], Laurent Pallanca[8], Johana Panduro[3], Luca Pasquini[8], Thibaut Paumard[2], Isabelle Percheron[8], Karine Perraut[5], Guy Perrin[2], Pierre-Olivier Petrucci[5], Andreas Pflüger[1], Oliver Pfuhl[1], Thanh Phan Duc[8], Philipp M. Plewa[1], Dan Popovic[8], Sebastian Rabien[1], Andrés Ramírez[8], Jose Ramos[3], Christian Rau[1], Miguel Riquelme[8], Gustavo Rodríguez-Coira[2], Ralf-Rainer Rohloff[3], Alejandra Rosales[1], Gérard Rousset[2], Joel Sanchez-Bermudez[3], Sylvia Scheithauer[3], Markus Schöller[8], Nicolas Schuhler[8], Jason Spyromilio[8], Odele Straub[2], Christian Straubmeier[4], Eckhard Sturm[1], Marcos Suarez[8], Konrad R. W. Tristram[8], Noel Ventura[5], Fédéric Vincent[2], Idel Waisberg[1], Imke Wank[4], Felix Widmann[1], Ekkehard Wieprecht[1], Michael Wiest[4], Erich Wiezorrek[1], Markus Wittkowski[8], Julien Woillez[8], Burkhard Wolff[8], Senol Yazici[1,4], Denis Ziegler[2], Gérard Zins[8]

[1]Max Planck Institute for Extraterrestrial Physics, Garching, Germany; [2]LESIA, Observatoire de Paris, PSL Research University, CNRS, Sorbonne Universités, UPMC Université Paris 6, Université Paris Diderot, Sorbonne Paris Cité, France; [3]Max Planck Institute for Astronomy, Heidelberg, Germany; [4]I. Physikalisches Institut, University of Cologne, Germany; [5]Institut de Planétologie et d'Astrophysique de Grenoble (IPAG), Université Grenoble Alpes, CNRS, IPAG, France; [6]CENTRA — Universidade de Lisboa — Faculdade de Ciências, Portugal; [7]CENTRA — Universidade do Porto — Faculdade de Engenharia, Portugal; [8]ESO; [9]Observatoire de Genève, Université de Genève, Switzerland; [10]ONERA, The French Aerospace Lab, Châtillon, France; [11]European Space Agency, Space Telescope Science Institute, Baltimore, USA; [12]Unidad Mixta Internacional Franco-Chilena de Astronomía (CNRS UMI 3386), Departamento de Astronomía, Universidad de Chile, Santiago, Chile; [13]Max Planck Institute for Radio Astronomy, Bonn, Germany; [14]Leiden Observatory, The Netherlands; [15]Department of Physics, University of California, Berkeley, USA

With the arrival of the second generation instrument GRAVITY, the Very Large Telescope Interferometer (VLTI) has entered a new era of optical interferometry. This instrument pushes the limits of accuracy and sensitivity by orders of magnitude. GRAVITY has achieved phase-referenced imaging at approximately milliarcsecond (mas) resolution and down to ~100-microarcsecond astrometry on objects that are several hundred times fainter than previously observable. The cutting-edge design presented in Eisenhauer et al. (2011) has become reality. This article sketches out the basic principles of the instrument design and illustrates its performance with key science results obtained during commissioning: phase-tracking on stars with K ~ 10 mag, phase-referenced interferometry of objects fainter than $K \gtrsim 17$ mag, minute-long coherent integrations, a visibility accuracy of better than 0.25 %, and spectro-differential phase and closure phase accuracy better than 0.5 degrees, corresponding to a differential astrometric precision of a few microarcseconds (μas).

GRAVITY was developed in a collaboration between the Max Planck Institute for Extraterrestrial Physics, LESIA of Observatoire de Paris/CNRS/UPMC/Université Paris Diderot and IPAG of Université Grenoble Alpes/CNRS, the Max Planck Institute for Astronomy, the University of Cologne, CENTRA–Centro Multidisciplinar de Astrofísica (Lisbon and Porto) and ESO.

GRAVITY was shipped to Paranal in July 2015 (Figures 1 and 2). After roughly one year of installation and commissioning, the instrument was offered to the scientific community for the first time in October 2016. The observations we report here include objects and results that were out of reach for any previous interferometric instrument. Most notable are observations of the Galactic Centre black hole Sagittarius A* (Sgr A*) and the nearby star S2 (Figure 3); the microquasar SS 433; and 50-microarcseconds accuracy astrometry of the M-dwarf binary system GJ 65. More details about GRAVITY and early commissioning results can be found in GRAVITY Collaboration (2017 a, b, c and d).

Phase referencing optical interferometry for the VLTI

As part of GRAVITY, each of the four 8.2-metre Unit Telescopes (UT) has been equipped with a Coudé Infrared Adaptive Optics (CIAO) system, which corrects atmospheric perturbations and stably injects the light from two adjacent astrophysical objects into optical fibres. Two fibres per telescope feed two integrated optics beam combiners: one for each object. Each beam combiner pairwise combines the telescopes and samples the resulting six fringe patterns at four phase-shifted locations. Those 24 outputs are dispersed by a spectrometer and imaged onto a detector. One of the two beam combiners serves as a fringe-tracker. It is equipped with a low-resolution spectrometer and a fast camera optimised to measure the fringe phase at kHz frequency. The fringe-tracker measures and corrects atmospheric piston perturbations in real time, which permits long integration times on the second beam combiner.

The active stabilisation of the science channel allows the integration time to be increased from a few milliseconds (atmospheric coherence time) to hundreds of seconds. The resulting leap in sensitivity opens up a wide range of applications, from very faint targets at low spectral resolution to moderately bright targets at high spectral resolution. Furthermore, GRAVITY provides dual-field astrometry by precisely measuring the optical delay between two distinct objects with a dedicated metrology system. This yields object separations with an exquisite accuracy of a few tens of μas.

Both single-field (where a beam splitter injects the light from a single object into the two fibres) and dual-field modes are offered to the community, with a spectral resolution up to 4000 and a limiting magnitude of $K = 8$ in single-field mode using the 1.8-metre Auxiliary Telescopes (ATs) and $K = 10$ on the 8-metre UTs depending on weather conditions. In dual-field mode, the offered limiting magnitude is 0.5 magnitudes fainter on the fringe-tracker, and 3.5 magnitudes on the science channel. Dual-field astrometry is still under commissioning. The first observations show residuals as low as 50 μas when following objects over several months.

Figure 1. After ten years of design and realisation in Europe, GRAVITY was shipped to Chile and brought up to Cerro Paranal in these two trucks in July 2015.

Figure 2. GRAVITY in the integration hall immediately after shipment.

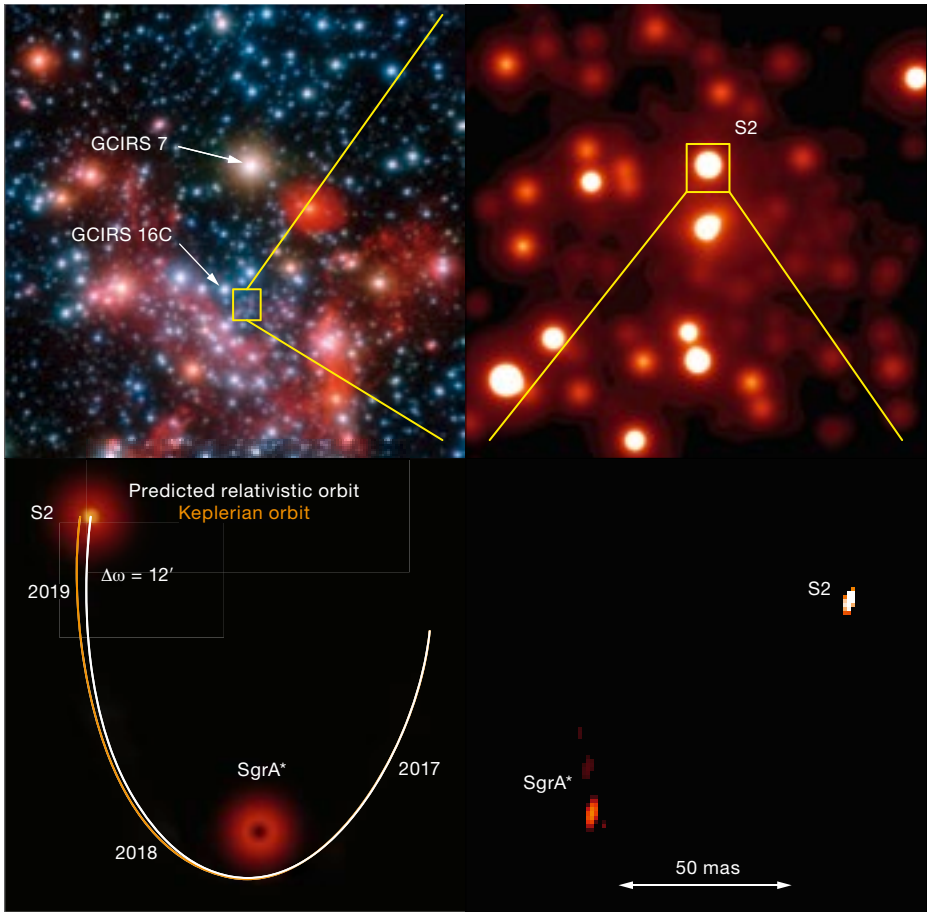

Figure 3. Top left: The central 20 arcseconds in the Galactic Centre with the adaptive optics and fringe-tracking reference stars. Top right: The central arcsecond as seen with the VLT instrument NAOS-CONICA (NACO). Bottom left: The shift between the predicted Keplerian (yellow) and relativistic (white) orbits of S2 amounts to 12 arcminutes. Bottom right: Reconstructed image from the first detection of Sgr A* by GRAVITY on 21 September 2016. The slight elongation is due to the geometry of the observatory projected on sky and is not intrinsic to the source.

Dynamics around the Galactic Centre black hole

Probing the gravitational potential around the Galactic Centre black hole Sgr A* (for example, Genzel et al., 2010) has been the primary science case and design driver of the instrument, hence the name GRAVITY (Paumard et al., 2008). The stellar orbits in the Galactic Centre are thus far perfectly Keplerian and give the best estimate of the black hole mass and its distance from Earth. The S stars within one arcsecond of Sgr A* provide ideal test particles, probing space-time in the vicinity of the black hole. With GRAVITY we want to detect general relativity effects in the orbits of those stars as deviations from Keplerian motion. S2 is the best-suited star for this experiment known so far.

Sgr A* is also surrounded by an inflow/outflow region known to exhibit flares: outbursts of energy that occur approximately once per day. The short timescale and large-amplitude brightness variations indicate that the flaring occurs a few Schwarzschild radii from the central mass. If confirmed this means the flares are additional probes for measuring the gravitational potential near the event horizon.

The Galactic Centre observations provide a good illustration of the various GRAVITY subsystems: the very bright M1 supergiant GCIRS 7 is picked up by the star separators to feed the CIAO infrared wavefront

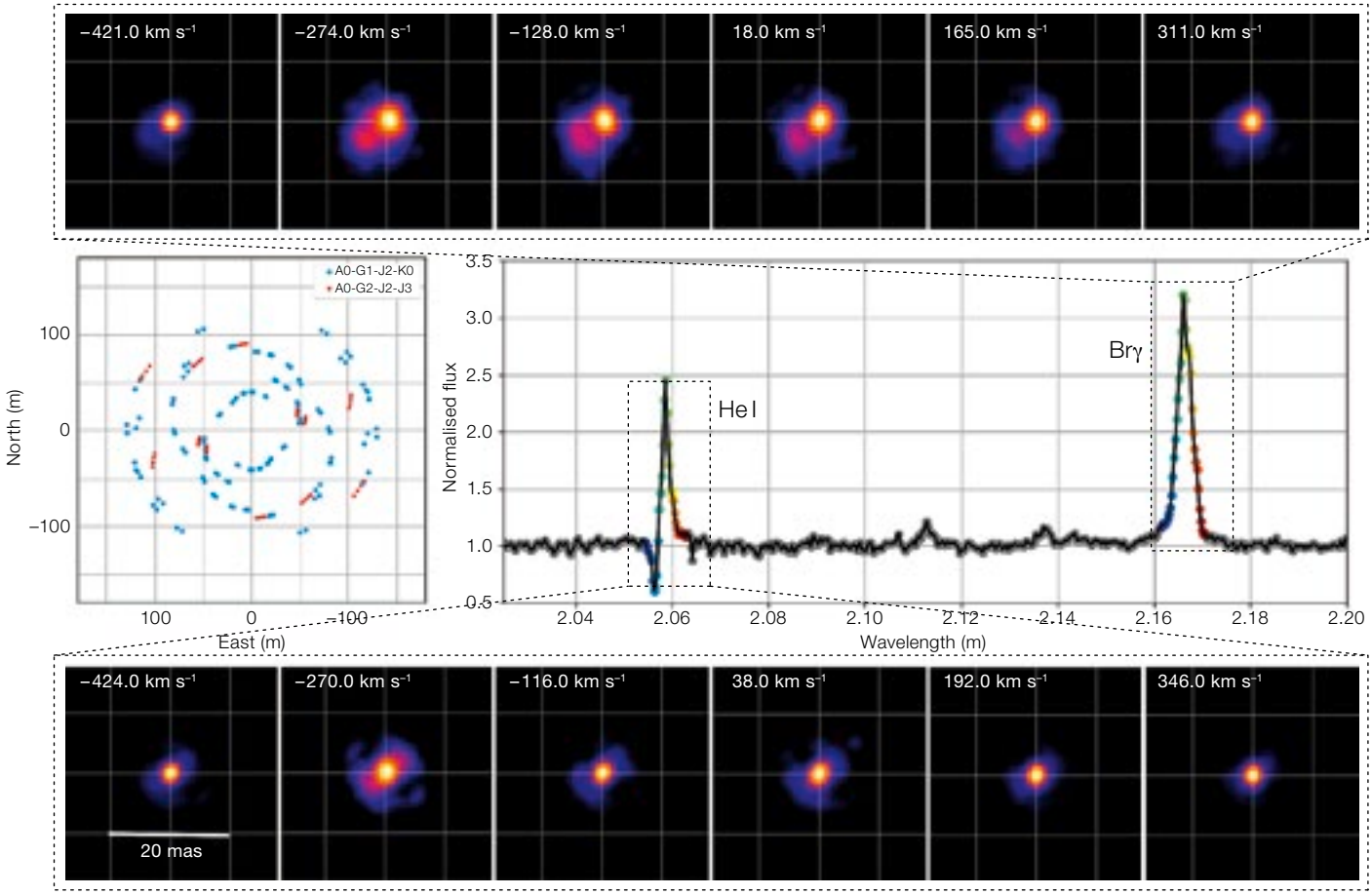

Figure 4. (Above) Interferometric imaging of η Car. Middle left: UV coverage of the GRAVITY observations. Middle right: Normalised GRAVITY spectrum of η Car. Top (bottom): Six of the reconstructed images across the Brγ (He I) line.

sensors; the blue supergiant GCIRS 16C (K = 9.8) feeds the fringe-tracker; and S2 and Sgr A* feed the science channel. Another nearby star serves as a local calibrator. S2 and GCIRS 16C show closure phases close to zero and visibilities around unity, indicating that they are isolated and unresolved (i.e., ideal astrometric references).

The Galactic Centre observations began in September 2016 with fireworks. The very first long exposures detected a moderate flare from Sgr A* (K = 15), with visibility and phase signatures that are typical for a binary system. Reconstructed images (Figure 3) revealed two objects in the interferometric beam: Sgr A* in its flaring state and S2. Since the initial observations, we have been monitoring Sgr A* on a monthly basis. Surprisingly, we detected the infrared counterpart of Sgr A* at all times in various brightness states. At the same time we followed S2 over its orbit with a measurable day-to-day motion.

The continuous monitoring during 2017 provides us with the astrometric baseline necessary for the detection of general relativistic deviations in S2's orbit. Only GRAVITY and the VLTI will allow the detection of S2's Schwarzschild precession soon after the pericentre flyby in spring 2018.

As we anxiously await the pericentre approach, we are constantly improving the instrument calibration and data reduction. Based on signal-to-noise calculations we are confident that in the near future, the observations will reach K ~ 19 sensitivity and contrast ratios of a few hundred. This additional increase in sensitivity will hopefully permit the detection of faint stars — which are predicted to exist based on stellar density extrapolations — with orbital periods lasting a few years or even a few months. If found, these stars could allow the detection of higher-order relativistic perturbations such as Lense-Thirring precession and frame dragging, and ultimately provide a direct measurement of the black hole's spin.

Spectro-imaging of Eta Carinae at milliarcsecond resolution

Eta Carinae (η Car) is one of the most intriguing luminous blue variables in the Galaxy. Models of its radiation from infrared to X-ray wavelengths imply that its core contains a binary star. The stellar wind from the secondary star creates a cavity inside the wind from the primary. Using the array of ATs, we imaged η Car with GRAVITY in February 2016. The high spectral resolution mode (R = 4000) allowed us to map η Car's wind-wind collision zone in atomic hydrogen (Brγ at 2.1661 μm) and, for the first time, in

atomic helium (He I at 2.0587 µm; Figure 4). The first and last image of each series reveal the continuum image of η Car, a compact structure of 5 milliarcseconds in size. This is the primary wind (Weigelt et al., 2016).

The GRAVITY data also confirm the presence of the wind-wind collision cavity observed with the VLTI instrument Astronomical Multi-BEam combineR, AMBER (Weigelt et al., 2016) at a velocity of −275 km s^{-1}. The bright arc-like feature in the south-east, observed at blue-shifted velocities, could be part of the hot wind due to a shock between the cavity arms after the most recent periastron passage in 2014 (Madura et al., 2013). The He I images show how ultraviolet photons from the secondary star ionise the wind from the primary. These images illustrate GRAVITY's imaging capabilities, with six simultaneous baselines and the full *K*-band at high spectral resolution. It reveals the stellar and wind parameters of large stars like η Car, and ultimately predicts their evolution and fate.

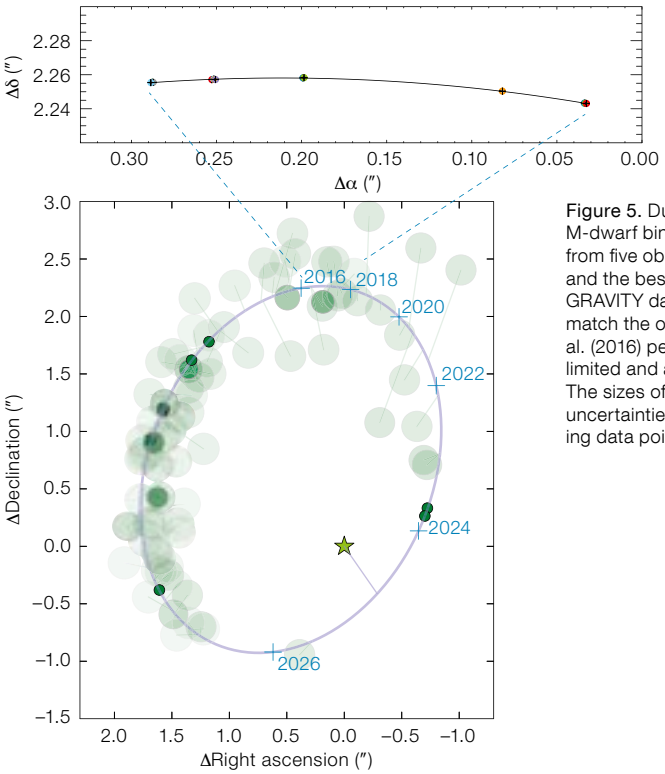

Figure 5. Dual-beam astrometry of the M-dwarf binary GJ 65. Top: Astrometry from five observing epochs in 2016–2017 and the best quadratic fit (black) to the GRAVITY data. Bottom: The GRAVITY data match the orbit of GJ 65 from Kervella et al. (2016) perfectly well, based on seeing limited and adaptive optics observations. The sizes of the discs represent the uncertainties of the single telescope imaging data points.

Towards dual-field astrometry

The dual-field design of GRAVITY paves the way for interferometric narrow-angle astrometry (Shao & Colavita, 1992). Differential phase measurements between the fringe-tracker and science channels remove most sources of systematic uncertainty. However, one needs to measure the differential optical path delay between the two fringes by means of GRAVITY's metrology system. The fundamental limitation becomes the atmospheric fluctuations, which — for separations of a few arcseconds — average out to about 10 microarcseconds within minutes. Reaching such accuracy will allow, for example, the detection of the reflex motion of a low-mass star (0.1–0.5 $M_\odot$) due to the presence of an Earth-mass planet on a one-year orbit.

In that respect, the well-studied binary GJ 65 AB, 2.68 pc from the Sun, is promising. Its two very-low-mass M-dwarf components (~ 0.12 $M_\odot$ each; Kervella et al., 2016) orbit each other in 26.28 years with a semi-major axis of 2.05 arcseconds. We observed GJ 65 AB repeatedly with the AT array and GRAVITY between August 2016 and October 2017. Our measurements (Figure 5) show an unprecedented accuracy of ~ 50 microarcseconds, and we detect the orbital acceleration. Further observations will be able to detect Jovian planets around nearby M-dwarf binaries such as GJ 65. The detection of Earth-like planets requires improved modelling and correction of the various systematic errors in order to achieve the design goal of 10-microarcsecond accuracy.

Accretion and ejection mechanisms in the binary T Tauri system S CrA

We have observed both components of the binary system S Coronae Australis (S CrA North and South) using GRAVITY and the UT array. This system (130 pc from Earth) consists of an early G-type primary (*K* = 6.6) and an early *K*-type secondary star (*K* = 7.3). Each component is a classical T Tauri star. With an apparent separation of 1.4 arcseconds, we have been able to employ the dual-field mode, thereby doubling the flux in each channel compared to single-field observations. We swapped between the two components to observe both at high resolution (*R* = 4000). Our *K*-band continuum observations show a disc around each component with half-flux radii of about 0.1 astronomical units (au), and inclinations and position angles identical within the uncertainties of a few degrees. This reveals that the two stars formed from the fragmentation of a common disc. Moreover, the variations of the interferometric quantities as a function of wavelength through the emission lines from atomic hydrogen in S CrA North reveal complex dynamics in a compact region (0.06 au) located well within the dust sublimation radius. This region is twice as large as the inner truncation radius below which accretion onto the star is magnetically driven. This suggests the coexistence of a stellar wind with magnetospheric accretion onto S CrA North (Figure 6).

A high-mass X-ray binary at microarcsecond accuracy

The high-mass X-ray binary (HMXB) BP Cru consists of a slowly rotating neutron star (GX 301-2) accreting from the wind of its blue hypergiant companion (Wray 977; Kaper et al., 2006). Like most X-ray binaries, the orbital system size

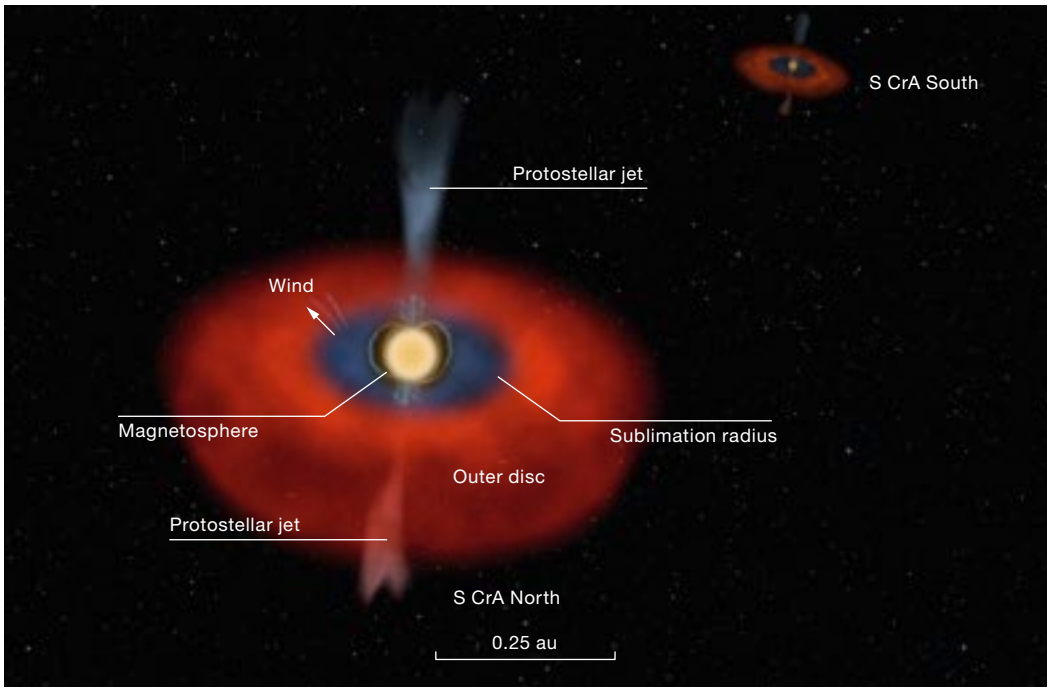

Figure 6. Artist's impression of the S CrA binary T Tauri system. GRAVITY data reveal details at an unprecedented small scale. The northern component shows a complex mixture of ejection and accretion between the scale of the magnetosphere (0.03 au) and of the sublimation radius (0.1–0.15 au). The spin axes of the two accretion discs are almost aligned, suggesting that they formed from a common precursor disc. The contrast between the large separation (1.4 arcseconds or about 200 au) and the small size of each component has been artificially reduced in this artist's impression.

(< 1 mas) is smaller than the resolution of even the largest optical/near-infrared interferometers. However, using the technique of spectral differential interferometry, it is possible to obtain spatial information on much smaller scales of a few microarcseconds. BP Cru was observed with GRAVITY and the UTs in high spectral resolution (R = 4000) with a total on-source integration of 2100 s. The differential visibility and phase across the Brγ line of atomic hydrogen (shown in Figure 7) resolve the centroid shift and extension of the flux distribution as a function of velocity. The data reveal an extended (~ 4 R_*) and distorted wind around the donor star, as well as the possible presence of a gas stream previously predicted from the X-ray lightcurve (Leahy & Kostka, 2008). The GRAVITY phase errors of 0.2 degrees correspond to a

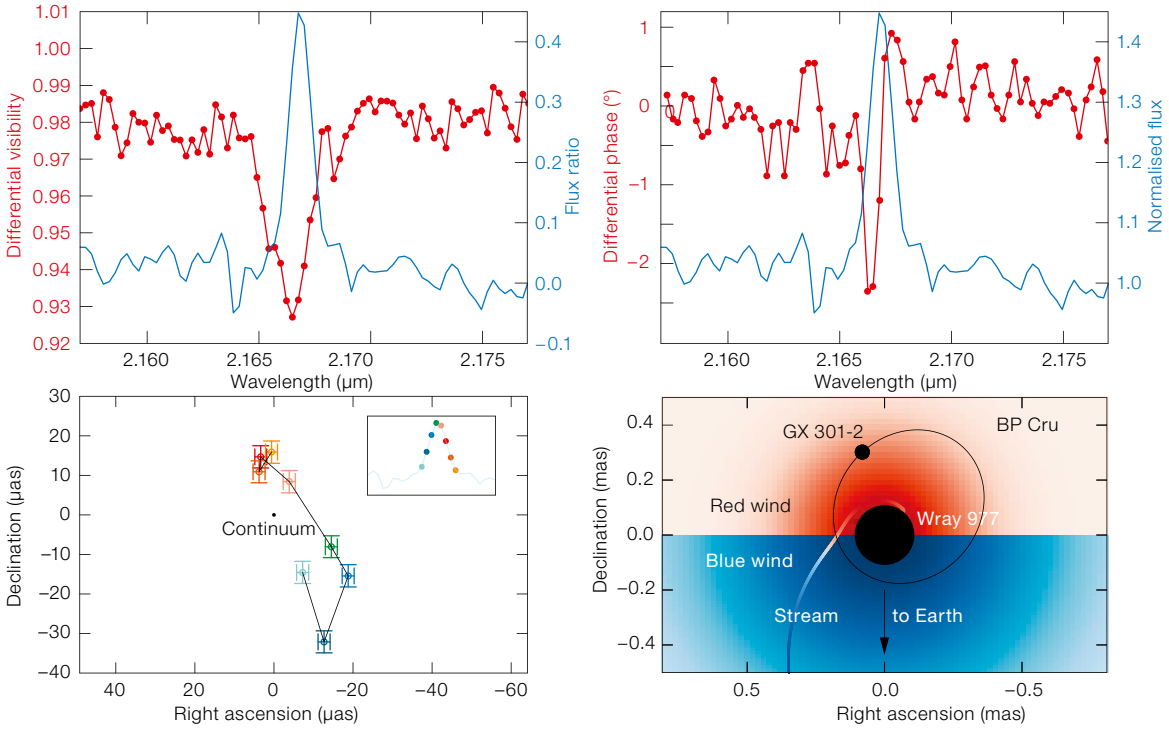

Figure 7. Tracing the inner region of the HMXB BP Cru. The upper figures show the differential visibility (left) and phase (right) for the UT1–UT4 baseline across the Brγ line as well as the flux profile. Their combination measures the centroid position and extension of the flux distribution as a function of velocity, shown in the lower left panel, with typical errors of 2 microarcseconds. The data show an extended and distorted wind around the donor star, with a blue side about two times larger than the red side. Further, the data support the presence of a gas stream (bottom right), as predicted from X-ray data to explain the asymmetry probed by the differential phases.

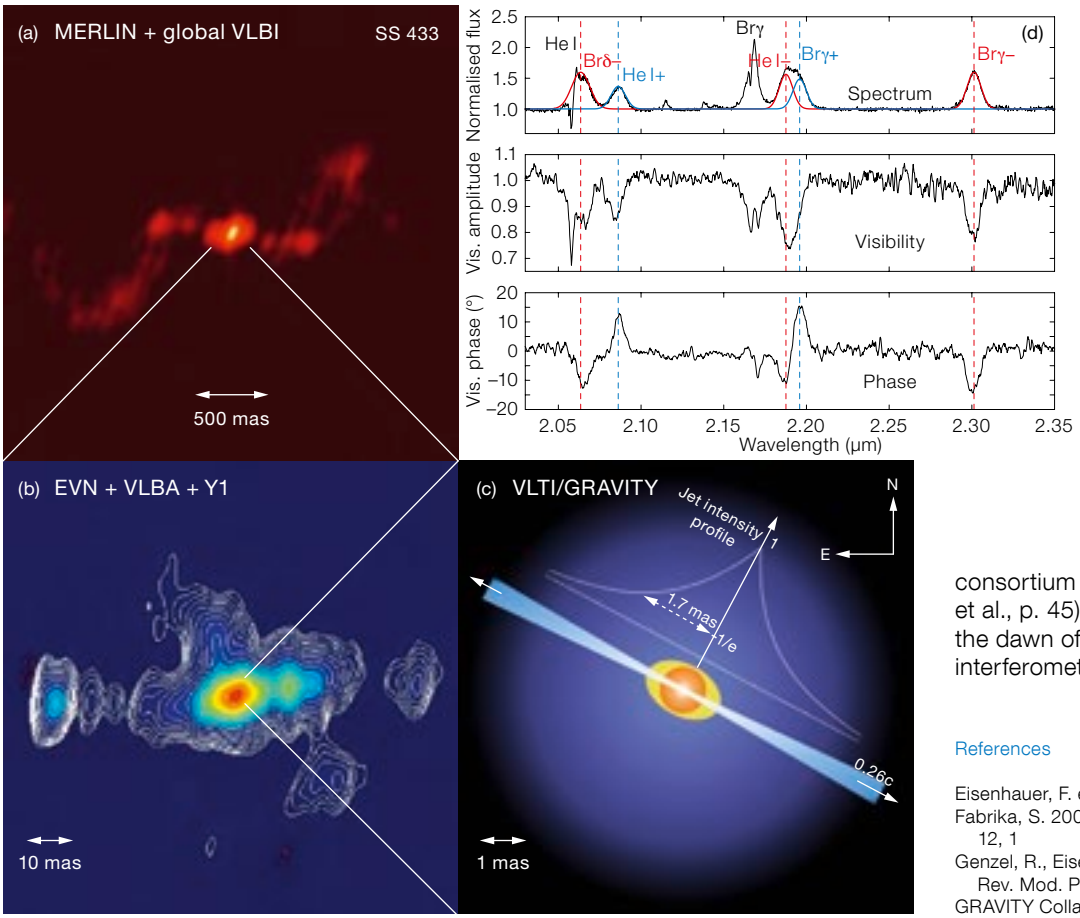

Figure 8. The microquasar SS433. The large-scale structure of the relativistic jets of SS 433 has been previously studied with radio interferometry using the Multi-Element Radio Linked Interferometer Network (MERLIN), the Very Long Baseline Interferometer (VLBI) and the European VLBI Network (EVN) (panels a and b). For the first time GRAVITY has spatially resolved the wind and redshifted (v/c ~ 0.26) emission lines from the baryonic jet. The *K*-band spectrum from GRAVITY shows several lines from the jet (shown in panel d as red/blue for the receding/approaching jets) in Brγ, Brδ and He I, as well as stationary lines from Brγ and He I. Differential visibilities and phases are seen across all lines (d), allowing models of the emission regions at sub-milliarcsecond scales (c).

centroid difference of 2 microarcseconds for a 100-metre baseline.

First optical interferometry of a microquasar

The high sensitivity of GRAVITY allowed the first near-infrared interferometric observation of a microquasar at a sub-milliarcsecond scale. The well-known X-ray binary SS 433 (K = 8.2, V = 13.0) is the only source in the galaxy known to accrete persistently in excess of its Eddington rate. The super-critical accretion drives massive winds and powerful precessing relativistic jets (Fabrika, 2004).

With 80 minutes of on-source exposure time with the UTs in high spectral resolution, GRAVITY simultaneously resolved all of these components. The winds were seen in the continuum emission (partially resolved at a size of ~ 0.8 mas) with evidence for bipolar outflows seen in the stationary (i.e., non-jet) Brγ emission line. Differential interferometry at several redshifted emission lines (v/c ~ 0.26) revealed the spatial structure of the relativistic jets (Figure 8).

While the large-scale structure of the jets had previously been studied at radio wavelengths (Paragi et al., 2001), we have spatially resolved its baryonic jet emission lines (Margon et al., 1979) for the first time. The jet emission peaks surprisingly close to the binary, and is well-modelled with a resolved (~ 2 mas) intensity profile that is exponentially decreasing.

GRAVITY has entered the science phase

The results presented in this article are only selected examples of early science from GRAVITY. The wider community has benefited from GRAVITY's performance since 2016, with two Science Verification runs in June and September and open-time operation since October 2016. With additional results from PIs outside of the consortium (Mérand et al., p. 16; Kraus et al., p. 45), The Messenger celebrates the dawn of a new era for optical interferometry.

References

Eisenhauer, F. et al. 2011, The Messenger, 143, 16
Fabrika, S. 2004, Astrophys. & Space Phys. Rev., 12, 1
Genzel, R., Eisenhauer, F. & Gillessen, S. 2010, Rev. Mod. Phys., 82, 3121
GRAVITY Collaboration: Abuter, R. et al. 2017a, A&A, 602, A94
GRAVITY Collaboration: Garcia Lopez, R. et al. 2017b, A&A, 608, A78
GRAVITY Collaboration: Petrucci, P. O. et al. 2017c, A&A, 602, L11
GRAVITY Collaboration: Waisberg, I. et al. 2017d, ApJ, 844, 72
Kaper, L., van der Meer, A. & Najarro, F. 2006, A&A, 457, 595
Kervella, P. et al. 2016, A&A, 593, A127
Leahy, D. A. & Kostka, M. 2008, MNRAS, 384, 747
Madura, T. I. et al. 2013, MNRAS, 436, 3820
Margon, B. et al. 1979, ApJ, 233, 63
Paragi, Z. et al. 2001, Ap&SS Suppl., 276, 131
Paumard, T. et al. 2008, *The Power of Optical/IR Interferometry: Recent Scientific Results and 2nd Generation Instrumentation*, ed. Richichi, A., Delplancke, F., Paresce, F. & Chelli, A., (Berlin Heidelberg: Springer-Verlag), 313
Shao, M. & Colavita, M. M. 1992, A&A, 262, 353
Weigelt, G. et al. 2016, A&A, 594, A106

Notes

Principal authors: Thibaut Paumard, Oliver Pfuhl, Andreas Eckart, Karine Perraut, Wolfgang Brandner and Paulo Garcia.

DOI: 10.18727/0722-6691/5049

GRAVITY Science Verification

Antoine Mérand[1]
Jean-Philippe Berger[2]
Willem-Jan de Wit[1]
Frank Eisenhauer[3]
Xavier Haubois[1]
Thibaut Paumard[4]
Markus Schoeller[1]
Markus Wittkowski[1]
Julien Woillez[1]
Burkhard Wolff[1]

[1] ESO
[2] Institut de Planétologie et d'Astrophysique de Grenoble, Université Grenoble Alpes, CNRS, France
[3] Max Planck Institute for Extraterrestrial Physics, Garching, Germany
[4] LESIA, Observatoire de Paris, PSL Research University, CNRS, Sorbonne Universités, UPMC Université Paris 6, Université Paris Diderot, Sorbonne Paris Cité, France

In the time between successfully commissioning an instrument and before offering it in the Call for Proposals for the first time, ESO gives the community at large an opportunity to apply for short Science Verification (SV) programmes. In 2016, ESO offered SV time for the second-generation Very Large Telescope Interferometer instrument GRAVITY. In this article we describe the selection process, outline the range of science cases covered by the approved SV programmes, and highlight some of the early scientific results.

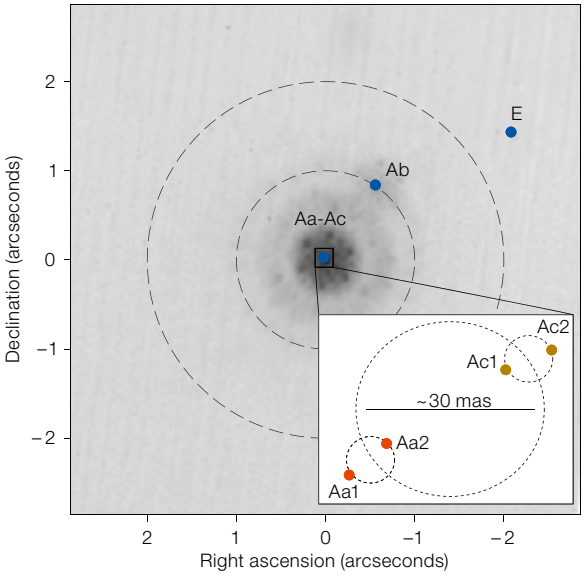

Figure 1. This is a Sparse Aperture Masking image of the system HD 93206 taken with NACO using the K_s filter. The position of the Aa-Ac, Ab and E components are represented by blue dots. Two concentric dashed rings encircle the central 2–4 arcseconds around HD 83206A. The inset diagram shows the quadruple system Aa-Ac, which is the main target of the observations.

ESO issued a call for SV on the Auxiliary Telescopes (ATs) in March 2016, just after the on-sky performance of GRAVITY was established (GRAVITY Collaboration, 2017) and the Science Operations team had been trained in operating the instrument. In total, 43 proposals were received. The SV proposals were evaluated by a team led by Jean-Philippe Berger, who was the Very Large Telescope Interferometer (VLTI) Programme Scientist at the time. The panel consisted of members of the Instrument Operation Team and the GRAVITY consortium. Their main task was to assess the feasibility and scientific merits of each project, and later to acquire the observations and carry out the data reduction. All information regarding SV can be found on the GRAVITY SV page[1].

20 programmes were selected to showcase the spectro-imaging capabilities of GRAVITY and to enable its performance — in terms of sensitivity, wide simultaneous spectral coverage and improved spatial information — to be compared to the Astronomical Multi-BEam combineR (AMBER), the VLTI instrument it most closely resembles. Two SV runs of nine nights each were scheduled in June and September 2016 and observations were carried out in service mode by the SV team. The instrument operations were smooth, but it was challenging to complete all the programmes in the allocated time as they required multiple changes to the AT configurations. Despite this, there was no substantial loss of time and ultimately 14 programmes were considered fully or almost completed, with six programmes either partially completed or not completed. We present some highlights from four SV programmes here.

The quadruple massive stars in HD 93206

Almost all massive stars are found in multiple systems: Sana et al. (2014) showed that 90 % of massive stars have at least one companion, while 30 % belong to triple or higher-degree systems. In addition to detecting and cataloguing systems for statistical studies, it is necessary to investigate individual systems to test massive star formation scenarios. The late-O/early-B type system HD 93206, also known as QZ Car, is the most massive quadruple star system known, totalling 90 $M_\odot$. The GRAVITY observations of HD 93206 (Programme ID 60.A-9175, Principal Investigator [PI]: Sanchez-Bermudez) were used to improve on NAOS–CONICA (NACO) sparse aperture masking (SAM) observations (Figure 1). The reconstructed GRAVITY image shows Aa and Ac clearly but does not resolve each component as a binary (Figure 2). Previous observations with the Precision Integrated Optics Near-infrared Imaging ExpeRiment (PIONIER) and the less precise NACO/SAM separation for Aa-Ac are also shown. The new analysis excludes the presence of a companion up to 5 magnitudes fainter in this 150-milliarcsecond field of view.

In addition to spatially resolving Aa-Ac as a binary, GRAVITY's spectroscopic resolution allowed two lines to be detected: hydrogen Brγ lines (2.1661 µm), which trace shocks in the winds from the hot stars, and helium lines (2.058 µm & 2.112 µm), which are photospheric. These GRAVITY observations show that the Brγ emission is very compact and does not result from the interaction of winds from Aa and Ac. An alternate explanation is that the emission results from wind interactions within the Aa and Ac binaries. Future observations using GRAVITY with the Unit Telescopes (UTs) should result

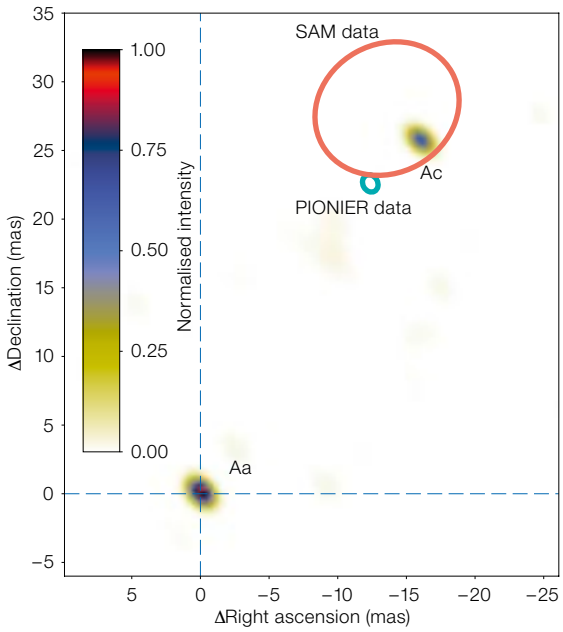

Figure 2. BiSpectrum Maximum Entropy Method (BSMEM) reconstructed interferometric image of HD 93206A. The components of the outer binary Aa-Ac are labelled on the figure. The colour scale represents the normalised intensity. Cyan and red ellipses show the 1-σ positions of the Ac component based on PIONIER and NACO observations respectively (Sana et al., 2014). The positional difference between the PIONIER and GRAVITY epochs is due to orbital motion.

in better sensitivity and enable the detection of a weak interferometric signal in Brγ within the Aa and/or Ac binaries.

The evolved binary star Ups Sgr

Ups Sgr is an interacting binary in an advanced stage of evolution, in which the stripped donor has lost its hydrogen envelope and is now experiencing a second episode of mass loss during core helium burning. The spectroscopic binary has an orbital period of 138 days (Koubsky et al., 2006). The binary is also surrounded by a dusty torus with an inner rim diameter of 20 milliarcseconds, as detected by the MID-infrared Interferometric instrument (MIDI) on the VLTI (Netolický et al., 2009). Bonneau et al. (2011) detected over-resolved Hα emission with the Centre for High Angular Resolution Astronomy (CHARA) interferometer using the Visible spEctroGraph and polArimeter (VEGA).

This system was imaged by GRAVITY (Programme ID 60.A-9177, PI Gies) and complemented by *H*-band data from the Michigan InfraRed Combiner (MIRC) on CHARA. Preliminary results indicate that GRAVITY can resolve the inner binary with a separation of a few milliarcseconds. A significant amount of light (~ 60–70 %) is detected from an over-resolved circumbinary disc; the flux ratio between the disc and the binary shows a chromatic wavelength dependence across the spectral channels. An additional asymmetry in the system was detected, likely from resolved structure in the inner region of the disc. The team is in the process of reconstructing images while simultaneously fitting for binary separation, with the goal of producing snapshots of the system at different orbital phases.

The complex young stellar binary system CO Ori

Programme 60.A-9159 (PI Davies) used the short baseline configuration (8–30 m) of the ATs to observe both components of the CO Ori young stellar object binary system. The single-field mode was used to observe the primary (*K* = 3.0 magnitudes). Located 2 arcseconds away, the secondary (*K* = 6.0) required GRAVITY's unique dual-field mode and was observed by the GRAVITY spectrograph while the primary was used for fringe tracking. Both the circumprimary and circumsecondary *K*-band emission were successfully spatially resolved for the first time. This confirmed the previous result from Rodgers et al. (2003) that the secondary star is responsible for the Brγ emission observed towards the system. Together with GRAVITY's detection of circumsecondary continuum emission, the presence of this line (typically associated with the accretion process in young stars) provides strong evidence for the presence of a circumsecondary accretion disc.

The team is using geometrical models to determine the orientation of the circumprimary and circumsecondary material. The continuum closure phases for both binary components provide no strong indication of a deviation from a centrosymmetric brightness distribution at the distances probed. The team is therefore focusing their modelling on the continuum visibilities. Their results indicate the presence of a disc around the primary CO Ori A (full width at half maximum [FWHM] = 2.31 ± 0.04 milliarcseconds; inclination, *i* = 30.2 ± 2.2 degrees; position angle [PA] = 40.6), while the circumsecondary emission more likely comprises a disc (FWHM = 0.96 ± 0.55) and an extended halo component. This halo component is likely attributed to scattered light (for example, Pinte et al., 2008).

The primary science goal of this programme was to determine the relative orientation of the discs in the binary system. However, the *K*-band emission from CO Ori B was more compact than anticipated and astronomers were unable to determine the orientation of the circumsecondary emission. Instead, efforts were redirected to the secondary scientific aim of probing the origin of the variable extinction (UX Ori phenomena) associated with CO Ori A.

The inclination of the circumprimary emission is below that found for the discs of other UX Ori-type stars (*i* ~ 30–70 degrees; Eisner et al., 2004; Pontoppidan et al., 2007; Chapillon et al., 2008; Kreplin et al., 2013; Vural et al., 2014; Kreplin et al., 2016). Thus, rather than emanating from a disc (for example, Natta et al., 1997), CO Ori A provides the first indication that in some cases the UX Ori phenomena may be attributed to irregularities in a dusty outflow (for example, Tambovtseva & Grinin, 2008). These results are presented in greater detail in Davies et al. (2017).

The planet-hosting debris disc around β Pic

Medium-resolution GRAVITY observations of the young star β Pic (HD 39060,

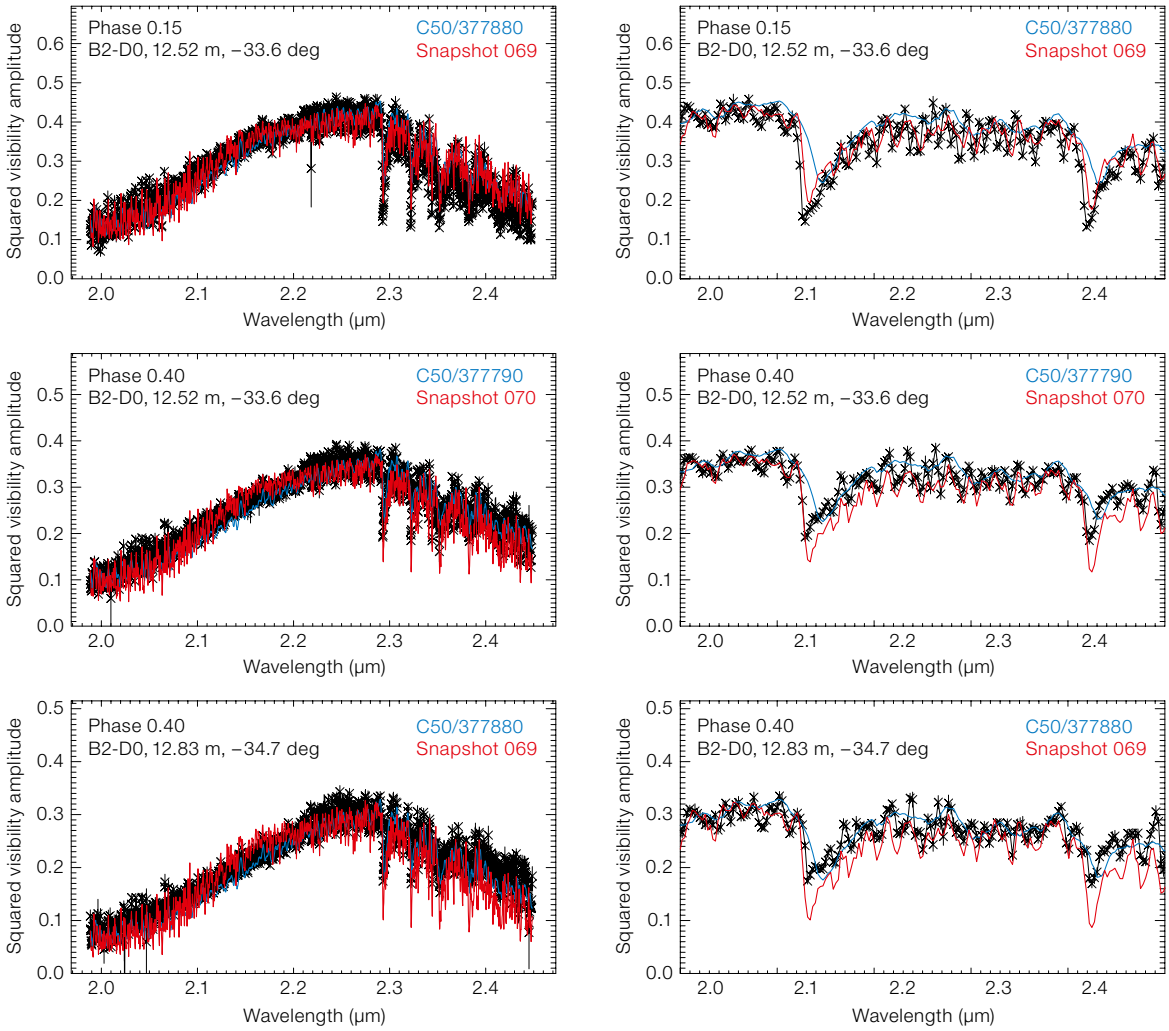

Figure 3. GRAVITY observations of the Mira star R Peg. Left: Visibilities (black) of R Peg in June, September, and November 2016 at visual phases 0.15, 0.40 and 0.65. Also shown are predictions by the best-fit CODEX models (blue) and RHD simulations (red). The wavelength range covers 1.98–2.45 μm and corresponds to the full wavelength coverage of the GRAVITY instrument (Wittkowski et al., in preparation). Right: Zooming in on the wavelength range around the CO (2-0 and 3-1) bandheads at 2.29 μm and 2.32 μm.

A6V, 19.3pc, ~ 12 Myr) were carried out using the compact VLTI configuration (Programme ID 60.A-9161, PI Defrère). β Pic is a prime target for understanding planetary system formation and evolution. Since the discovery of its planetary system (Smith & Terrile, 1984) successive generations of telescopes have reported the detection of an edge-on debris disc. The disc has several distinctive features suggestive of a multiple-belt system (Telesco et al., 2005); star-grazing comets arranged into two families (Beust et al., 1990; Kiefer et al., 2014); circumstellar gas (for example, Roberge et al., 2006; Dent et al., 2014); and a planetary companion (~ 10 M_{Jup}) orbiting the star with a semi-major axis of ~ 9 astronomical units (au) (Lagrange et al., 2009). The existence of other planets also seems likely (Freistetter et al., 2007) and may explain several asymmetries identified in the debris disc, including a warp at ~ 50 au, inclined by approximately 4 degrees with respect to the outer disc (Augereau et al., 2001; Lagrange et al., 2012).

Over the past few years, the close environment (less than a few au) of β Pic has been the focus of several studies trying to detect a predicted sub-stellar companion. In particular, closure phase measurements with AMBER and PIONIER excluded the presence of companions a few hundred times fainter than the central star at angular separations up to approximately 100 milliarcseconds (i.e., a brown dwarf of about 30 M_{Jup} at the age of β Pic; Absil et al., 2010). No companion has been detected at the current precision level, although accurate squared visibilities obtained with PIONIER have revealed the presence of resolved circumstellar emission, with an integrated brightness amounting to approximately 1.4 % of the stellar brightness in the *H*-band (Defrère et al., 2012).

If the scattering of stellar light in the outer disc is seen edge-on, it may help to explain the spectral shape of the measured excess. However, current models fail to reproduce the total value of this excess, and hot material must also be present in the innermost region of the planetary system. The prevailing scenario is the presence of hot exozodiacal dust as proposed for older A-type stars (for example, Ertel et al., 2014).

However, the exact amount of hot dust, its location and its chemical properties remain unclear, particularly due to the lack of multi-wavelength information. GRAVITY has a crucial role to play here by providing the first medium-resolution

spatially resolved observations of the inner planetary system. The SV data confirm the presence of resolved circumstellar emission that depends on the wavelength and the baseline orientation, unlike previous observations of this excess obtained in the *H*-band (Defrère et al., 2012). Thorough radiative-transfer modelling is currently underway to produce a disc model that will fit the observed visibilities and reveal the nature of this puzzling excess emission.

The Mira-type star R Peg

Low- to intermediate-mass stars, including our Sun, evolve into red giants and subsequently into asymptotic giant branch (AGB) stars. Mass loss increases during AGB evolution and eventually dominates the subsequent stellar evolution. AGB mass loss is driven by interplay between pulsations that extend the atmosphere, dust formation in the extended atmosphere, and radiation pressure on the dust. However, the details of these interrelated processes remain unknown.

Recent one-dimensional dynamic model atmospheres, based on self-excited pulsation models of oxygen-rich Mira stars, predicted a regular sinusoidal variation of the photospheric radius and the irregular chaotic variability of the outer molecular layers (Cool Opacity-sampling Dynamic EXtended [CODEX] models; Ireland et al., 2008, 2011). Similarly, three-dimensional radiation hydrodynamic (RHD) simulations of AGB stars by Freytag & Höfner (2008) showed shock waves that are overall roughly spherically expanding, and are similar to those from the one-dimensional models with certain additional non-radial structures. Comparisons by Wittkowski et al. (2016) of AMBER data with both CODEX and RHD models showed that predictions by both types of models are indeed consistent and can explain observations at individual epochs. PIONIER imaging observations by Wittkowski et al. (2017) confirmed the predicted effects of non-radial structures on clumpy dust formation.

Early long-term narrow-band monitoring of Mira variables at the Palomar Testbed Interferometer by Thompson et al. (2002) showed the expected sinusoidal variation in a near-continuum bandpass for two sources with different phase lags. Since then, this predicted variability over a stellar cycle has not been convincingly confirmed. AMBER observations, along with observations from other facilities, showed agreement with CODEX models at individual epochs but could not convincingly show the longer-term variability.

GRAVITY observations promised to deliver stronger observational constraints at any epoch, allowing us to verify the model-predicted variability of the visibility spectra. This expectation was based on the high spectral resolution of GRAVITY, which can be reached over the whole *K*-band; the higher expected S/N on the target visibility spectra due to the longer integration times on the science spectrometer; and the higher expected accuracy of calibrated visibilities, due to the better stability of the instrument as compared to previous campaigns with AMBER.

The first such observations were attempted by a team led by Markus Wittkowski, Gioia Rau and Andrea Chiavassa (Programme ID 60.A-9176). The Mira variable R Peg was observed in June, September and November 2016. The latest epoch was part of the follow-up programme 098.D-0647 (PI Wittkowski). Calibrator star observations interleaved the R Peg observations. Data were obtained in the high spectral resolution and split polarisation modes, and were reduced using the GRAVITY pipeline (version 1.0.5). The data obtained with the science spectrometer were compared to those from the faster low-resolution fringe tracker and gave a consistent height of the calibrated visibility. This confirms a good absolute calibration of the visibility data.

Figure 1 shows preliminary results of the visibility data covering the full *K*-band for the example of one baseline at the three epochs. The best-fit CODEX model atmospheres as well as the best-fit three-dimensional radiation hydrodynamic (RHD) simulations by Freytag & Höfner (2008) are also shown. These fits were obtained in the same way as for the AMBER data of AGB stars (Wittkowski et al., 2016). The projected baseline lengths and position angles at the three epochs are very similar. These preliminary results suggest a decreasing visibility at a near-continuum bandpass around 2.25 µm along visual variability phases 0.15, 0.40, and 0.65, which corresponds to an increasing continuum radius. At the same time, the visibility dip at the CO bandheads relative to the nearby near-continuum decreases along these phases. This suggests a decreasing contribution by extended CO layers. Furthermore, the comparison to one- and three-dimensional dynamic model atmospheres shows a good agreement between the observations and models in the shape of the visibility function. Note that these are preliminary results and a more detailed analysis will appear in Wittkowski et al. (in preparation).

This preliminary analysis promises that GRAVITY will provide measurements of the pulsation of the photosphere and extended atmosphere of AGB stars in unprecedented detail. Comparisons to the newest models (for example, Freytag et al., 2017) will enable further insights into the processes of convection and pulsation in these atmospheres.

References

Absil, O. et al. 2010, A&A, 520, L2
Augereau, J. C. et al. 2001, A&A, 370, 447
Beust, H. et al. 1990, A&A, 236, 202
Bonneau, D. et al. 2011, A&A, 532, A148
Chapillon, E. et al. 2008, A&A, 488, 565
Davies, C. L. et al. 2017, arxiv.org:1711.10244
Defrère, D. et al. 2012, A&A, 546, L9
Dent, W. R. F. et al. 2014, Science, 343, 1490
Eisner, J. A. et al. 2004, ApJ, 613, 1049
Freytag, B. & Höfner, S. 2008, A&A, 483, 571
Freytag, B. et al. 2017, A&A, 600, A137
GRAVITY Collaboration 2017a, A&A, 602, A94
Ireland, M. J. et al. 2008, MNRAS, 391, 1994
Ireland, M. J. et al. 2011, MNRAS, 418, 114
Kishimoto, M. 2016, A&A, 590, A96
Koubsky, P. et al. 2006, A&A, 459, 849
Kreplin, A. et al. 2013, A&A, 551, A21
Kreplin, A. et al. 1997, ApJ, 491, 885
Netolický, M. et al. 2009, A&A, 499, 827
Pinte, C. et al. 2008, ApJ, 673, L63
Pontoppidan, K. M. et al. 2007, ApJ, 656, 980
Rodgers, B. M., Pierpoint, L. M. & van der Bliek, N. S. 2003, AAS Abstracts, 35, 1257
Sana, H. et al. 2014, ApJS, 215, 15
Sanchez-Bermudez, J. et al. 2017, ApJ, 845, 57
Tambovtseva, L. V. & Grinin, V. P. 2008, Astronomy Letters, 34, 231
Vural, J. et al. 2014, A&A, 564, A118
Thompson, R. R. et al. 2002, ApJ, 577, 447
Wittkowski, M. et al. 2016, A&A, 587, A12
Wittkowski, M. et al. 2017, A&A, 601, A3

Links

[1] GRAVITY Science Verification: https://www.eso.org/sci/activities/vltsv/gravitysv.html

DOI: 10.18727/0722-6691/5050

MUSE WFM AO Science Verification

Bruno Leibundgut[1]
Roland Bacon[2]
Yara L. Jaffé[1]
Evelyn Johnston[1]
Harald Kuntschner[1]
Fernando Selman[1]
Elena Valenti[1]
Joël Vernet[1]
Frédéric Vogt[1]

[1] ESO
[2] CRAL, Observatoire de Lyon, Saint Genis Laval, France

The goal of Science Verification (SV) as part of the transition into operations is to carry out scientific observations to test the end-to-end operations of a new instrument or new instrument modes. The Multi Unit Spectroscopic Explorer, (MUSE; Bacon et al., 2010), at the Very Large Telescope (VLT) can be operated in several modes. The wide-field mode has been offered since Period 94 (October 2014) for natural-seeing observations. With the commissioning of the Adaptive Optics Facility (AOF; Arsenault et al., 2017) the wide-field mode can be supported by ground-layer adaptive optics through four artificial laser guide stars and the adaptive optics module, Ground Atmospheric Layer Adaptive OptiCs for Spectroscopic Imaging (GALACSI). The MUSE wide-field mode adaptive optics Science Verification (hereafter referred to MUSE WFM AO SV) was scheduled from 12–14 August 2017. Out of 41 submitted proposals, 19 observing programmes were scheduled, covering a wide range of science topics and amounting to an allocation of 42 hours. This included sufficient oversubscription to cover all expected observing conditions. Due to inclement weather during the original SV nights, two more nights were allocated on 16 and 17 September 2017 to observe more programmes. In total, seven programmes were completed, six programmes received partial data, and the remaining six projects could not be started. We summarise here the planning, execution and first results from the Science Verification.

Proposal solicitation and submission

The Call for MUSE WFM AO SV Proposals was issued on 18 May 2017[1] and was advertised *via* the ESO Science Newsletter[2]. With the call, the MUSE WFM AO SV webpage[3] was also launched. In total, 41 proposals were received by the deadline on 14 June 2017. The MUSE WFM AO SV team evaluated all proposals and the selection was discussed at a videoconference on 7 July 2017. The cutoff line was defined at 42 hours of allocated time, which resulted in 19 programmes being allocated time. All Principal Investigators (PIs) were informed of the results of the selection process on 13 July and the successful PIs were requested to provide the Phase 2 material by 31 July. All PIs complied with this deadline.

The selected programmes covered many different science topics including: globular clusters, nuclear stellar clusters in nearby galaxies, massive star clusters in the Small Magellanic Cloud (SMC), supernova remnants, blue compact and nearby starburst galaxies, star formation in nearby galaxies, the gas distribution around galaxies, galaxy clusters, and the gas content and star formation activity in galaxies at $z = 1$.

Observations

The first two SV nights (12 & 13 August) were completely lost due to inclement weather (low temperatures and snow) and technical issues with the hexapod of the secondary mirror unit on VLT Unit Telescope 4 (UT4). The road to the mountaintop was closed during the night of 12 August due to the freezing conditions. In total, this amounted to a loss of 20 hours.

The last night of the first SV run (14 August) was more successful. We were able to observe two globular clusters, the central cluster of the Sagittarius dwarf galaxy, a young massive cluster in the SMC, a star formation region in a nearby galaxy, a galaxy cluster at $z = 1.46$, and star formation clumps in a distant ($z \approx 3$) galaxy cluster. The adaptive optics (the deformable secondary mirror and GALACSI) worked without major problems throughout the night.

Two additional SV nights were allocated to compensate for the bad weather on 16 and 17 September, and these had varying conditions. Data for a few more SV programmes could be obtained. They included observations of a blue compact galaxy, star formation in dwarf galaxies, the nucleus of a nearby galaxy, sites of supernovae, the influence of black holes at the centres of galaxies, and a second epoch for the massive cluster in the Small Magellanic Cloud.

Overall, 13 out of the 19 selected programmes were observed. Good image quality (~ 0.6 arcseconds) could be achieved for natural seeing above one arcsecond and in excellent atmospheric conditions an image quality better than 0.4 arcseconds could be obtained. In addition to the difficult weather conditions, the main reasons for not starting more programmes were conflicts with observing programmes at other Unit Telescopes (UTs) due to laser collisions. Visitor mode programmes at all UTs take precedence over laser observations. Any time the lasers cross the beam of another telescope, the Adaptive Optics Facility (AOF) observations have to be postponed and rescheduled. With only a limited amount of SV time available, such collisions prevented us from starting more programmes. The seeing conditions during parts of the nights were also less favourable, so the image quality of the more ambitious programmes could not be achieved.

Archive and data processing

All raw data are publicly available through the ESO Science Archive. The MUSE WFM AO SV webpage contains direct links to the raw data. The ESO data quality control group reduced all SV data. A new version of the MUSE data reduction pipeline was released at the beginning of October, which includes handling of the MUSE WFM AO data and supports all of the new modes used during the SV run. The SV webpage provides a link to the new pipeline version.

A few first scientific results

The following provides a sample of some preliminary results obtained during MUSE

Elena Valenti

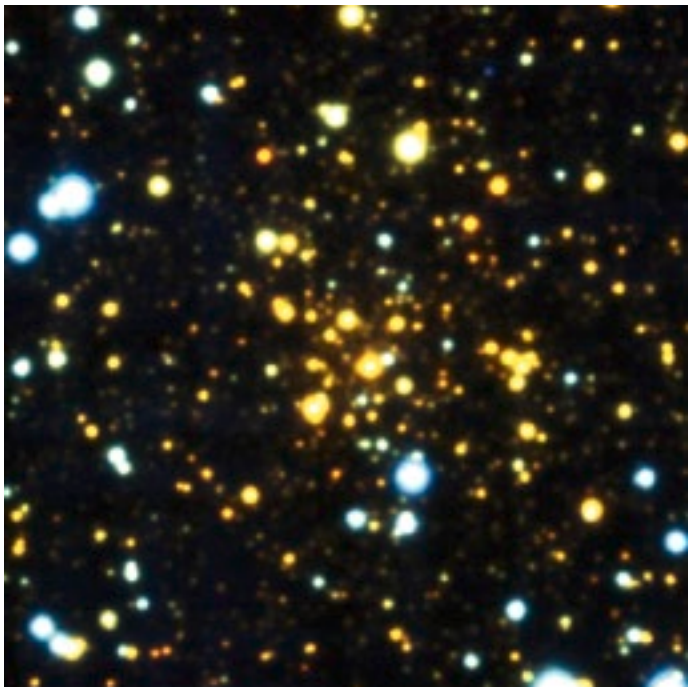

Figure 1. Colour composite of VVV CL001. This image shows almost the full 1 × 1 arcminute field of MUSE in WFM.

Elena Valenti

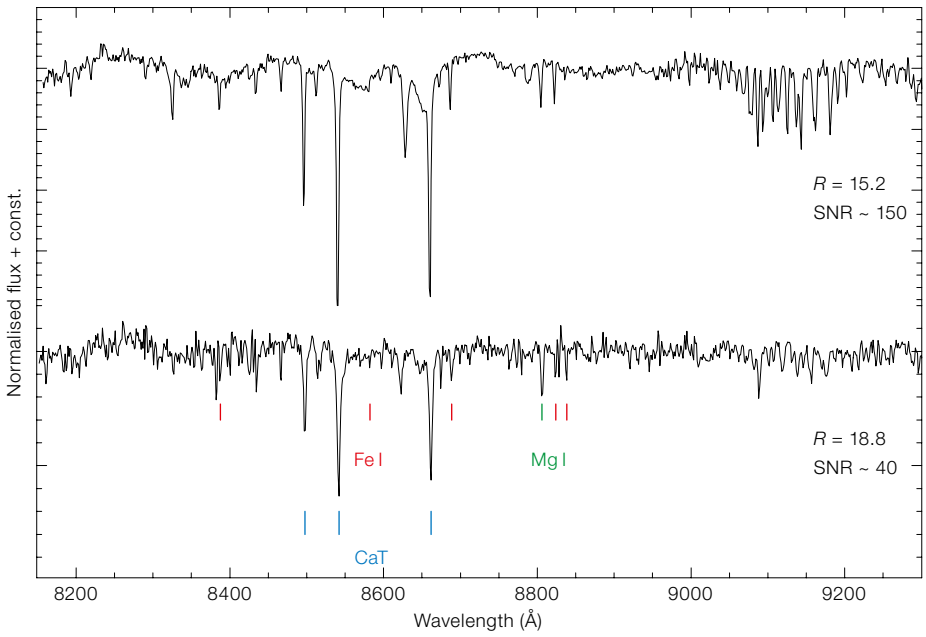

Figure 2. Ca triplet region of two stars in VVV CL001.

WFM AO SV and demonstrates the scientific potential of this new mode of MUSE.

Globular cluster VVV CL001

The heavily obscured (A_V ~ 10) globular cluster VVV CL001 (Figure 1) was observed to measure the kinematics of the cluster and the metallicities of individual stars. The cluster is in close proximity to another globular cluster, UKS-1, and they are possibly gravitationally bound. The radial velocity of VVV CL001 as obtained from individually resolved stars and compared to UKS-1 might reveal that they are at the same distance behind the Galactic Centre, providing evidence for the first binary globular cluster system known in the Milky Way.

The observations were taken with a seeing of approximately one arcsecond, with an average ground-layer turbulence fraction of ~35 % and an average coherence time of ~4.5 ms. The adaptive optics helped to reach deeper into the cluster, providing a stable and uniform image quality of ~0.6 arcseconds across the whole field of view.

After processing the data with the latest MUSE pipeline (version 2.2), the final data cube has been sliced along the wavelength axis into 3681 monochromatic images (i.e., single plane) sampling the targets from 4750 to 9350 Å with a wavelength step of 1.25 Å. Finally, the spectra for all detected stars in the *R* and *I* images have been extracted by running point-spread-function (PSF) fitting photometry on all 3681 single planes. Such a "photometric approach" for the spectral extraction allows for the proper handling of stellar blends, as well as a refinement of the sky subtraction. Indeed, sky residual signatures in the final data cube are removed through the PSF fitting, which estimates and subtracts the local sky for each star.

Spectra for more than 900 stars have been obtained in a 1 × 1 arcminute area in the cluster centre. The two spectra are examples of the quality of information that can be extracted around the Ca infrared triplet (Figure 2). Radial velocity measurements are expected for the entire stellar sample, while Fe, Ca and Mg abundances will be possible only for the brighter sources (i.e., spectra with signal-to-noise ≥ 40).

Massive star cluster

Most massive stars are born in binary systems and hence their evolution is likely to be heavily influenced by their close companion. NGC 330 is a young massive cluster in the Small Magellanic Cloud. Spectroscopy of stars in the outskirts of NGC 330 had already been obtained (Evans et al., 2006; Martayan et al., 2007a,b), revealing a particularly low binary fraction (4 %) but also many Be stars. The compact central cluster (with more than 100 stars with initial masses above 8 $M_\odot$; Sirianni et al., 2001) could not been resolved with existing instrumentation. Given the strong primordial mass segregation revealed by the Hubble Space Telescope (Sirianni et al.,

2001; Figure 3), the most massive stars — and binary products — are expected to be located in the cluster core. Given the high source density in the cluster core, AO-supported observations are required. In the MUSE image (Figure 3) many sources have a companion within less than an arcsecond of separation.

Five dithering positions of 540 seconds each were obtained during MUSE WFM AO SV with relative offset between the positions of about 0.7 arcseconds. All dithering positions were combined into a master cube. The full width at half maximum of the spatial PSF (measured on the white-light image) is about 0.8 arcseconds and shows little variation over the field of view. Compared to the seeing conditions during the observations (seeing between 0.8 and 1.6 arcseconds) the Ground Layer Adaptive Optics correction (GLAO) provided a significant improvement.

The spectra (Figure 4) were extracted over 2 × 2 spaxels and normalised to the continuum. Stars 1 and 2 are red/yellow and blue supergiants, with $V \sim 13.5$; stars 3 and 4 are fainter cluster members ($V \sim 16.5$) with star 4 showing double-peak Balmer emission reminiscent of Be-star features. MUSE gathered spectroscopy of hundreds of massive stars in less than one hour of observation.

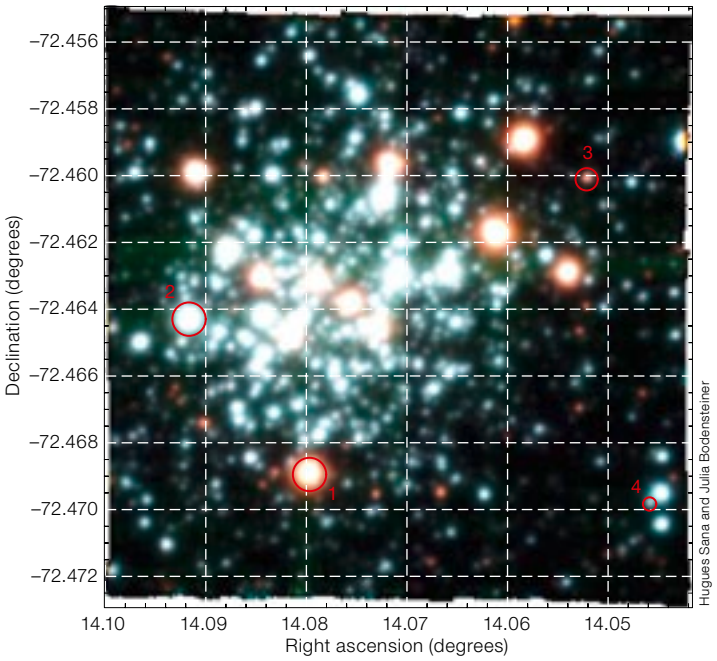

Figure 3. True-colour image of NGC 330. Spectra of the labelled stars are shown in Figure 4.

Starbursts

Extended starbursts in dwarf galaxies affect their hosts dramatically. Feedback from massive stars into the interstellar medium determines how the galaxy will form stars in the future and whether star formation will stop completely. Previous VIsible Multi-Object Spectrograph (VIMOS) observations indicate that in Haro 14, a blue compact galaxy, new star formation is triggered by shock waves created by stellar winds and supernovae from a previous epoch. Emission-line images reveal the location and progress of star formation.

Haro 14 is an excellent laboratory to investigate the star formation and feedback processes in dwarf galaxies. The central regions contain two temporally and spatially distinct episodes of star formation with ages of approximately 6 Myr

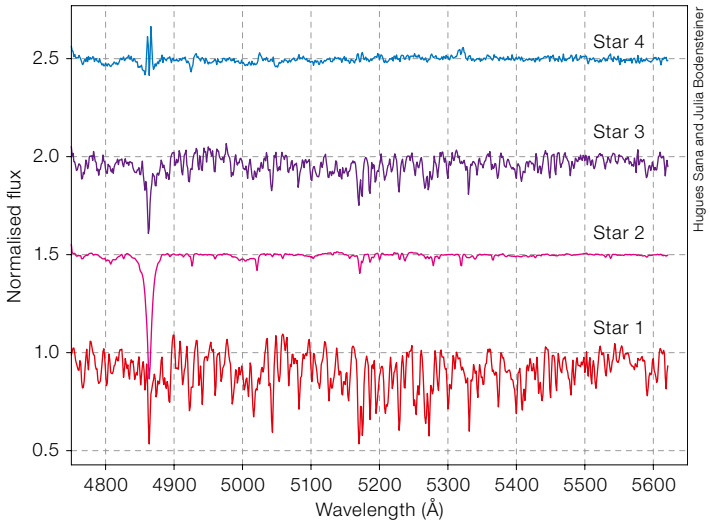

Figure 4. (Above) Spectra of four stars in NGC 330.

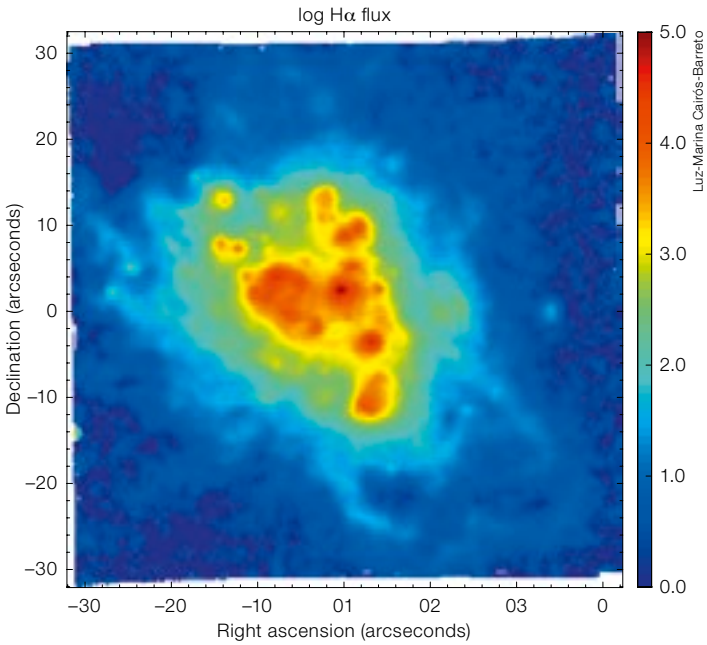

Figure 5. (Right) Hα emission in the compact blue dwarf galaxy Haro 14.

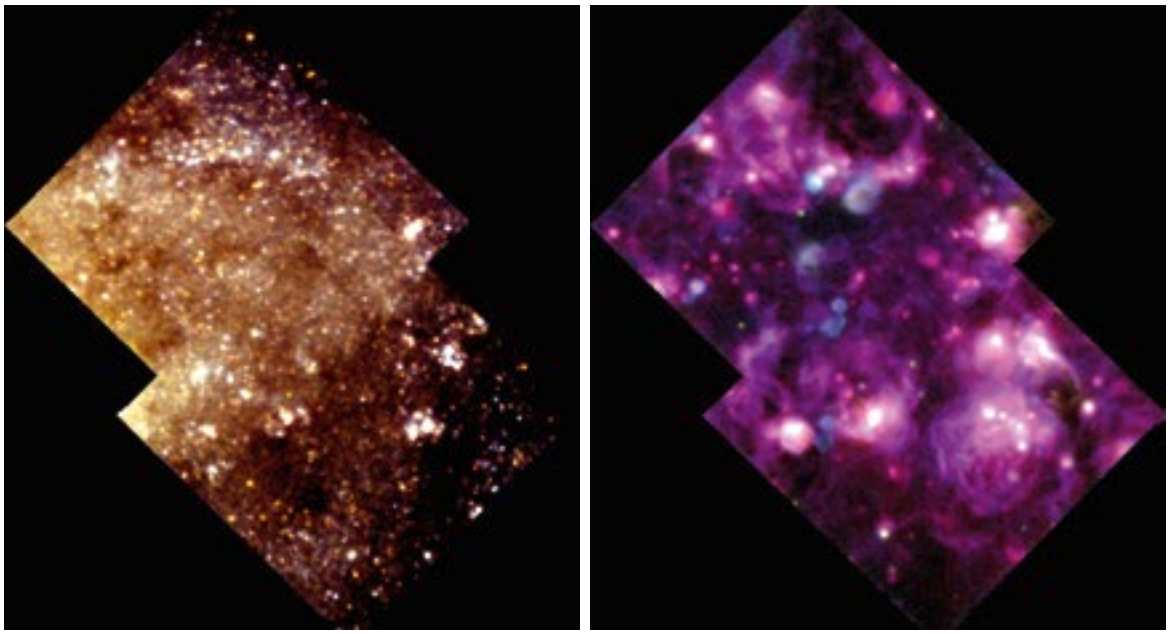

Angela Adamo and Michele Fumagalli

Figure 6. Continuum image (left) and emission-line image (right) of NGC 7793 from the same MUSE data cube Each pointing shows the full MUSE field (1 × 1 arcminutes across).

and 10–30 Myr. The VIMOS data also reveal a horseshoe-like structure — most probably a superbubble — as well as numerous filaments of ionised gas and many faint knots close to the superbubble and filaments. MUSE AO-corrected data (Figure 5) are essential to resolve the interaction of stars and gas in the new sites of star formation (i.e., in the walls of the shell-like and bubble structures), to follow the ionised gas filaments to larger distances (between 0.8 kpc and 2 kpc), and to investigate the fate of the outflows (super-winds) in the galaxy.

Tracing star formation at galactic scales

Stellar feedback can also be observed through the emission lines tracing star formation. The most prominent lines at optical wavelengths are Hα, [O III] and [S II], which trace different temperatures and densities in the interstellar medium. Compared to the distribution of stars, these emission sites provide insight into the interactions of stellar radiation and winds with the interstellar medium. Combined with the cold molecular gas measured with the Atacama Large Millimeter/submillimeter Array (ALMA), a complete picture of the state of the interstellar matter in a galaxy can be traced.

The nearby spiral galaxy NGC 7793 was observed during MUSE WFM AO SV. The nuclear star cluster of the galaxy was used as the AO tip-tilt star. The image quality on the final MUSE cubes is ~0.6 arcseconds (with small variations in the blue and red part of the spectral range), which — at the galaxy's distance of 3.5 Mpc — corresponds to a physical size of only 10 pc. NGC 7793 is classified as an Sd spiral.

The left-hand image of Figure 6 is a three-colour composite of the stellar continuum of the galaxy at ~4900 Å (blue), at ~6300 Å (green), and at ~7000 Å (red), extracted from the final MUSE data. In the continuum light, the young and more clustered stellar population and the diffuse field stellar population can be clearly distinguished. Dust lines are visible and trace the flocculent spiral arms. The right-hand image of Figure 6 is a three colour composite of emission lines. Hα emission is shown in the red channel, while [S II] 6717 Å and [O III] 5007 Å are in the blue and green channels, respectively.

Ionised gas fills the entire field of view, showing the effect of stellar feedback on the galactic interstellar medium. The [O III] emission is high within each H II region (white regions embedded in magenta filamentary structures), tracing massive, short-lived stars. The gradual change from bright pink to dark magenta filaments shows the optically-thick irregular boundaries of both giant and compact H II regions (Adamo et al., in preparation). The purple diffuse regions, bright in [S II] and [O III] but not in Hα, show the location of supernova remnants.

As part of the Hubble Treasury programme Legacy ExtraGalactic UV Survey (LEGUS[4]; Calzetti et al., 2015), detailed information on the young star cluster population and field stellar population of NGC 7793 exist (Adamo et al., 2017 & Sacchi et al., in preparation). Molecular gas at physical scales (~15 pc) has been mapped with ALMA, and giant molecular clouds with masses significantly above $10^5\ M_\odot$ have been detected (Bittle et al., in preparation). The full star formation lifecycle — from the emergence of dense gas from galactic-scale flows, to stellar birth, to subsequent feedback on small (below 10 pc) and large (kpc) scales — can be traced by combining the various datasets.

Gas around galaxies

One of the key questions in galaxy evolution is the interaction between galaxies and their immediate surrounding gas, called the circumgalactic medium (CGM). Observing the faint gas in emission is very challenging. A powerful alternative to study circumgalactic gas is to observe absorption lines in background quasar spectra. In the case of galaxy lenses, the different images of the quasar probe different sight lines around the lensing galaxy and hence the gas distribution can be observed in absorption. Since galaxy

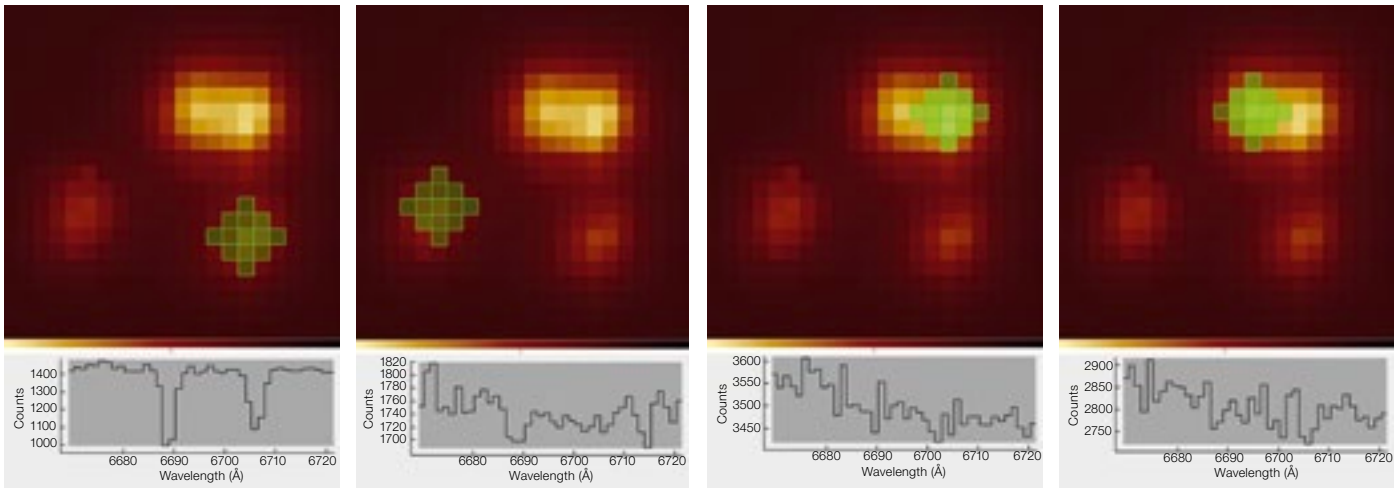

Figure 7. Four images of a lensed quasar, these are approximately 5 x 5 arcseconds in size. Spectra extracted from the green area are shown underneath each image.

lenses typically provide only a small separation between the quasar images, improved image quality is a big plus. Four lines of sight, with the smallest separation being only 0.7 arcseconds, were used to constrain the spatial distribution and homogeneity of the gas content around the massive foreground galaxy.

Figure 7 shows some of the first results from these observations. The yellow patches show the four images of the lensed quasar; the green marker indicates the area of the spectrum extraction shown on the bottom. The lensing galaxy in the centre of the four quasar images is not visible. Ca II H and K absorption at the redshift of the lensing galaxy (z = 0.661) can be seen towards one of the quasar images (left panel) and not towards the other three. This asymmetry in the Ca II distribution might indicate gas flows on scales of 7–13 kpc or smaller.

Galaxy clusters

Galaxy clusters at high redshift (z > 1) differ from clusters in the local Universe. High-redshift clusters contain a population of star-forming galaxies at their cores, while nearby clusters are dominated by old passive galaxies. This new population at high redshift has recently been detected through millimetre observations with ALMA. It is of great interest to study the internal dynamics of these galaxies, requiring observations of a cluster core to be made with the highest possible angular resolution.

Stach et al. (2017) identified ultra/luminous infrared galaxies (U/LIRGS) from their ALMA 1.2-millimetre continuum emission. MUSE WFM AO SV observations of the z = 1.46 cluster (Figure 8) confirm [O II] 3727 Å emission from several sources. This cluster was selected for study from a SCUBA-2 870 μm survey of high redshift clusters due to the strong overdensity of submillimetre sources in the cluster centre. Stach et al. (2017) used ALMA to resolve the four sources seen in the low-resolution SCUBA-2 map of this field into thirteen individual millimetre-bright galaxies, of which at least eleven are spectroscopically confirmed as members of the cluster from the ALMA and MUSE observations. The U/LIRGs with molecular emission lines detected in the ALMA 1.2-mm or 3-mm data cubes, corresponding to CO(2-1) or CO(5-4) at the cluster redshifts, are labelled with "CO". This significant overdensity of luminous starburst galaxies in this cluster shows a reversal of the star-formation rate-density trend seen in the local Universe, where dense environments are less active than the surrounding low-density field. This has been predicted by theoretical models

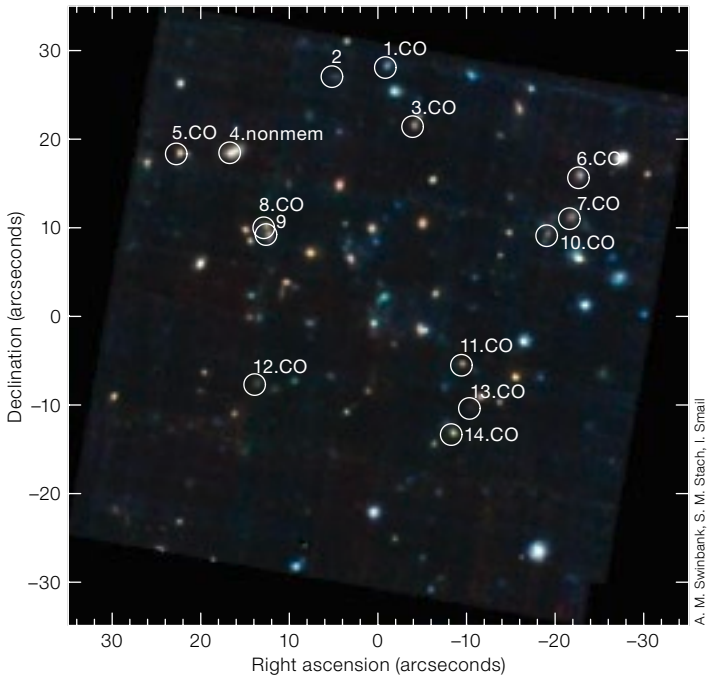

Figure 8. True-colour image of the cluster XCS2215-1738. Counterparts of ALMA sources are marked.

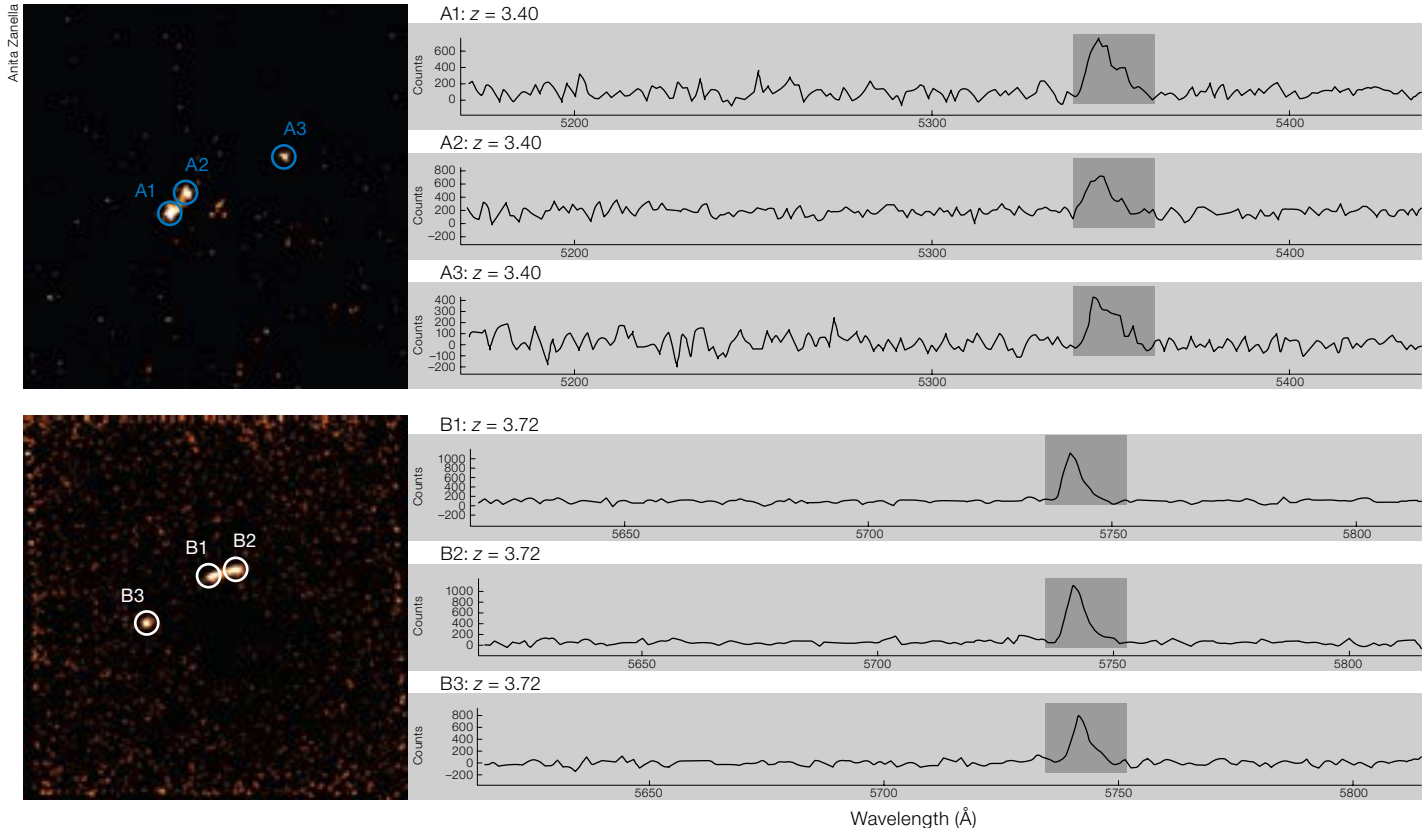

Figure 9. Lyα emission in lensed, high-redshift galaxies; the images are cutouts from a full MUSE field. Lyα spectra for the marked sources are shown on the right.

that couple the formation and evolution of galaxies with the growth of the structures they inhabit. The ALMA and MUSE data shown here are published in Stach et al. (2017).

High-redshift galaxies

During the most active phase of star formation in the Universe (between $z = 1$ to $z = 3$), galaxies display a clumpy structure. Star formation appears to proceed in large regions (up to 2 kpc) but the role of these star formation regions in the evolution of the host remains unclear. By observing lensed galaxies, the individual clumps can be isolated and the shape of the Lyα line provides insight into the influence of such regions on the host. If the star-forming regions are disrupted quickly then they will not change the overall structure of the galaxy, but with significant lifetimes they will strongly alter the history of the host. The MUSE WFM AO SV observations of two lensed galaxies behind Abell 2895 provide information on the gas outflow rates and hence the expected lifetime of the clumps. Lyα images of the clumps and the shape of the Lyα lines are shown in Figure 9.

Prospects

The first MUSE ground-layer adaptive optics observations presented here demonstrate the great potential of this instrument mode. The improvement in image quality over the 1 × 1 arcminute field provides a capability that is not available anywhere else. The preliminary scientific results presented here are testimony to the wide range of science topics that can be addressed with the MUSE WFM supported by adaptive optics. The MUSE narrow-field mode still needs to be commissioned and promises a higher AO correction, albeit on a smaller field in the red. The Science Verification for this mode is planned for August 2018.

Acknowledgements

We received excellent support at the telescope from the Telescope and Instrument Operators Claudia Reyes, Diego Parraguez and Israel Blanchard. Pascale Hibon was the operations support scientist during the observing nights. Anita Zanella and Bin Yan supported us at the telescope as the night astronomers. We would like to thank the following PIs who kindly provided the preliminary SV results presented in this article: Hugues Sana and Julia Bodensteiner, Luz Marina Cairós-Barreto, Angela Adamo and Michele Fumagalli, Ramona Augustin, Anita Zanella, Ian Smail, Stuart Stark and Mark Swinbank.

References

Adamo, A. et al. 2017, ApJ, 841, 131
Arsenault, R. et al. 2017, Messenger, 164, 2
Bacon, R. et al. 2010, SPIE, 7735, 7
Calzetti, D. et al. 2015, AJ, 149, 51
Evans, C. J. et al. 2006, A&A, 456, 623
Martayan, C. et al. 2007a, A&A, 462, 683
Martayan, C. et al. 2007b, A&A, 472, 577
Sirianni, M. et al. 2002, ApJ, 579, 275
Stach, S. M. et al. 2017, ApJ, 849, 154

Links

[1] Announcement of MUSE WFM AO SV call for proposals: http://www.eso.org/sci/publications/announcements/sciann17034.html
[2] May 2017 ESO science newsletter: http://www.eso.org/sci/publications/newsletter/may2017.html
[3] MUSE WFM AO SV webpage: http://www.eso.org/sci/activities/vltsv/musesv.html
[4] LEGUS survey webpage: https://legus.stsci.edu

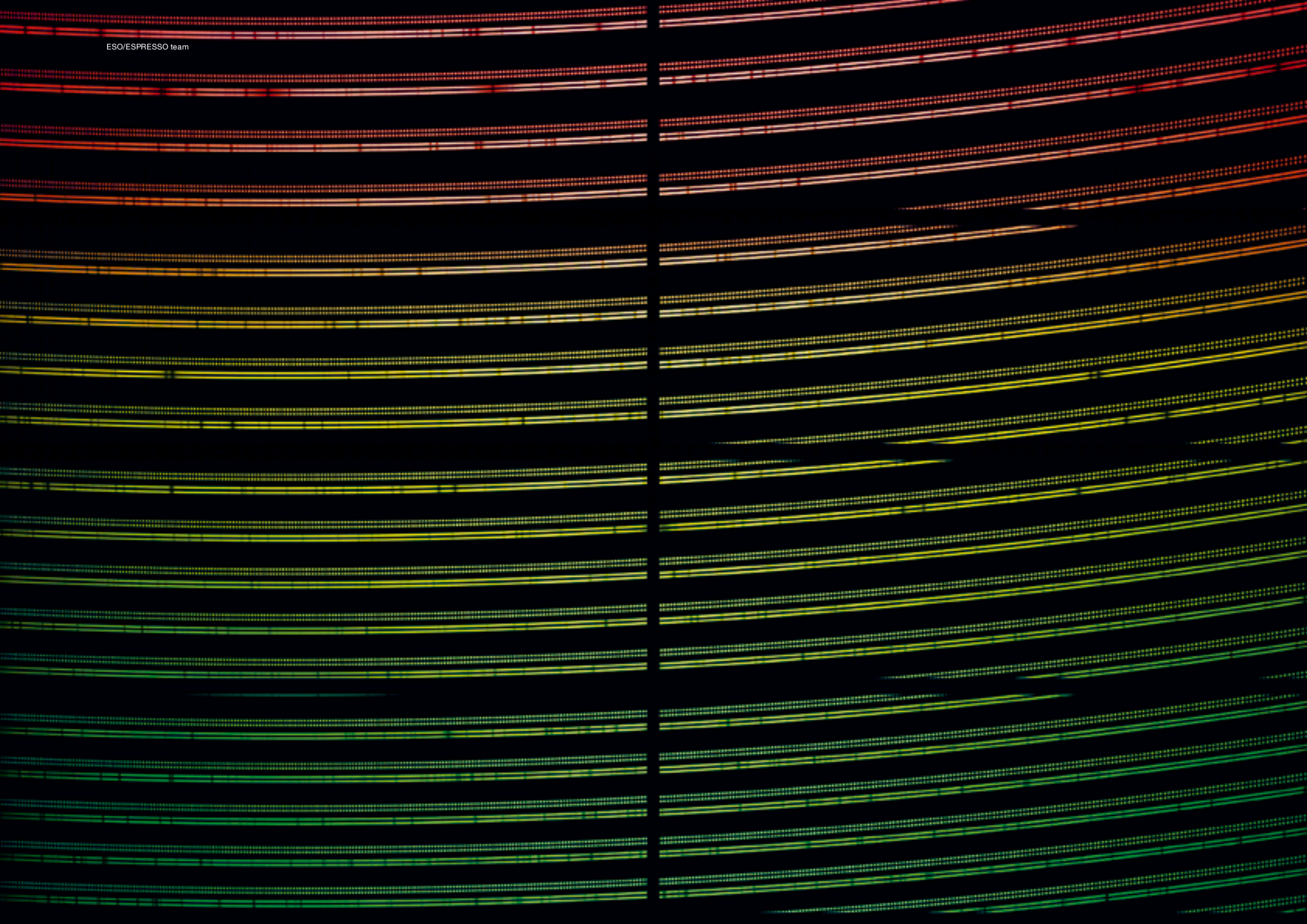
ESO/ESPRESSO team

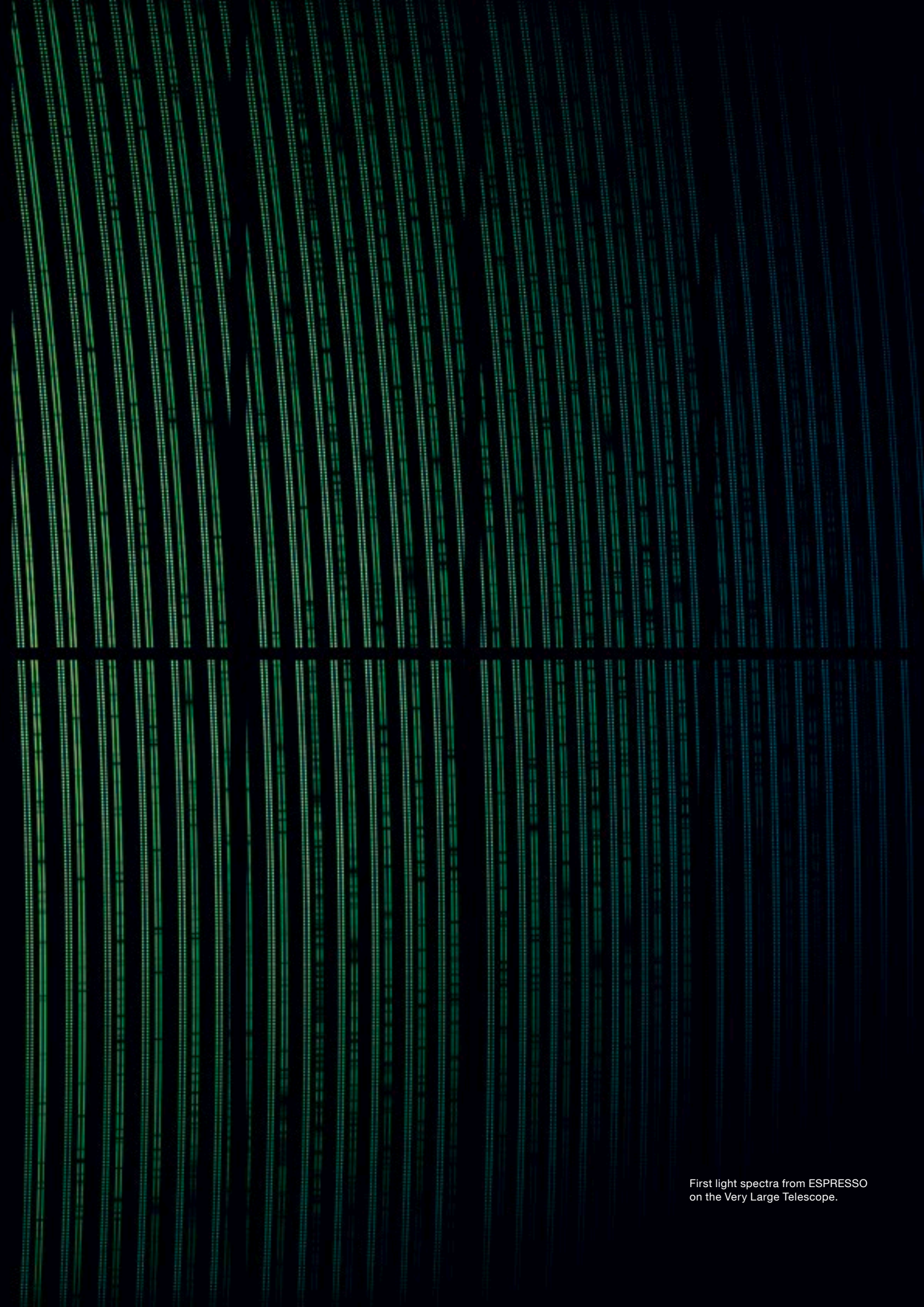

First light spectra from ESPRESSO on the Very Large Telescope.

Marco Gullieuszik 2017

A gallery of 50 galaxies observed by MUSE as part of the GASP project: RGB-band images (*g*, *r* and *z* filters, top) and the corresponding Hα emission intensity maps (bottom).

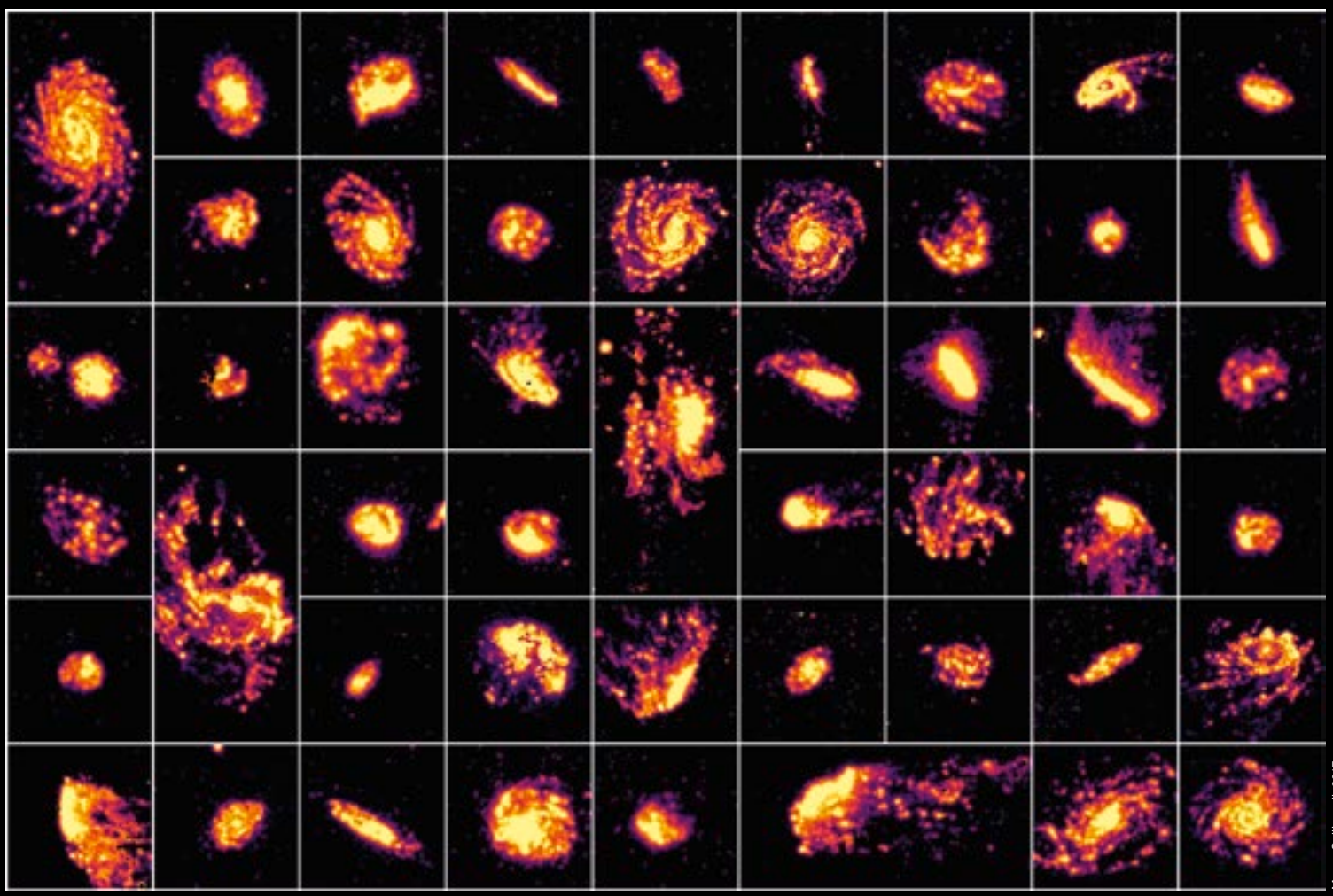

Marco Gullieuszik 2017

DOI: 10.18727/0722-6691/5051

Tales of Tails: Gas Stripping Phenomena in Galaxies with MUSE

Bianca M. Poggianti[1]
Marco Gullieuszik[1]
Alessia Moretti[1]
Yara L. Jaffé[2]
Jacopo Fritz[3]
Benedetta Vulcani[1,4]
Daniela Bettoni[1]
Callum Bellhouse[2,5]
Giovanni Fasano[1]
Mario Radovich[1]
& the GASP collaboration*

[1] INAF–Astronomical Observatory of Padova, Italy
[2] ESO
[3] Instituto de Radioastronomía y Astrofísica, UNAM, Morelia, Mexico
[4] University of Melbourne, Australia
[5] University of Birmingham, United Kingdom
[6] Specola Vaticana, Vatican State, Italy
[7] Center for Computational Astrophysics, Flatiron Institute, New York, USA
[8] University of Padova, Italy
[9] INAF–Astronomical Observatory of Trieste, Italy
[10] INAF–Istituto di Radioastronomia, Bologna, Italy
[11] Indian Institute of Astrophysics, Bangalore, India
[12] University of Innsbruck, Austria
[13] Université de Genève, Switzerland
[14] Macquarie University, Sydney, Australia
[15] Australian Astronomical Observatory, Sydney, Australia

The MUSE spectrograph is observing a sample of over 100 galaxies at z = 0.04–0.07 in order to investigate how environmental effects can cause galaxies to lose their gas. These galaxies have a wide range of galaxy stellar masses and environments, from clusters and groups to isolated galaxies, and have been selected because they show unilateral debris or tails suggestive of gas stripping. MUSE's large field of view, sensitivity, and spatial and spectral resolution allow us to study the physics of the stars and ionised gas in each galaxy in great detail, including the outskirts and extraplanar tails or debris out to 50–100 kpc away from each galaxy: a distance of more than ten times the galaxy's effective radius. We present the ongoing programme, GAs Stripping Phenomena in galaxies (GASP), and report on the first set of results.

* Alessandro Omizzolo[1,6], George Hau[2], Stephanie Tonnesen[7], Mauro D'Onofrio[8], Andrea Biviano[9], Sean McGee[5], Rosita Paladino[10], Koshy George[11], Michela Mapelli[1,12], Jan Bischko[12], Antonio Cava[13], Matt Owers[14], Warrick Couch[15]

Gas removal and galaxy evolution

A central question in galaxy formation and evolution is how gas flows in and out of galaxies. In the current hierarchical paradigm, the hot gas in dark matter halos cools and settles in the galactic disc, replenishing the cold gas reservoir necessary to form new stars. Any process that prevents the gas from cooling efficiently, or that removes gas from either the halo or the disc, has fundamental consequences for galaxy evolution. It is therefore of paramount importance to directly observe gas outflow and infall processes at work. Integral field spectrographs such as the Multi Unit Spectroscopic Explorer (MUSE) on the Very Large Telescope (VLT) can use both optical emission lines and light from stars to probe gas that is ionised by star formation, an active galactic nucleus (AGN), or shocks. Such observations can yield clues into stellar kinematics and star formation history.

Ram pressure stripping is believed to be an efficient mechanism to remove gas from a galaxy, affecting only the interstellar gas and not the stars. When a galaxy moves through a hot, dense intergalactic medium, the latter exerts pressure on the gas of the galaxy and can remove it from the disc and halo. The efficiency of this mechanism depends on the density of the intergalactic medium and the relative galaxy velocity. Ram pressure stripping therefore acts most strongly in galaxy clusters, but it has also been observed in galaxy groups and even pairs.

The GASP project

GASP (GAs Stripping Phenomena in galaxies with MUSE) is an ongoing ESO Large Programme studying gas removal processes in galaxies[1]. GASP is observing 114 galaxies at z = 0.04–0.07 in clusters, groups and the field, targeting 94 galaxies with optical signatures of unilateral debris or tails reminiscent of gas stripping processes, as well as a control sample of 20 disc galaxies with no morphological anomalies. The survey characteristics and strategy were presented in Poggianti et al. (2017a). The most important characteristic of the survey is its large coverage in area. At z = 0.04–0.07 the MUSE field of view covers 50–80 kpc and so it is possible to study extraplanar gas and stars out to large distances from the galactic disc using only one or two MUSE pointings.

The main goal of GASP is to study gas stripping in different environmental conditions in order to understand how, why and when gas is removed. We want to investigate the fraction of galaxies, the masses of the galaxies and their host halos, as well as the orbits, velocities and halo-centric distances for which gas-only removal processes are relevant.

The link between gas and star formation is another fundamental focus of the GASP programme. Overall, the star formation activity in galaxies has strongly declined since $z \sim 2$ owing to the combination of two effects: a large number of star-forming galaxies have evolved into passive galaxies where star formation has ceased, and the average rate of star formation has decreased in galaxies that are still producing stars. To understand the decline in star formation and the impact of gas removal processes on this galaxy quenching, it is crucial to study how gas stripping affects the stellar history in the GASP galaxies. The MUSE data reveal whether the star formation activity is globally enhanced or suppressed during the stripping, as well as how the quenching of star formation proceeds within each galaxy and over what timescales.

Tales of tails

MUSE observations began in 2015 (ESO Period 96) with a sample of cluster galaxies. From these data we obtained a wide range of diagnostics including: spatially resolved morphologies and kinematics of gas and stars, gas metallicity and ionisation parameters, gas densities and masses, dust extinction, star formation densities, stellar mass densities,

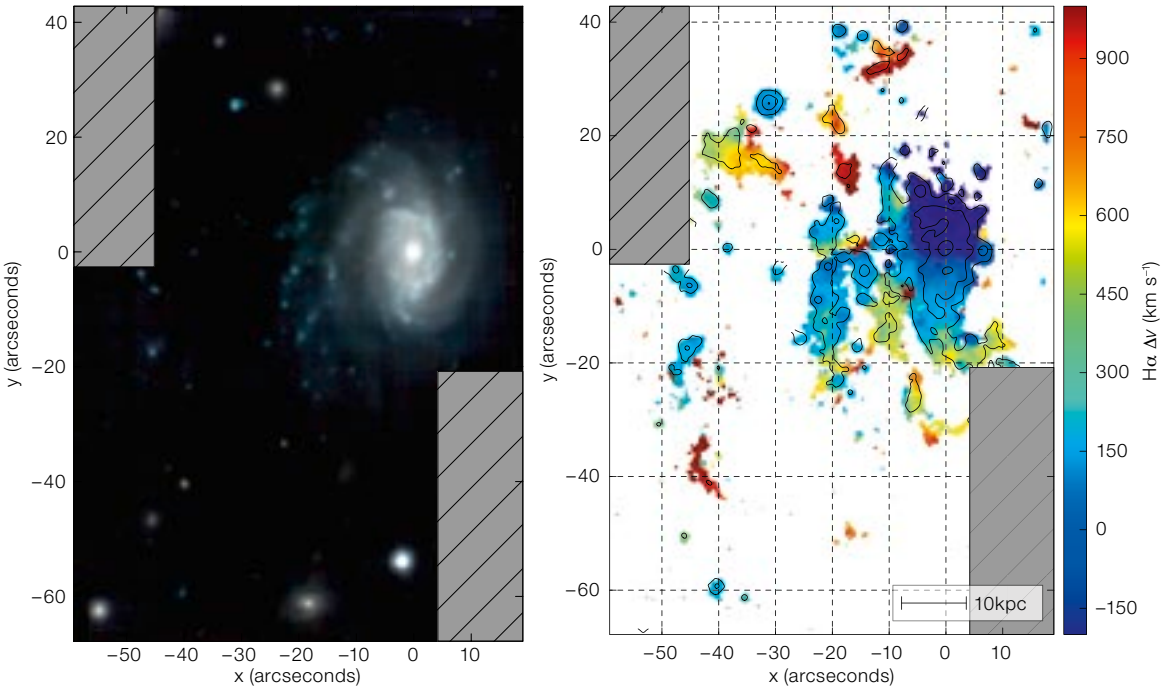

Figure 1. The GASP galaxy JO201, one of the most spectacular cases of ram pressure stripping, was studied using two MUSE pointings. It is crossing the massive cluster A85 at supersonic speed, moving towards the observer along the line of sight, and has lost 50 % of its total gas mass so far. Left: RGB (5000–6000 Å; 6000–7000 Å; 7000–8000 Å) MUSE image. Right: Hα velocity map, showing the complex velocity structure of the gas, which includes rotation in the disc, and a high velocity (> 200 km s^{-1}) component that corresponds to stripped gas dragging behind the galaxy (Bellhouse et al., 2017).

ionisation mechanisms, luminosity-weighted stellar ages, and star formation history. These quantities trace each galaxy's history in detail and can reveal the mechanisms that drive gas removal.

By design, the evidence for gas stripping in the GASP targets varies significantly. Some targets have long tails that are visible even in broadband optical images, while others contain only subtle indications of initial or mild stripping (see Poggianti et al., 2016 for the classification). Some of the most striking examples of ram pressure stripping in action have been presented in dedicated individual publications (Poggianti et al., 2017a; Bellhouse et al., 2017; Fritz et al., 2017; Gullieuszik et al., 2017; Moretti et al., 2017).

Common features in the GASP galaxies

The tails are much more prominent in Hα emission than in the optical and can extend out to over 100 kpc from the galactic disc (see p. 28, Figures 1 and 3). The stripped gas is ionised through stellar photoionisation due to ongoing star formation within the stripped gas. The gas tails are characterised both by regions of diffuse Hα emission and kinematically cold knots that are bright in Hα; these cold knots are identified as giant H II regions and complexes. A significant fraction of the total star formation related to each system takes place outside of the disc.

The morphology and kinematics of the gas are consistent with ram pressure stripping, and we can estimate the fraction of gas lost before the epoch of observation by considering both the extent of Hα within the disc and the increasing ram pressure as the galaxy infalls into the cluster. A comparison of gas and stellar kinematics shows that the latter is totally undisturbed, which was expected as ram pressure only affects the gas. The gas retains the velocity of the stars at the location of the disc from which it was stripped and continues to rotate coherently with the galaxy until several kiloparsecs away from the main galaxy body.

The stripping proceeds from the outside in, with the outermost regions of the disc stripped first (Figures 2 and 3). Clear post-starburst signatures are left in the regions of the disc that have recently been stripped, while strong star formation continues within the remaining gas and especially where the gas is compressed. From the MUSE data we can reconstruct the history of star formation in broad, logarithmically-spaced age bins, and observe where stars formed in each epoch at each location (Figure 3).

While it is commonly believed that ram pressure stripping is efficient only in low-mass galaxies and in the most massive clusters, we find extreme ram pressure stripping even in massive galaxies (10^{11} $M_{\odot}$) and in relatively low-mass clusters (with velocity dispersions of 500–600 km s^{-1}). The galaxies possessing the longest tails are at their first infall into the cluster and they are located at low projected cluster-centric radii and high velocities relative to the cluster redshift: the optimal conditions for ram pressure stripping. Our results are in agreement both with the standard analytic scenario of ram pressure stripping (Gunn & Gott, 1972), and detailed hydrodynamic simulations of galaxies falling into clusters, which show long tails of stripped material with the correct conditions for star formation (Tonnesen & Bryan, 2012). These findings are consistent with a fast-acting mechanism that significantly alters the gas content of galaxies on their first passage through the dense intergalactic medium (Jaffé et al., 2017).

Ram pressure and AGN

The mechanism responsible for the gas ionisation at any point in each galaxy can be assessed from spatially-resolved diagnostic diagrams of emission line

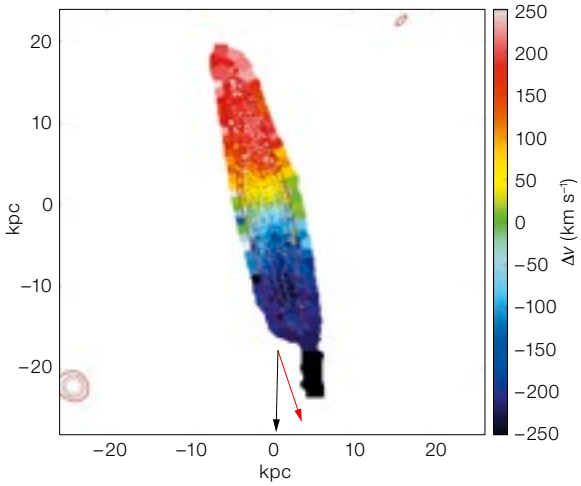

Figure 2. The GASP sample comprises a number of galaxies with truncated Hα discs. The gas stripping proceeds from the outside in, and the gas has already been removed from the outer disc regions in these objects. JO36 is an example of this (Fritz et al., 2017) and its stellar velocity map (left) is more extended than the map of the Hα-emitting gas (right). JO36 experienced a burst of star formation between 20 and 500 Myr ago in the outer regions of the disc, which are now devoid of gas and passively evolving. The inner disc is still gas-rich and forming stars, and X-ray data indicate the presence of a deeply obscured AGN that is hidden at optical wavelengths.

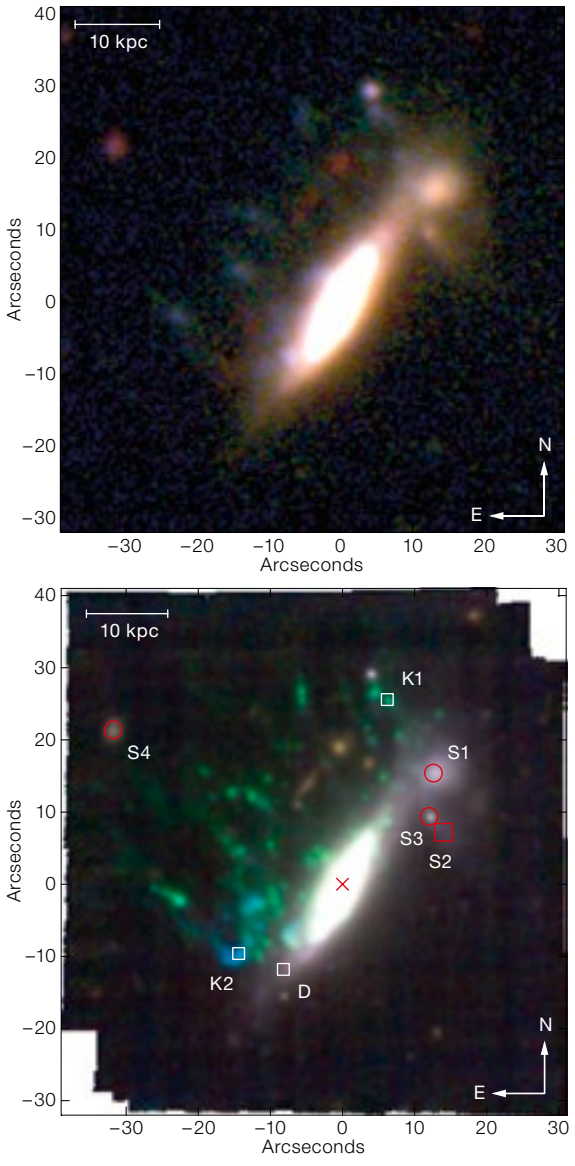

Figure 3. JO204 is seen almost edge-on while falling into a cluster approximately along the plane of the sky. Left: RGB and [OIII], Hα and continuum images of J0204. The RGB (*uBV*) image in the top left shows faint traces of tails to the left of the disc, while in the bottom left panel a composite [OIII] 5007 Å (blue), Hα (green) and 7100–7200 Å continuum (red) image displays the striking tails of ionised gas (Gullieuszik et al., 2017). Below: This set of four figures shows the star formation rate in four age bins at each spatial location. Star formation was confined to the stellar disc until less than 600 Myr ago (two bottom panels), then the first extraplanar stars were formed in the stripped gas between 20 and 600 Myr ago while new stars were also forming everywhere in the disc (top right). At the time of the observations, ongoing star formation (< 20 Myr) is taking place throughout the tails and in the central part of the disc (top left).

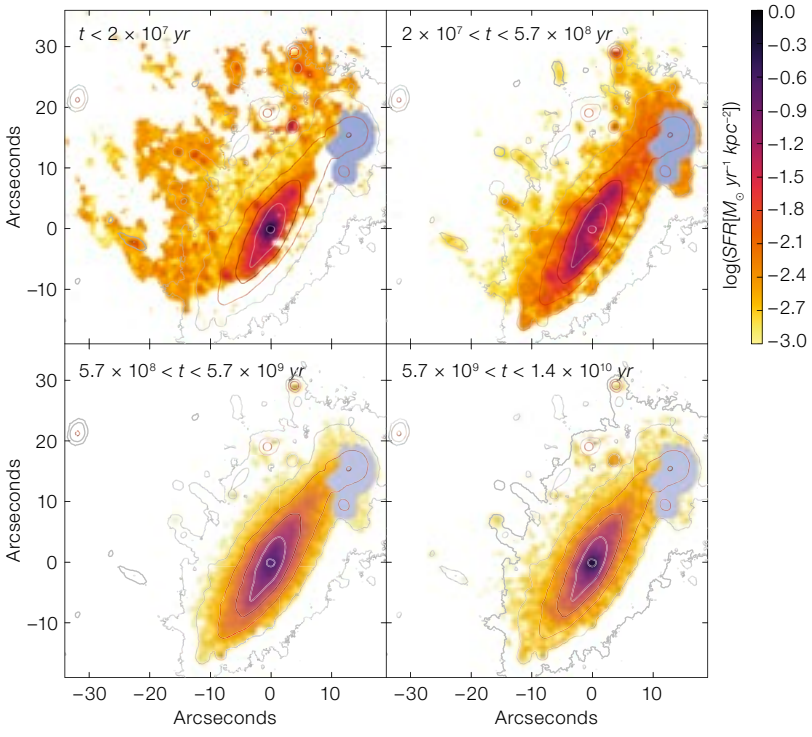

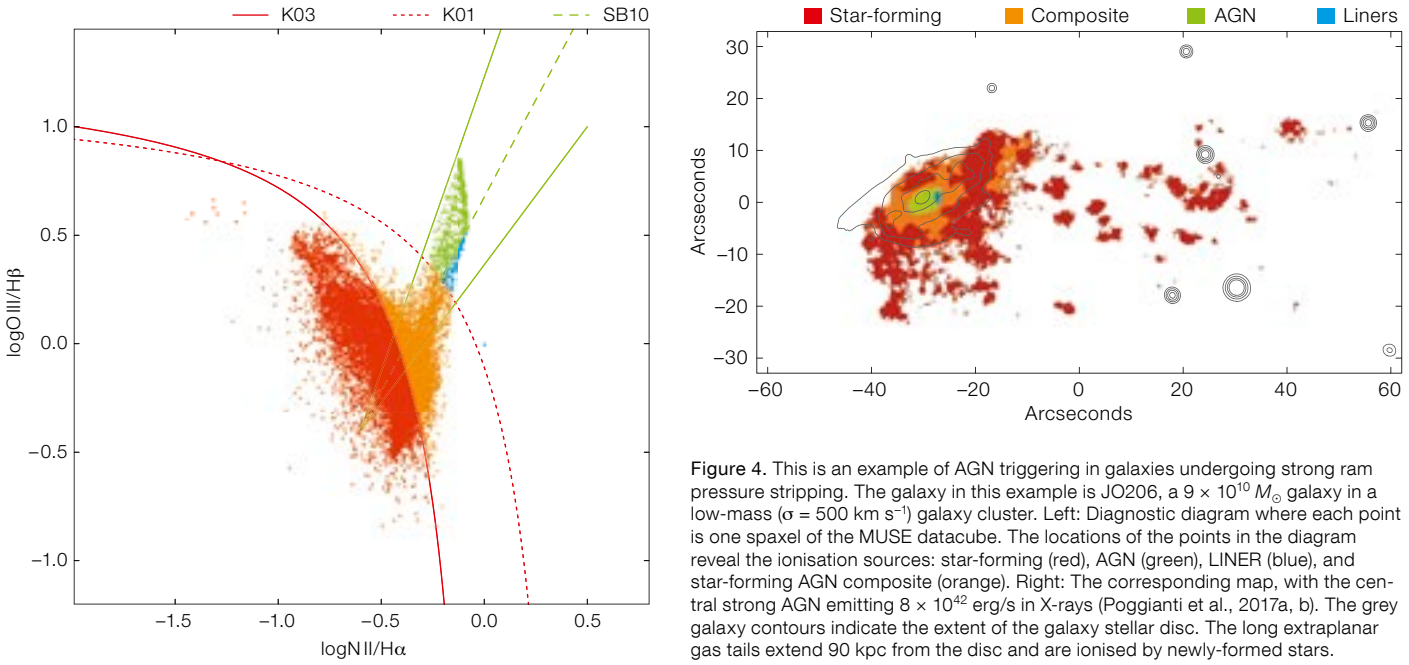

Figure 4. This is an example of AGN triggering in galaxies undergoing strong ram pressure stripping. The galaxy in this example is JO206, a 9 × 10^{10} $M_{\odot}$ galaxy in a low-mass (σ = 500 km s^{-1}) galaxy cluster. Left: Diagnostic diagram where each point is one spaxel of the MUSE datacube. The locations of the points in the diagram reveal the ionisation sources: star-forming (red), AGN (green), LINER (blue), and star-forming AGN composite (orange). Right: The corresponding map, with the central strong AGN emitting 8 × 10^{42} erg/s in X-rays (Poggianti et al., 2017a, b). The grey galaxy contours indicate the extent of the galaxy stellar disc. The long extraplanar gas tails extend 90 kpc from the disc and are ionised by newly-formed stars.

ratios as measured from MUSE spectra (Figure 4). As GASP data began to pour in, one of the first unexpected results was the high incidence of AGN in the galaxies undergoing the strongest stripping: six out of seven galaxies with the most spectacular tails host a central AGN. Five of these display typical Seyfert 2 emission line ratios and one is a low-ionisation nuclear emission-line region (LINER) powered by a low-luminosity AGN, which was confirmed by data from the Chandra X-ray Observatory. Although the sample is still too small to draw definitive statistical conclusions, this fraction is surprisingly high compared to the low occurrence of AGN activity among emission line galaxies in clusters (3 %) and the general field (8 %) at similar redshifts.

This "AGN excess" may result from ram pressure causing gas to flow towards the galaxy centre, or from an enhancement in the stripping strength due to energy injection from the AGN, or both. The proximity of the sample galaxies to the cluster core and their high relative speeds strongly support the hypothesis that ram pressure triggers AGN activity and not *vice versa*. How this occurs is still unknown, as simulations of ram pressure in the presence of an AGN do not yet exist. However, hydrodynamic simulations have shown that when gas in a galaxy disc interacts with a non-rotating intracluster medium, it loses angular momen-

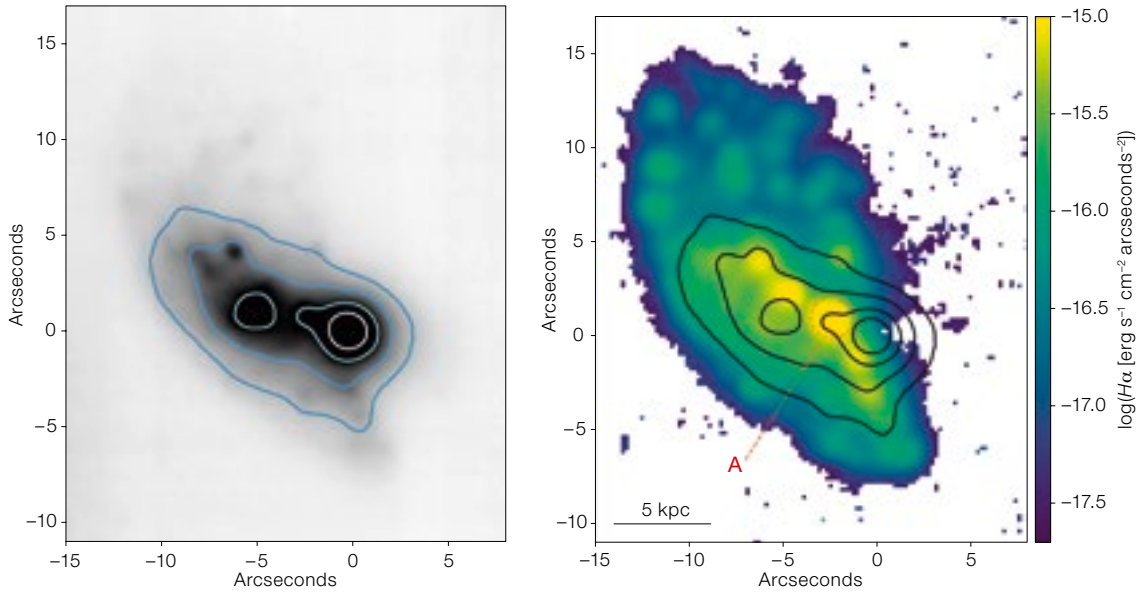

Figure 5. P96949 is the only merger found in the GASP sample so far. A late-type galaxy is merging with an early-type galaxy of similar mass (~ 10^{10} $M_{\odot}$), inducing high levels of star formation activity and the formation of a tidal dwarf galaxy in the compression zone between the two galactic nuclei. In the MUSE white-light image (left), the two galaxy centres are visible as the two peaks in the stellar light contours. The Hα intensity map (right) shows the regions of enhanced star formation. The forming dwarf galaxy is enclosed by the red dotted circle (Vulcani et al., 2017b).

tum and can therefore spiral into the galaxy's central region. Oblique shocks in a flared galaxy disc might also play a role.

These results put forward ram pressure as a possible, albeit as yet unknown, mechanism for feeding the central supermassive black hole of an AGN with gas (Poggianti et al., 2017b; ESO Release eso1725[2]). A complete census of AGN activity among galaxies in different stages of gas stripping, from initial stripping to peak and post stripping, must await the completion of the survey.

Ongoing work, data release and prospects

At the time of writing, three quarters of the GASP data have been taken. The first ESO GASP data release was published on 26 October 2017 and is accessible from the ESO archive[3]. As observations approach completion, we will finish the statistical analysis of the GASP sample and begin to address more general questions including:

– What is the amount of stars contributed by the stripping to the intracluster light and what are their metallicities?
– What is the amount and metallicity of the stripped gas?
– What are the characteristics of the star formation activity happening outside galaxy discs?
– What are the common features in gas stripping phenomena, when do the long tails form and how long do they last?
– And finally, how many galaxies undergo gas stripping depending on environment, and by what mechanism?

While observations of our group and field sample are still ongoing, our preliminary analysis shows that various phenomena can give rise to optical morphologies resembling gas stripping. Among the galaxies analysed so far there are good candidates of stripping in groups, low-mass clusters and even filaments (Vulcani et al., in preparation). There is also an interesting case of likely gas accretion — instead of removal — onto an isolated galaxy (Vulcani et al., 2017a), and the only case so far of a merger in GASP (Vulcani et al., 2017b, Figure 5).

Multi-wavelength follow-up studies of GASP include: the Atacama Pathfinder EXperiment, APEX CO(2-1) observations (completed, Moretti et al., in preparation); Atacama Large Millimeter/submillimeter Array (ALMA) CO(2-1) and CO(1-0) observations, approved for ALMA Cycle 5; JVLA C-array HI imaging (completed); and ongoing far-ultraviolet and near-ultraviolet imaging using the Ultraviolet Imaging Telescope (UVIT) on Astrosat (George et al., in preparation). The combination of MUSE and ancillary data will provide a panoramic view of the stellar content and the ionised, neutral and molecular gas.

Acknowledgements

We are very grateful to the ESO staff at Paranal and Garching for carrying out and supporting this programme. Benedetta Vulcani acknowledges the support from an Australian Research Council Discovery Early Career Researcher Award (PD0028506). This work was co-funded under the Marie Curie Actions of the European Commission (FP7-COFUND).

References

Bellhouse, C. et al. 2017, ApJ, 844, 49
Fritz, J. et al. 2017, ApJ, 848, 132
Gunn, J. E. & Gott, J. R. 1972, ApJ, 176, 1
Gullieuszik, M. et al. 2017, ApJ, 846, 27
Jaffé, Y. L. et al. 2017, submitted to MNRAS
Moretti, A. et al. 2017, submitted to MNRAS
Poggianti, B. et al. 2016, AJ, 151, 78
Poggianti, B. et al. 2017a, ApJ, 844, 48
Poggianti, B. et al. 2017b, Nature, 548, 304
Tonnesen, S. & Bryan, G. L. 2012, MNRAS, 422, 1609
Vulcani, B. et al. 2017a, ApJ, in press
Vulcani, B. et al. 2017b, ApJ, 850, 163

Links

[1] The GASP website: http://web.oapd.inaf.it/gasp/index.html
[2] ESO Press Release: https://www.eso.org/public/news/eso1725/
[3] GASP's first data release: http://www.eso.org/sci/publications/announcements/sciann17080.html

ESO/GASP collaboration

MUSE observations of the galaxy JO206 from the GASP programme. Red shows the glow from ionised hydrogen and white shows where most of the stars are located.

DOI: 10.18727/0722-6691/5052

Unveiling the Nature of Giant Ellipticals and their Stellar Halos with the VST

Marilena Spavone[1]
Massimo Capaccioli[1,2]
Nicola R. Napolitano[1]
Enrichetta Iodice[1]
Aniello Grado[1]
Luca Limatola[1]
Andrew P. Cooper[3]
Michele Cantiello[4]
Duncan A. Forbes[5]
Maurizio Paolillo[2]
Pietro Schipani[1]

[1] INAF–Astronomical Observatory of Capodimonte, Italy
[2] University of Naples Federico II, Italy
[3] Institute for Computational Cosmology, Durham, United Kingdom
[4] INAF–Astronomical Observatory of Teramo, Italy
[5] Centre for Astrophysics & Supercomputing, Swinburne University, Australia

Observations of diffuse starlight in the outskirts of galaxies provide fundamental constraints on the cosmological context of galaxy assembly in the Lambda Cold Dark Matter model, which predicts that galaxies grow through a combination of *in-situ* star formation and accretion of stars from other galaxies. Accreted stars are expected to dominate in the outer parts of galaxies. Since dynamical timescales are longer in these regions, substructures related to accretion, such as streams and shells, can persist over many Gyr. In this work we use extremely deep *g*- and *i*-band images of six massive early-type galaxies (ETGs) from the VEGAS survey to constrain the properties of their accreted stellar components. The wide field of view of OmegaCAM on the VLT Survey Telescope (VST) also allows us to investigate the properties of small stellar systems (such as globular clusters, ultra-compact dwarfs and satellite galaxies) in the halos of our galaxies. By fitting light profiles, and comparing the results to simulations of elliptical galaxy assembly, we have identified signatures of a transition between relaxed and unrelaxed accreted components and can constrain the balance between *in-situ* and accreted stars.

Early-type galaxy stellar halos

The Lambda Cold Dark Matter (ΛCDM) galaxy formation theories predict that galaxies grow through a combination of *in-situ* star formation and accretion of stars from other galaxies. Accreted stars are expected to dominate in the outer parts of galaxies because they have much lower binding energies in the remnant system than stars formed by dissipative collapse. The structural properties of the outer parts of galaxies and their correlations with stellar mass and other observables might therefore provide ways of testing theoretical predictions of growth by accretion.

Cosmological simulations of galaxy formation predict trends in these quantities with mass that lead to systematic variations in the average shape, amplitude, and extent of azimuthally averaged surface brightness profiles (Cooper et al., 2013). Unfortunately, the accreted debris is also expected to have extremely low surface brightness (μ_v ~ 29 mag arcseconds^{-2}) on average and therefore to be very hard to separate from the background sky in conventional photometric observations. In theoretical models massive ETGs accumulate the bulk of their stellar mass by accretion, predominantly through about ten mergers of low stellar mass ratio (Cooper et al., 2015).

From an observational perspective, the connections between different mechanisms of mass growth and the "structural components" inferred from images of ETGs are not straightforward. If the bulk of the stars really are accreted, then the "stellar halo" should be identified with at least the structural component that dominates the observed stellar mass. However, other empirical components might also be accreted. *In-situ* stars in ETGs are extremely difficult to distinguish if they are also spheroidal and dispersion-supported and have old, metal-rich stellar populations resembling those of the dominant accreted component(s) with which they have been thoroughly mixed by violent relaxation.

Cosmological dynamical simulations can help by suggesting plausible interpretations for features in the surface brightness profiles of ETGs in the context of specific galaxy formation theories. In particular, simulated galaxies show evidence of substructure in the form of inflections or breaks, at which the surface brightness profile becomes either steeper or shallower (for example, Cooper et al., 2013; Rodriguez-Gomez et al., 2016). These inflections also correspond to variations in the ratio between individual accreted components as a function of radius. Most simulations predict that the transition between *in-situ* and accretion-dominated regions should be almost imperceptible in the azimuthally averaged profiles of typical ETGs.

Observational work has clearly identified features in ETG surface brightness profiles and kinematic distributions that are indicative of substructure in the accreted component (Bender et al., 2015). Some of these features occur at distances of many effective radii and hence at very low surface brightness, which could be interpreted as evidence for multiple accreted components in the context of the models mentioned above. Using different techniques with observations of different depths, several authors have concluded that the profiles of massive ETGs are not well described by a single Sérsic law component, once thought to be near universal for spheroidal galaxies, suggesting that three or more Sérsic components may be required for an accurate description of typical ETGs.

The VEGAS survey

The study of galaxy stellar halos, historically hampered by their faintness, has recently benefited from the new generation of very-wide-field imaging instruments. We are taking advantage of the wide field of view and high spatial resolution of the VLT Survey Telescope (VST) at ESO's Paranal Observatory to carry out a multi-band imaging survey of nearby ETGs, named VEGAS (VST Early-type GAlaxies Survey; Capaccioli et al., 2015). The large field of view of the OmegaCAM mounted on the VST (one square degree matched by pixels 0.21 arcseconds wide), together with its high efficiency and spatial resolution, allows us to map the surface brightness of a galaxy out to isophotes encircling about 95 % of the total light using a reasonable integration.

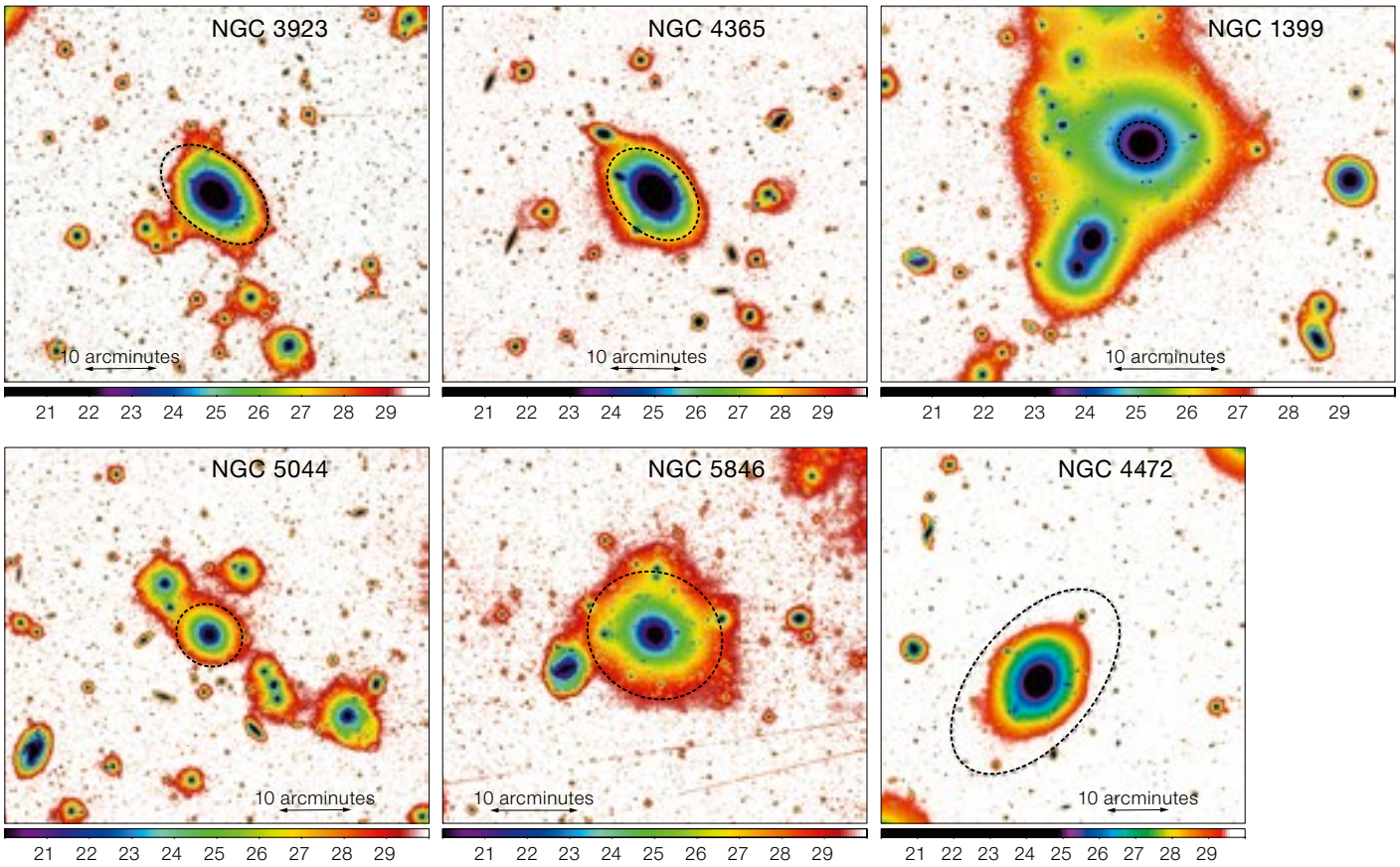

Figure 1. VST *g*-band sky-subtracted images of the galaxies analysed in this work. The colour scale represents surface brightness in mag arcseconds^{-2}. North is up, east is to the left. We point out that the stellar halos often extend even further than it is possible to visualise in these images, as shown by the profiles in Figure 3.

The main products of the VEGAS survey are: 1) a two-dimensional light distribution out to 8–10 effective radii (R_e), galaxy structural parameters and diffuse light component, inner substructures as a signature of recent cannibalism events; 2) radially-averaged surface brightness profiles and isophote shapes out to 10 R_e; 3) colour gradients and the connection with galaxy formation theories; 4) detection of external low-surface-brightness structures of the galaxies and the connection with the environment; and 5) a census of small stellar systems (globular clusters, ultra-compact dwarfs and galaxy satellites) out to ~ 20 R_e from the main galaxy centre and their photometric properties.

The data used in this work consist of exposures in *g* and *i* Sloan Digital Sky Survey bands obtained with VST and OmegaCAM, in both service and visitor mode, for the giant ETGs (Figure 1) NGC 3923, NGC 4365, NGC 5044 and NGC 5846, along with similar data on NGC 4472 and NGC 1399 (Capaccioli et al., 2015 and Iodice et al., 2016).

The data reduction procedure followed is described by Capaccioli et al. (2015) and Spavone et al. (2017). We adopted a "step-dither" observing strategy for galaxies with large angular extents, consisting of a cycle of short exposures centred on the target and on offset fields ($\Delta = \pm 1$ degree). With such a technique the background can be estimated from exposures taken as close as possible, in space and time, to the scientific images. This ensures better accuracy, reducing the uncertainties at very faint surface brightness levels.

Results

The isophotal analysis of the VEGAS galaxies is performed on the final mosaic in each band with the IRAF task ELLIPSE, which computes the intensity, $I(a,\theta)$, azimuthally sampled along an elliptical path described by an initial guess for the isophote centre (X,Y), ellipticity ε, and semi-major axis position angle θ at different semi-major axis lengths.

We find an increase in ellipticity in the outer regions of all the galaxies, indicating the presence of a more flattened outer component with a significant gradient in position angle. From the isophotal analysis we also extract very deep surface brightness profiles (μ_g ~ 30 mag arcseconds^{-2}). In the left panel of Figure 2 we plot these profiles as a function of galactocentric radius normalised to the effective radius R/R^e. This comparison shows that we have two kinds of profiles in our sample: those with "excess" light in the outer regions, which tend to flatten in these regions; and those for which the surface brightness falls off more rapidly. The differences in the shape of the light profiles may be signatures of different dynamical states for the stellar halos surrounding

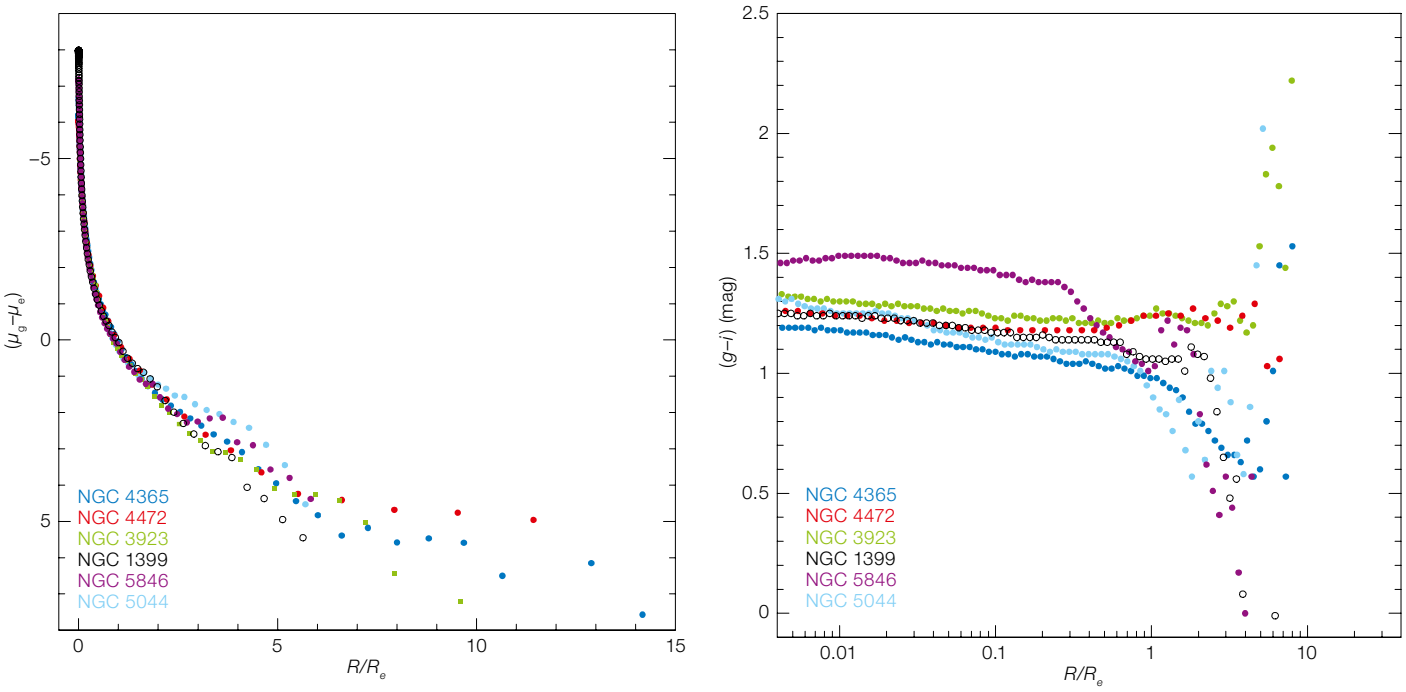

Figure 2. Left: Azimuthally-averaged surface brightness profiles in the *g*-band scaled to their effective magnitude, as a function of galactocentric radius normalised to the effective radius, R/R_e. Right: The (*g*–*i*) colour profiles of the galaxies in our study.

these galaxies. The mean (*g*–*i*) colour profiles for galaxies in our sample are shown in the right panel of Figure 2. The colours of all our galaxies are redder than those typically found for ETGs, since they all show the presence of dust lanes, shells, and other signs of ongoing interactions. The colours develop a steeper gradient at a different radius for each galaxy, becoming bluer (for NGC 1399, NGC 4365, NGC 5044 and NGC 5846) or redder (for NGC 3923 and NGC 4472). We will show later that the discontinuities observed in the colour profiles, ellipticities and position angles correspond to the transition radii observed in each surface brightness profile, which are defined as the locations of the transition between two different fit components.

Since there is considerable evidence in the literature that the light profiles of many of the most massive ETGs are not fitted well by a single Sérsic law and at least one additional component is needed (Seigar et al., 2007; Donzelli et al., 2011), our analysis focuses on the fit of projected one-dimensional (ellipsoidally averaged) surface brightness profiles of our sample galaxies. This second component is sometimes interpreted as evidence for a stellar halo. The overall profile is composed of different contributions and therefore theory suggests that the surface brightness profiles of ETGs should be described by the superposition of different components. For this reason, we first present models of the surface brightness profiles of galaxies in our sample with a double Sérsic law (r^{-n}), or with an exponential profile (n = 1) on the outer component. The result of these fits and their residuals are shown in Figure 3.

From this analysis we have identified a radius for each galaxy in our sample that marks the transition between the inner and outer components of our two-component fit. We label this empirically defined "transition radius" R_{tr}. This transition occurs at very faint levels of surface brightness (μ_{tr}) for all our galaxies. Moreover, a discontinuity in the ellipticity, position angle, and (*g*–*i*) colour profile of each of the six galaxies occurs around R_{tr} (see Spavone et al., 2017).

The relative contribution of the outer halo with respect to the total galaxy light (f_{h}) estimated from these fits ranges from 27 % to 64 %. Since there is no clear reason to believe that the outer component in a fit such as this accounts for most of the accreted mass in massive elliptical galaxies, these halo mass fractions should be considered a lower limit for the total accreted mass.

Numerical simulations predict that stars accreted by brightest cluster galaxies (BCGs) account for most of the total galaxy stellar mass (~ 90 % on average), while *in-situ* stars only contribute significantly to the surface brightness profiles out to R ~ 10 kpc (Cooper et al., 2013, 2015; Rodriguez-Gomez et al., 2016). The overall accreted profile is built up of contributions from several significant progenitors. For this reason, theory suggests that the surface brightness profile of an ETG should be well described by the superposition of an inner Sérsic profile, representing the sub-dominant *in-situ* component in the central regions, with another Sérsic profile representing the dominant superposition of the relaxed phase-mixed accreted components, and an outer diffuse component representing unrelaxed accreted material (streams and other coherent concentrations of debris), which does not contribute significant surface density to the brighter regions of the galaxy.

Following these theoretical predictions, we described the surface brightness

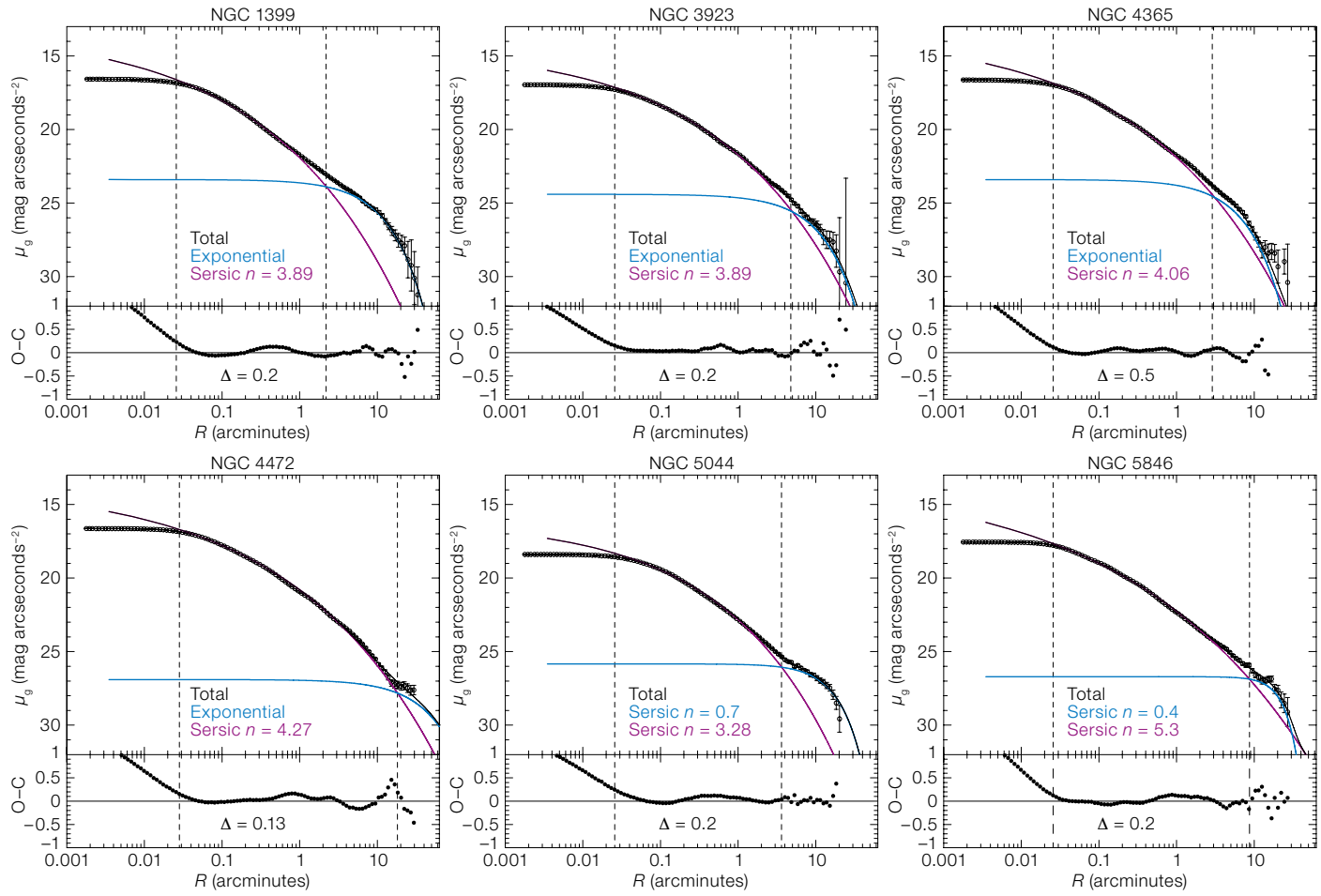

Figure 3. VST *g*-band profiles of NGC 1399, NGC 3923, NGC 4365, NGC 4472, NGC 5044, and NGC 5846 plotted on a logarithmic scale. The blue line is a fit to the outer regions, while the magenta line is a fit to the inner regions with a Sérsic profile, and the black line is the sum of the components in each fit. The dashed lines indicate the core of the galaxy, which was excluded from the fit, and the transition point between the two components, respectively.

profiles of our six galaxies with a three-component model: a Sérsic profile for the centrally concentrated *in-situ* stars, a second Sérsic for the relaxed accreted component, and an exponential component for the diffuse and unrelaxed outer envelope. To mitigate the degeneracy in parameters and provide estimates of accreted components that are closely comparable to the results of numerical simulations, we fixed $n \sim 2$ (allowing small variations of ±0.5) for the *in-situ* component of our three-component fits (Cooper et al., 2013). The results of these fits are shown in Figure 4. From this plot it appears that, as argued by Cooper et al. (2015), the radius R_{tr} identified in Figure 2 marks the transition between different accreted components in different states of dynamical relaxation, rather than between *in-situ* and accreted stars. From the fitting procedure we estimated the contributions of the outer exponential "envelopes" to the total galaxy mass; these range from 28 % to 60 % for the galaxies in our sample. We also estimate the fractions of total accreted mass, which range from 83 % to 95 %.

Comparison with theoretical predictions

In the previous section, we identified inflections in the surface brightness profiles of galaxies in our sample that may correspond to transitions between regions dominated by debris from different accreted progenitors in different dynamical states. In Figure 5 we compare the accreted mass ratios inferred from our observations (filled red triangles) with other observational estimates for BCGs (Bender et al., 2015; Seigar et al., 2007; Iodice et al., 2016), with theoretical predictions from semi-analytic particle-tagging simulations by Cooper et al. (2013, 2015), and with the Illustris cosmological hydrodynamical simulations (Rodriguez-Gomez et al., 2016).

We find that the stellar mass fraction of the accreted component derived for galaxies in our sample is fully consistent with both published data for other BCGs (despite considerable differences in the techniques and assumptions involved) and the theoretical models of Cooper et al. (2013, 2015). In Figure 5 we also compare the stellar mass fractions obtained for the outermost exponential component of our multi-component fit (open red triangles) with the mass fraction associated with unbound debris streams from surviving cluster galaxies in the simulations of Cooper et al. (2015). We found that the

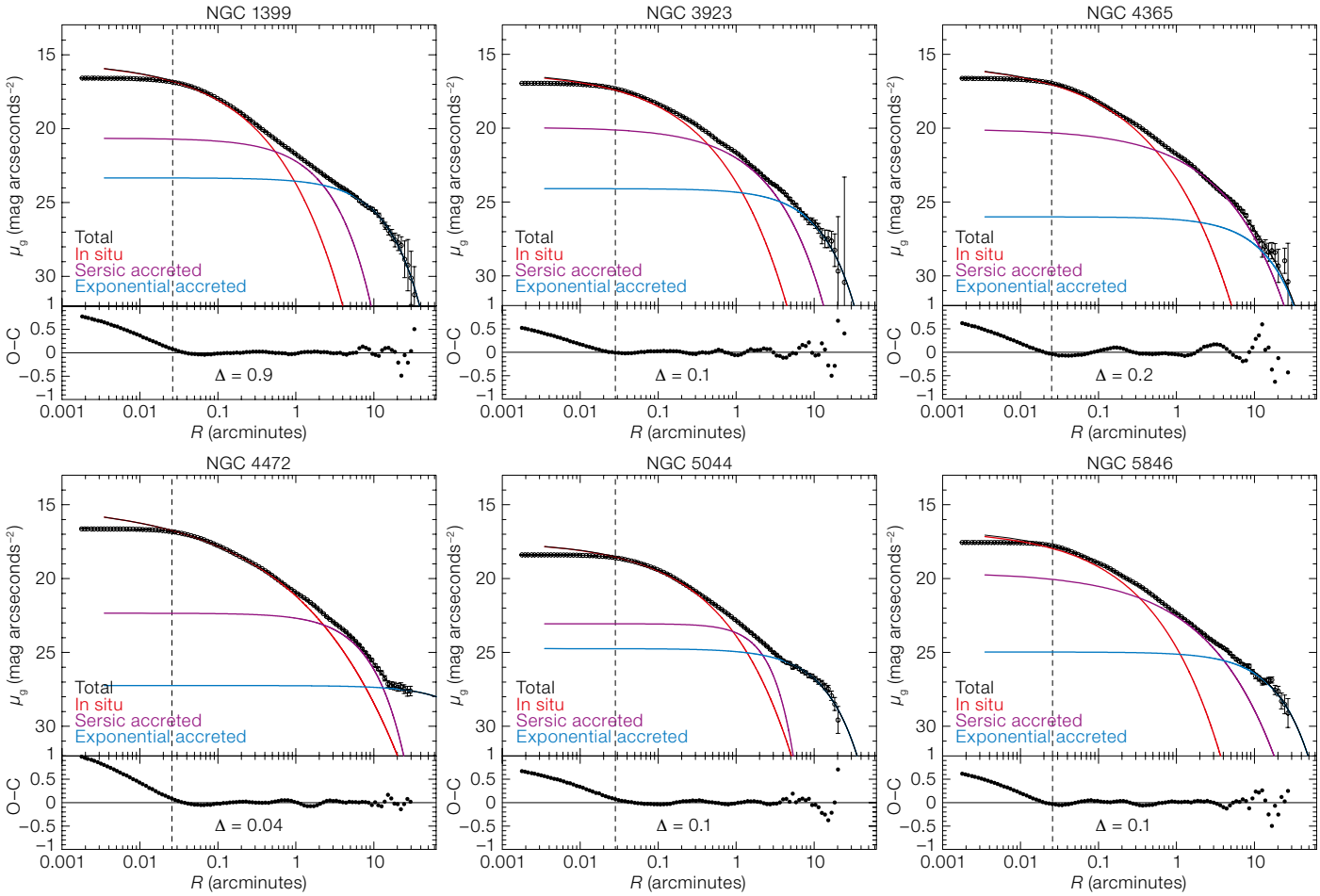

Figure 4. VST *g*-band profiles of NGC 1399, NGC 3923, NGC 4365, NGC 4472, NGC 5044, and NGC 5846, fitted with a three-component model motivated by the predictions of theoretical simulations.

mass fraction in this component of our fits is consistent with these values from the simulations, suggesting that such components may give a crude estimate of the mass distribution associated with dynamically unrelaxed components originating from disrupting or recently disrupted galaxies, as argued by Cooper et al. (2015).

Clues to the origin of stellar halos

Our analysis suggests that the surface brightness profiles of the galaxies in our study are best reproduced by multi-component models. For each of the galaxies in our study we can identify at least one inflection in the surface brightness profile. These inflections occur at very faint surface brightness levels ($24.0 \leq \mu_g \leq 27.8$ mag arcseconds^{-2}). They appear to correlate with changes in the trend of ellipticity, position angle, and colour with radius, where the isophotes become flatter and misaligned and the colours become bluer beyond the inflections. This suggests that these inflections mark transitions between physically distinct components in different states of dynamical relaxation.

A variety of possible interpretations for such features have been suggested, based on theoretical models. Upward inflections (shallower outer slopes) might reflect transitions between either an inner *in-situ*-dominated region and an outer accretion-dominated region, or else between two accreted components (Font et al., 2011). Downward inflections can occur within the profiles of debris from single progenitors alone, corresponding to the characteristic apocentric radius of its stars (Cooper et al., 2010; Deason et al., 2013) and therefore need not represent a transition between two separate components. We do not observe significant changes in surface brightness or other properties at the transition point between the inner two components of our theoretically motivated three-component fits. This is perhaps not surprising because simulations predict that the *in-situ* accreted transition is hardly noticeable in very massive galaxies, for the most part because the *in-situ* stars account for a relatively small fraction of the total mass even in the bright body of the galaxy. It is encouraging that we see a variety of profile inflections in our photometric investigation of this small subset of the VEGAS sample and that these are broadly consistent with expectations based on state-of-the-art theoretical models.

Our results suggest that, with the complete sample of extremely deep surface brightness profiles from the full survey, we will be able to investigate the late stages of massive galaxy assembly statistically,

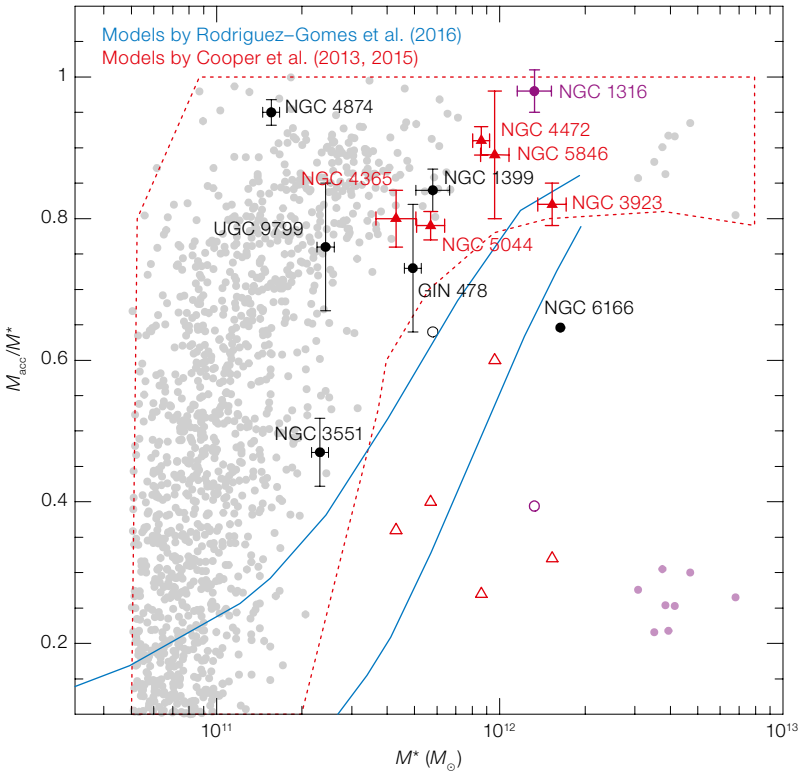

Figure 5. Accreted mass fraction versus total stellar mass for ETGs. Our VEGAS measurements are given as red filled and open triangles (see text for details). Black circles correspond to other BCGs from the literature. Red and blue regions indicate the predictions of cosmological galaxy formation simulations by Cooper et al. (2013, 2015) and Rodriguez-Gomez et al. (2016), respectively. Purple-grey points show the mass fraction associated with the streams from Table 1 in Cooper et al. (2015) for comparison to the observations shown by open symbols.

thereby distinguishing dynamically evolved systems from those that are still reaching dynamical equilibrium, and probing the balance between *in-situ* star formation and accretion across a wide range of stellar mass. This is a promising route to constraining cosmological models of galaxy formation such as those we have compared with here, which predict fundamental, relatively tight correlations between the present-day structure of massive galaxies and the growth histories of their host dark matter halos.

Acknowledgements

M. Spavone wishes to thank the ESO staff for their support during the observations at the VST. The data reduction for this work was carried out with the computational infrastructure of the INAF–VST Center at Naples (VSTceN). M. Spavone acknowledges financial support from the VST project (PI M. Capaccioli).

References

Bender, R. et al. 2015, ApJ, 807, 56
Capaccioli, M. et al. 2015, A&A, 581, A10
Cooper, A. P. et al. 2013, MNRAS, 434, 3348
Cooper, A. P. et al. 2015, MNRAS, 451, 2703
Deason, A. J. et al. 2013, ApJ, 763, 113
Donzelli, C. J. et al. 2011, ApJ, 195, 15
Font, A. S. et al. 2011, MNRAS, 416, 2802
Iodice, E. et al. 2016, ApJ, 820, 42
Rodriguez-Gomez, V. et al. 2016, MNRAS, 458, 2371
Seigar, M. S. et al. 2007, MNRAS, 378, 1575
Spavone, M. et al. 2017, A&A, 603A, 38S

ESO/GASP collaboration

The Visible and Infrared Survey Telescope for Astronomy (VISTA).

DOI: 10.18727/0722-6691/5053

Dissecting the Core of the Tarantula Nebula with MUSE

Paul A. Crowther[1]
Norberto Castro[2]
Christopher J. Evans[3]
Jorick S. Vink[4]
Jorge Melnick[5]
Fernando Selman[5]

[1] Department of Physics & Astronomy, University of Sheffield, United Kingdom
[2] Department of Astronomy, University of Michigan, Ann Arbor, USA
[3] UK Astronomy Technology Centre, Royal Observatory, Edinburgh, United Kingdom
[4] Armagh Observatory, United Kingdom
[5] ESO

We provide an overview of Science Verification MUSE observations of NGC 2070, the central region of the Tarantula Nebula in the Large Magellanic Cloud. Integral-field spectroscopy of the central 2 × 2 arcminute region provides the first complete spectroscopic census of its massive star content, nebular conditions and kinematics. The star formation surface density of NGC 2070 is reminiscent of the intense star-forming knots of high-redshift galaxies, with nebular conditions similar to low-redshift Green Pea galaxies, some of which are Lyman continuum leakers. Uniquely, MUSE permits the star formation history of NGC 2070 to be studied with both spatially resolved and integrated-light spectroscopy.

Tarantula Nebula

The Tarantula Nebula (30 Doradus) in the Large Magellanic Cloud (LMC) is intrinsically the brightest star-forming region in the Local Group and has been the subject of numerous studies across the electromagnetic spectrum. Its low (half-solar) metallicity and high star formation intensity are more typical of knots in high-redshift star-forming galaxies than local systems thanks to its very rich stellar content (Doran et al., 2013). Indeed, 30 Doradus has nebular conditions that are reminiscent of the galaxies known as Green Peas. These are local extreme emission-line galaxies that are analogues of high-redshift, intensely star-forming galaxies, some of which have been confirmed as Lyman continuum leakers (for example, Micheva et al., 2017).

The Tarantula Nebula is host to hundreds of massive stars that power the strong Hα nebular emission, comprising main sequence OB stars, evolved blue supergiants, red supergiants, luminous blue variables and Wolf-Rayet (WR) stars. The proximity of the LMC (50 kpc) permits individual massive stars to be observed under natural seeing conditions (Evans et al., 2011). The exception is R136, the dense star cluster at the LMC's core that necessitates the use of adaptive optics or the Hubble Space Telescope (HST; see Khorrami et al., 2017, Crowther et al., 2016). R136 has received particular attention since it hosts very massive stars (≥ 100 $M_{\odot}$; Crowther et al., 2016) that are the potential progenitors of pair-instability supernovae and/or merging black holes whose gravitational wave signatures have recently been discovered with LIGO.

Star formation in the Tarantula Nebula began at least 15–30 Myr ago, as witnessed by the cluster Hodge 301, whose stellar content is dominated by red supergiants. There was an upturn in its rate of star formation within the last 5–10 Myr, which peaked a couple of Myr ago in NGC 2070, the central ionised region that hosts R136. Star formation is still ongoing, as witnessed by the presence of massive young stellar objects and clumps of molecular gas observed with ALMA (Indebetouw et al., 2013). The interplay between massive stars and the interstellar medium also permits the investigation of stellar feedback at high spatial and spectral resolutions (for example, Pellegrini, Baldwin & Ferland, 2011).

MUSE observations of NGC 2070

NGC 2070, the central region of the Tarantula Nebula, was observed with the Multi Unit Spectroscopic Explorer (MUSE) as part of its original Science Verification programme at the Very Large Telescope (VLT) in August 2014. MUSE is a wide-field, integral-field spectrograph, providing intermediate-resolution (R ~ 3000 at Hα) spectroscopy from 4600–9350 Å over one square arcminute with a pixel scale of 0.2 arcseconds. Four overlapping MUSE pointings provided a 2 × 2 arcminute mosaic which encompasses both the R136 star cluster and R140 (an aggregate of WR stars to the north). See Figure 1 for a colour-composite of the central 200 × 160 pc of the Tarantula Nebula obtained with the Advanced Camera for Surveys (ACS) and the Wide Field Camera 3 (WFC3) aboard the HST. The resulting image resolution spanned 0.7 to 1.1 arcseconds, corresponding to a spatial resolution of 0.22 ± 0.04 pc, providing a satisfactory extraction of sources aside from R136. Four exposures of 600 s each for each pointing provided a yellow continuum signal-to-noise (S/N) ≥ 50 for 600 sources. A total of 2255 sources were extracted using SExtractor, while shorter 10- and 60-second exposures avoided saturation of strong nebular lines. Absolute flux calibration was achieved using *V*-band photometry from Selman et al. (1999). An overview of the dataset, together with stellar and nebular kinematics, is provided by Castro et al. (submitted to A&A).

Spatially resolved nebular properties

We present colour-composite images extracted from the MUSE datacubes in Figure 2, highlighting the stellar content and ionised gas, respectively. Figure 2a samples 6640, 5710 and 4690 Å, such that most stars appear white except for cool supergiants (orange; for example, Melnick 9 in the upper left) and WR stars, which appear blue owing to strong He II 4686 Å emission. Examples of the WR stars include R134 to the right of the central R136 star cluster and the R140 complex at the top, which hosts WN and WC stars, subsets of WR stars that have dominant lines of ionised nitrogen and ionised carbon respectively. In contrast, Figure 2b highlights the distribution of low-ionisation gas ([S II] 6717 Å, red), high-ionisation gas ([O III] 5007 Å, blue) and hydrogen (Hα, green). Green point sources generally arise from broad Hα emission from WR stars and related objects.

Owing to the presence of ionised gas throughout NGC 2070, our MUSE datasets enable the determination of nebular properties. Adopting a standard Milky Way extinction law, there is a wide variation in extinction throughout the region with

NASA, ESA, D. Lennon et al.

Figure 1. MUSE 2 × 2 arcminute mosaic (white square) superimposed on a colour-composite image of the Tarantula Nebula (corresponding to ~200 × 160 parsecs), obtained with the ACS and WFC3 instruments aboard HST.[1]

Figure 2. (a) VLT/MUSE colour-composite image of NGC 2070 (2 × 2 arcminutes) sampling 6640 Å (red), 5710 Å (green), and 4690 Å (blue). Blue sources are WR stars with prominent He II 4686 Å emission, while orange sources are predominantly red supergiants. (b) VLT/MUSE colour-composite image of NGC 2070 (2 × 2 arcminutes) sampling [S II] 6717 Å (red), Hα (green), and [O III] 5007 Å (blue).

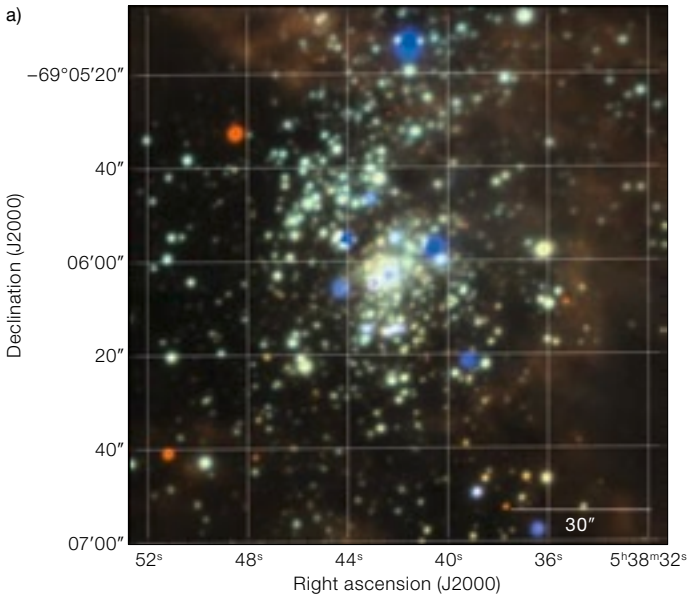

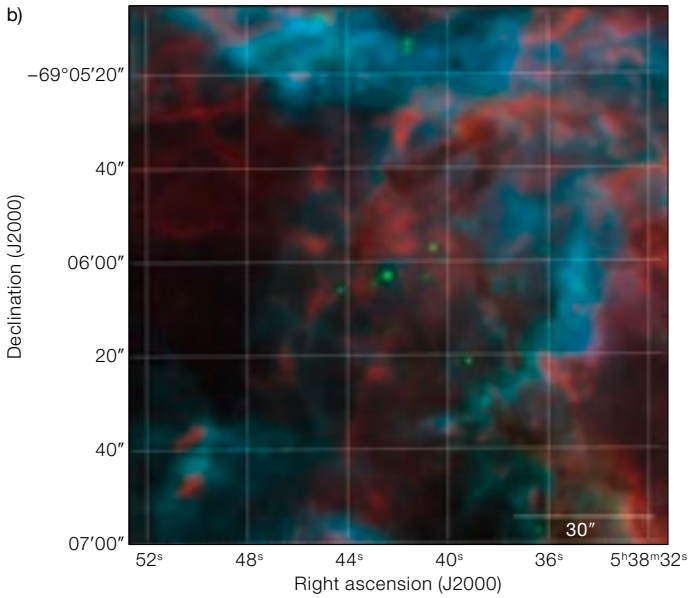

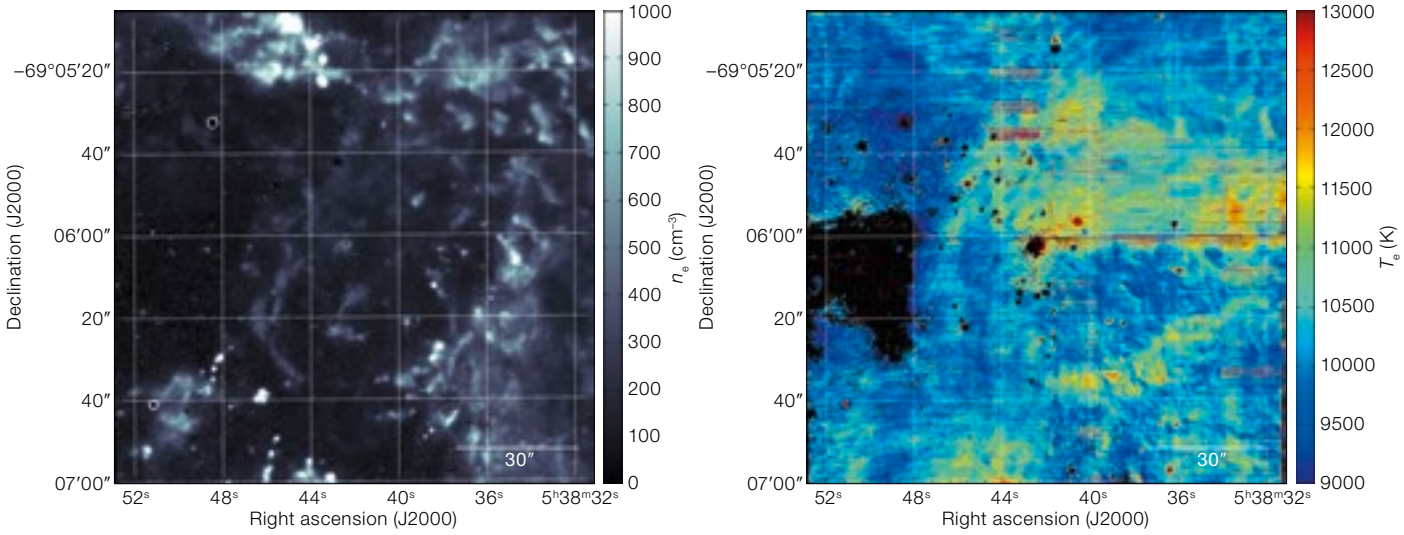

Figure 3. (Above) Distribution of gas density (left) and temperature (right) within the MUSE field of view, based on [S II] 6717/6731 Å and [S III] 6312/9069 Å diagnostics.

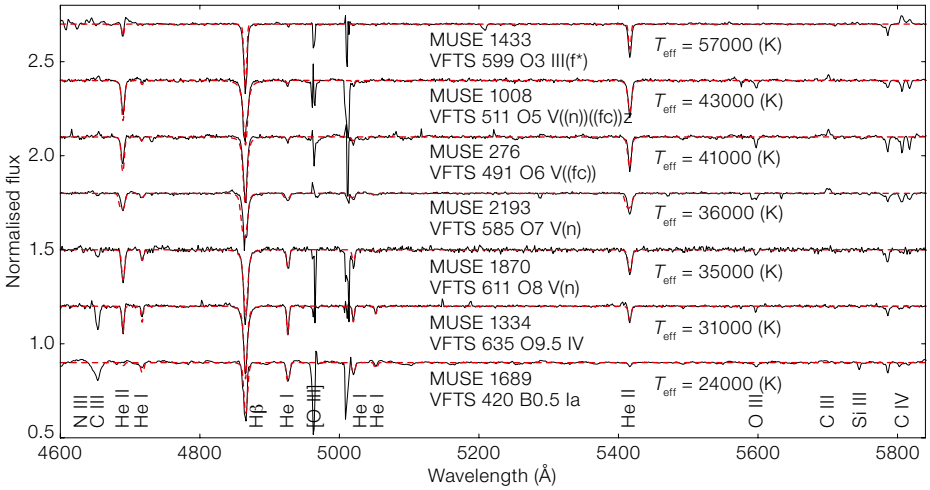

Figure 4. Blue to yellow spectroscopy of representative OB stars in NGC 2070 observed with VLT/MUSE (black solid lines), including spectral types from the VLT-FLAMES Tarantula survey, and temperatures from FASTWIND model fits (dashed red lines) to He I 4921 Å and He II 5412 Å.

coefficients spanning $0.15 \leq c(\mathrm{H}\beta) \leq 1.2$. On average, we found $c(\mathrm{H}\beta) = 0.55$ mag, which is in excellent agreement with long-slit results from Pellegrini, Baldwin & Ferland (2011). Nebular lines also permit the determination of electron densities and temperatures from [S II] and [S III] diagnostics as illustrated in Figure 3. The dust properties towards the Tarantula Nebula are known to be non-standard, with an average $c(\mathrm{H}\beta) = 0.6$ obtained from the law presented by Maíz-Apellániz et al. (2014) and $R = 4.4$, although this has little bearing on the nebular conditions determined here owing to the use of red spectral diagnostics.

Massive stars in NGC 2070

MUSE permits the first complete spectroscopic census of massive stars within NGC 2070. Previous surveys have been restricted to multi-object spectroscopy using slitlets or fibres (Bosch et al., 1999; Evans et al., 2011). Spectral lines in the blue are usually employed in the classification of OB stars, so the 4600 Å blue limit to MUSE has required the development of green and yellow diagnostics. Representative OB spectra from MUSE are presented in Figure 4 with classifications from blue spectroscopy using the Fibre Large Array Multi Element Spectrograph (FLAMES) on the VLT (Walborn et al., 2014). A spectroscopic analysis of 270 sources with He II 5412 Å absorption is now underway using the non-local thermodynamic equilibrium atmospheric code FASTWIND (Puls et al., 2005), yielding temperatures and luminosities from He I 4921 Å and He II 5412 Å. Preliminary fits to the illustrative spectra are also shown in Figure 4.

Ultimately we will determine the properties of all of the massive stars in NGC 2070 in order to fully characterise its recent star-formation history, substituting results from long-slit HST spectroscopy using the Space Telescope Imaging Spectrograph (STIS) for the central parsec of R136 (Crowther et al., 2016). Quantitative analysis of the MUSE data should also provide useful insights to incorporate into stellar evolution theory. For instance, Castro et al. (2014) suggested empirical boundaries for the zero- and terminal-age main sequences from their analysis of a large sample of OB stars. The MUSE data will enable a homogeneous analysis of a larger stellar sample, spanning a broad range of evolutionary stages (for example, main sequence, blue and red supergiants, and WR stars).

Of course, it is well known that massive stars prefer company, so it is likely that many of the MUSE point sources are multiple. Fortunately, the majority of

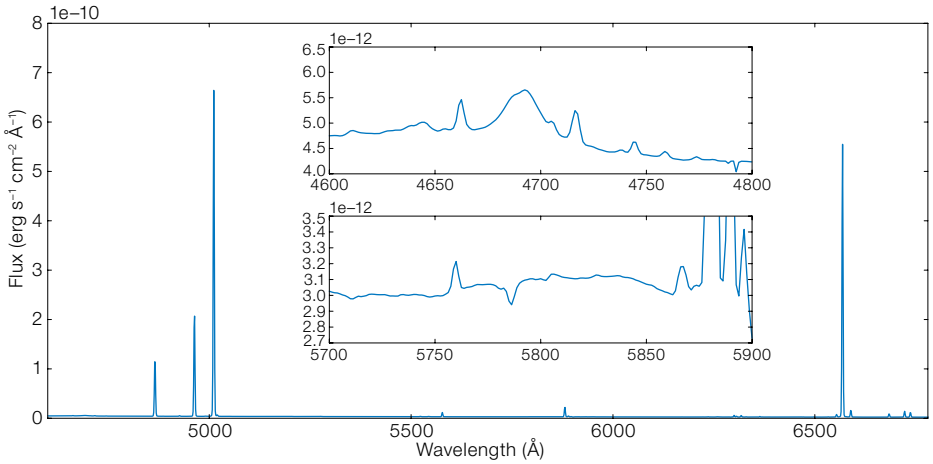

Figure 5. Integrated MUSE spectrum of NGC 2070, revealing a striking emission line spectrum, with characteristics reminiscent of Green Pea galaxies, plus WR bumps in the blue (upper inset, He II 4686 Å arising from WN stars) and yellow (lower inset, C IV 5801–12 Å due to WC stars).

massive stars in NGC 2070 have previously been monitored spectroscopically with VLT/FLAMES, revealing many short-period systems. In addition, 30 Doradus has been the target of the Chandra X-ray Visionary Programme (T-ReX) using the Advanced CCD Imaging Spectrometer (ACIS-I). This programme monitored X-ray emission from the Tarantula Nebula over 630 days, permitting longer-period systems to be identified. For example, Melnick 34, the blue emission-line star to the left of R136 in Figure 2a, has been revealed as an eccentric colliding-wind binary by its T-ReX variability (Pollock et al., 2017).

Integrated spectrum of NGC 2070

In addition to spectra of the spatially-resolved stars and gas in NGC 2070, it is possible to sum the MUSE observations to arrive at the integrated spectrum of the region. NGC 2070 would subtend 0.6 arcseconds if it were located at a distance of 10 Mpc, so MUSE offers the unique opportunity to study both the spatially-resolved properties of an intensively star-forming region and its aggregate characteristics. The integrated spectrum of NGC 2070 is presented in Figure 5. In addition to strong nebular lines, the high throughput of MUSE and the proximity of NGC 2070 allow a plethora of weaker features to be revealed in the integrated spectrum, including the non-standard density diagnostic C III 5517/5537 Å. Figure 5 also highlights broad blue (He II 4686 Å) and yellow (C IV 5801–12 Å) WR features in the integrated spectrum, with no evidence for a nebular contribution to the former. These are often observed in the integrated light of extragalactic star-forming regions.

Figure 6a compares the strong-line nebular characteristics of NGC 2070 with Sloan Digital Sky Survey (SDSS) star-forming galaxies and indicates similar high-excitation properties to those of Green Pea galaxies (Micheva et al., 2017). Analysis of the integrated spectrum reveals $c(\mathrm{H}\beta) = 0.57$ for a standard extinction law, such that the dereddened Hα luminosity is 1.5×10^{39} erg s^{-1}, corresponding to one-eighth of the entire Tarantula Nebula (Doran et al., 2013). The current star formation rate (SFR) for NGC 2070 is 0.008 $M_{\odot}$ yr^{-1}. This has been obtained by adopting a standard Kennicutt (1998) relation between Hα luminosity and SFR, modified for a Kroupa (2002) initial mass function by dividing by a factor of 1.5, and inferring a high star formation surface density of $\Sigma_{\mathrm{SFR}} \sim 10\ M_{\odot}$ yr^{-1} kpc^{-2}. Conditions are similar to clumps of intensively star-forming galaxies at high redshifts, as demonstrated in Figure 6b (adapted from Johnson et al., 2017).

Properties inferred from the integrated light of NGC 2070

The inferred age of the region from the equivalent width of Hα is ~4 Myr, implying a mass of $10^5\ M_{\odot}$ for an instantaneous burst of star formation. This is double the mass estimated for the central R136 cluster. In reality, there is an age spread of 0–10 Myr for massive stars within the entire Tarantula Nebula (Schneider et al., 2017), although the peak of star formation was inferred to be ~4.5 Myr ago, excluding R136 (which has an age of ~1.5 Myr; Crowther et al., 2016). The Hα-derived ionising output is 10^{51} photons s^{-1} for NGC 2070, equivalent to ~100 O7 V stars. This corresponds to ~300 O stars for the nebular derived age (Schaerer & Vacca, 1998), in good agreement with the number of MUSE sources that display He II 5412 Å absorption, albeit neglecting the (significant) contribution of the WR stars to the cumulative ionising output.

We derive log (O/H) + 12 = 8.25 for NGC 2070, adopting N^+ and S^{++} temperatures for singly- and doubly-ionised oxygen, respectively. However, the blue MUSE cutoff excludes the use of the stronger [O III] 4363 Å line. Direct determinations for the entire 30 Doradus region indicate a somewhat higher oxygen content (for example, log (O/H) + 12 = 8.33; Tsamis et al., 2003). Since WR line luminosities are metallicity dependent (Crowther & Hadfield, 2006) one would infer 20 mid-WN and five early WC stars in NGC 2070, or N(WR)/N(O) ≥ 0.08, by adopting LMC templates. This is in reasonable agreement with the resolved WR content of the MUSE field, namely 10 WN stars, 6 Of/WN stars and 2 WC stars. The rich star cluster R136 hosts four of the most massive WN5h stars in the region, but only contributes one third of the cumulative He II 4686 Å emission. In contrast, the less prominent R140 complex, which hosts two WN6 stars and one WC star, contributes another third of the He II 4686 Å emission and dominates the integrated C IV 5808 Å and C III 4650 Å flux. This arises from the relatively weak wind strengths of main sequence WN5h stars, as opposed to the significantly stronger emission from classical WN stars.

Strong-line calibrations are widely employed to infer the metallicity of extragalactic H II regions because of the faintness of auroral lines. Application of the commonly used calibrations from Pettini & Pagel (2004), using the N2 and

O3N2 indices, would imply a Small Magellanic Cloud (SMC)-like oxygen content of log (O/H) + 12 = 8.0, significantly lower than our direct determination. If one had to rely on strong-line diagnostics for NGC 2070, the use of SMC-metallicity WR templates from Crowther & Hadfield (2006) would suggest an unrealistically high number of mid-WN stars, and, in turn, N(WR)/N(O) ≥ 0.3. This would represent a severe challenge to current single/binary population synthesis models for a starburst region with 0.2 $Z_{\odot}$, in stark contrast with the N(WR)/N(O) ~ 0.07 and 0.4 $Z_{\odot}$ that has been obtained from our spatially resolved spectroscopy of the region.

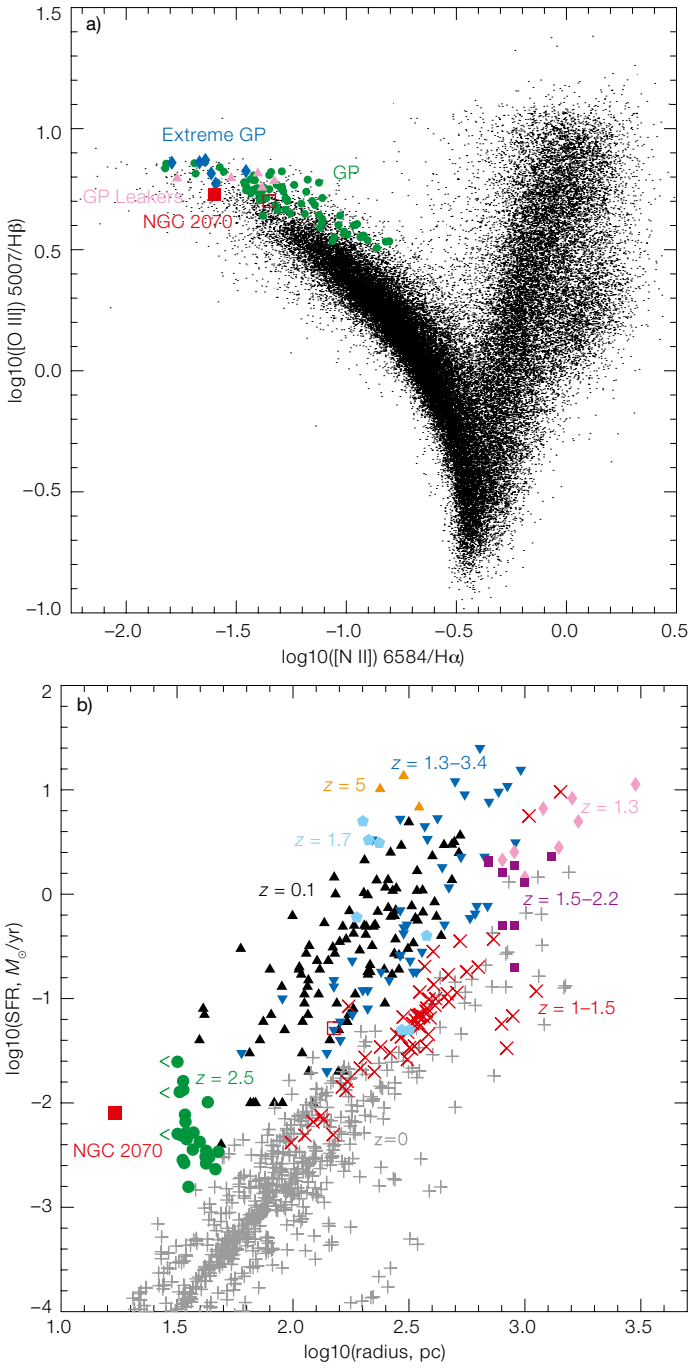

Figure 6. (a) BPT diagram (Baldwin, Phillips & Terlevich, 1981) illustrating the similarity in integrated strengths between NGC 2070/Tarantula (filled/open red square), Green Pea (green circles), extreme Green Pea (blue diamonds), and Lyman-continuum emitting Green Pea (pink triangles) galaxies, plus SDSS star-forming galaxies (black dots); updated from Figure 2 of Micheva et al. (2017). (b) Comparison between the integrated star-formation rate of NGC 2070/Tarantula (filled/open red square) and star-forming knots from galaxies, spanning a range of redshifts (adapted from Figure 2 of Johnson et al., 2017).

References

Baldwin, J. A., Phillips, M. M. & Terlevich, R. 1981, PASP, 93, 5
Bosch, G. et al. 1999, A&AS, 137, 21
Castro, N. et al. 2014, A&A, 570, 13
Crowther, P. A. et al. 2016, MNRAS, 458, 624
Doran, E. et al. 2013, A&A, 558, A134
Evans, C. J. et al. 2011, A&A, 530, A108
Kennicutt, R. C. 1998, ARA&A, 36, 189
Khorrami, Z. et al. 2017, A&A, 602, A56
Kroupa, P. 2002, Science, 295, 82
Indebetouw, R. et al. 2013, ApJ, 774, 73
Johnson, T. L. et al. 2017, ApJ, 843, L21
Maíz-Apellániz, J. et al. 2014, A&A, 564, A63
Micheva, G. et al. 2017, ApJ, 845, 165
Pellegrini, E. W., Baldwin, J. A. & Ferland, G. J. 2011, ApJ, 738, 34
Pettini, M. & Pagel, B. E. J. 2004, MNRAS, 348, L59
Puls, J. et al. 2005, A&A, 435, 669
Pollock, A. M. T. et al. 2017, MNRAS, in press
Schaerer, D. & Vacca, W. D. 1998, ApJ, 497, 618
Selman, F. et al. 1999, A&A, 341, 98
Schneider, F. et al. 2017, Science, in press
Tsamis, Y. et al. 2003, MNRAS, 338, 687
Walborn, N. et al. 2014, A&A, 564, A40

Links

[1] Hubble News Release: https://www.spacetelescope.org/news/heic1206

DOI: 10.18727/0722-6691/5054

VLTI Imaging of a High-Mass Protobinary System: Unveiling the Dynamical Processes in High-Mass Star Formation

Stefan Kraus[1]
Jacques Kluska[1]
Alexander Kreplin[1]
Matthew Bate[1]
Timothy Harries[1]
Karl-Heinz Hofmann[2]
Edward Hone[1]
John Monnier[3]
Gerd Weigelt[2]
Narsireddy Anugu[1]
Willem-Jan de Wit[4]
Markus Wittkowski[4]

[1] University of Exeter, United Kingdom
[2] Max-Planck-Institut für Radioastronomie, Bonn, Germany
[3] University of Michigan, Ann Arbor, USA
[4] ESO

High-mass stars exhibit a significantly higher multiplicity frequency than low-mass stars, likely reflecting differences in how they formed. Theory suggests that high-mass binaries may form by the fragmentation of self-gravitational discs or by alternative scenarios such as disc-assisted capture. Near-infrared interferometric observations reveal the high-mass young stellar object IRAS 17216-3801 to be a close high-mass protobinary with a separation of 0.058 arcseconds (~ 170 au). This is the closest high-mass protobinary system imaged to date. We also resolve near-infrared excess emission around the individual stars, which is associated with hot dust in circumstellar discs. These discs are strongly misaligned with respect to the binary separation vector, indicating that tidal forces have not yet had time to realign. We measure a higher accretion rate towards the circumsecondary disc, confirming a hydrodynamic effect where the secondary star disrupts the primary star's accretion stream and effectively limits the mass that the primary star can accrete. NACO *L'*-band imaging may also have resolved the circumbinary disc that feeds the accretion onto the circumstellar discs. This discovery demonstrates the unique capabilities of the VLTI, creating exciting new opportunities to study the dynamical processes that govern the architecture of close multiple systems.

There is strong observational support for the hypothesis that high-mass stars (> 10 $M_{\odot}$) can form through accretion from circumstellar discs (for example, Kraus et al., 2010; Boley et al., 2013; Johnston et al., 2015; Caratti o Garatti et al., 2017). These discs channel strong stellar winds and radiation in the polar direction, enabling the infall of material and allowing the star to grow beyond the limits imposed by radiation pressure and the classical Eddington barrier (for example, Kuiper et al., 2010).

While the detection of these discs is often interpreted as evidence for similarities between low- and high-mass star formation, it is also important to emphasise that the monolithic collapse scenario that has been developed for low-mass star formation is unable to explain the differences in multiplicity fractions observed between low-mass and high-mass stars. Surveys have found that ≥ 90 % of all O-type stars (> 16 $M_{\odot}$) are close multiple systems, while this fraction drops to 20 % for A-type stars (~ 3 $M_{\odot}$; Chini et al., 2014). In addition, the number of companions increases with the mass of the primary star. Various dynamical scenarios have been proposed to explain these remarkable characteristics. For instance, high-mass multiples might form via the fragmentation of self-gravitating discs (Kratter & Matzner, 2006), disc-assisted capture (Bally & Zinnecker, 2005), or through failed mergers in stellar collisions (Dale & Davies, 2006). Mass transfer processes during the early formation phase or dynamical three-body capture might also lead to the formation of close binaries of near-equal mass.

Testing these scenarios requires the discovery of high-mass protobinaries that are still in the process of forming. Given the large (kiloparsec) distance to these objects and their embedded nature, such studies need to be conducted at infrared or submillimetre wavelengths and at the highest achievable angular resolution. With its unprecedented 0.002-arcsecond angular resolution, the VLT Interferometer (VLTI) is well-suited to make such observations. In order to search for protobinary systems and to obtain new insights into the disc structure of high-mass young stellar objects (YSOs), we initiated an interferometric survey in the *K*-band using the Astronomical Multi-BEam combineR (AMBER) on the VLTI. The goal was to study the astronomical unit scale inner environment around high-mass YSOs at low spectral resolution (R = 35). The first results from this campaign were published in Kraus et al. (2010), where we detected an au-scale disc around the high-mass YSO IRAS 13481-6124.

GRAVITY and AMBER aperture synthesis imaging

Another source in our sample, IRAS 17216-3801, is a high-mass YSO located at a distance of 3.1 ± 0.6 kpc (Boley et al., 2013) with a bolometric luminosity of 6.1 × 10^4 $L_{\odot}$. Our VLTI observations resolve the system into a binary with a separation of 58 milliarcseconds (mas), corresponding to approximately 170 au at the distance of the source (Kraus et al., 2017). We estimate the component masses as 20 and 18 $M_{\odot}$, which makes the system about three times more massive and five times more compact than previously imaged high-mass multiple systems (for example, Sridharan et al., 2005). Most importantly, the mas-scale resolution achieved with the VLTI allows us to spatially resolve the discs around the individual components, which is the first time that this has been achieved for a high-mass protobinary system.

AMBER measurements taken in 2012 using the long Unit Telescope (UT) baselines (30–130 m) showed strong visibility and closure phase modulations that are characteristic of multiple systems, while the low visibility level indicated the presence of both disc and photospheric emission. As part of a VLTI GRAVITY Science Verification programme, we obtained medium spectral resolution (R = 500) on complementary Auxiliary Telescope (AT) baselines (11–34 m). The GRAVITY data recording sequence on IRAS 17216-3801 required less than one hour, but resulted in interferometric observables that changed dramatically on timescales of minutes (Figure 1), reflecting the changes in projected baselines that resulted from the Earth's rotation. The rapid changes in the visibility and phase signal allow us to constrain the object's structure with relatively little observing time.

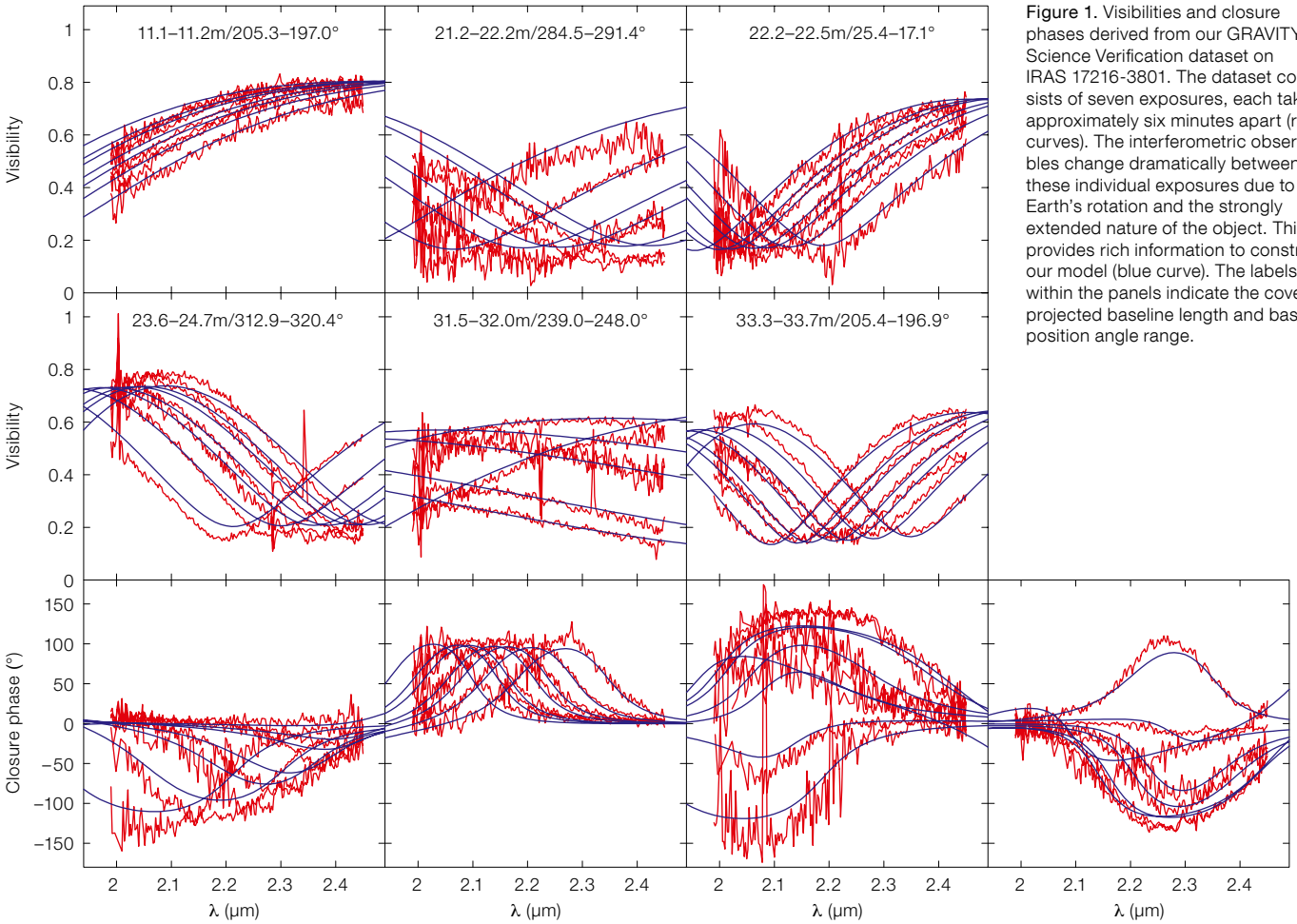

Figure 1. Visibilities and closure phases derived from our GRAVITY Science Verification dataset on IRAS 17216-3801. The dataset consists of seven exposures, each taken approximately six minutes apart (red curves). The interferometric observables change dramatically between these individual exposures due to the Earth's rotation and the strongly extended nature of the object. This provides rich information to constrain our model (blue curve). The labels within the panels indicate the covered projected baseline length and baseline position angle range.

The combined GRAVITY and AMBER data provide adequate uv-plane coverage for image reconstruction. In order to combine the two datasets, we needed to account for the orbital motion of the binary between 2012 and 2016. We therefore implemented an algorithm that rotated and scaled the uv-plane such that it compensated for the orbital motion between the two epochs, where the changes in binary separation and binary position angle were fitted as free parameters during the image reconstruction and model-fitting process. This method indicates that the separation remained constant between 2012 and 2016, while the binary position angle changed by 8° in the same time period.

Figure 2 (left) depicts the system at the 2016 epoch and clearly reveals a binary with 57.9 ± 0.2 mas separation (170 au at 3.1 kpc). Both components are associated with spatially resolved emission, where the emission around the northern component (A) is more extended than around the southern component (B) and also clearly misaligned with respect to the binary separation vector. In order to characterise this extended emission, we fitted an analytic model to the visibility and closure phase data, which includes the photospheric emission from the stars and the discs around each star, and the extended emission is represented with a Gaussian component. We parameterised the discs with a radial temperature power law, where the disc emission extends between an inner and outer radius. Our model indicates that the circumprimary and circumsecondary discs are seen under intermediate inclination angles (60° ± 10° and 38° ± 10°, respectively, where 0° corresponds to face-on viewing geometry). The circumsecondary disc is roughly aligned (position angle 159° ± 15°) with the binary separation vector of 166.8° ± 0.2°, while the circumprimary disc is strongly misaligned (position angle 67° ± 7°; see sketch in Figure 2, right).

Both discs seem to feature an opacity hole in the inner regions at radii of 2.77 ± 0.39 mas (circumprimary disc) and 2.49 ± 0.42 mas (circumsecondary disc). This is a well-known effect in low- and intermediate-mass YSOs (for example, Lazareff et al., 2017) and has also been observed in the high-mass YSO IRAS 13481-3601 (Kraus et al., 2010). The derived inner disc radii likely indicate the region close to the star where the temperatures are too high for dust grains to exist.

NACO imaging and a potential circumbinary disc

We also imaged the system using NACO adaptive optics imaging in several near-infrared filters (including a *J*-band filter and narrow-band filters in *H* and *K*). When

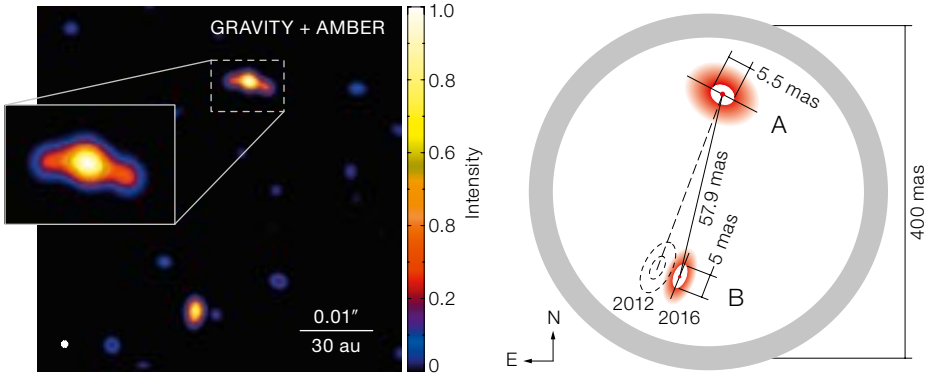

Figure 2. Far left: Aperture synthesis image reconstructed from our GRAVITY (AT) and AMBER (UT) datasets. Left: Sketch of the IRAS 17216-3801 system, as derived with model-fitting techniques.

comparing these images with the point spread function (PSF) measured on a dedicated PSF calibrator star, there is a clear "notch" south of the primary star, indicating that we marginally resolve the 58 mas binary also with NACO (1.64 μm image in Figure 3, top-left and bottom panels).

In another image taken with the *L*′-band filter, we detect a surprisingly extended structure with a half width at half maximum (HWHM) size of ~250 mas (Figure 3, top-right and bottom). Hydrodynamic simulations predict that a binary should truncate the circumbinary disc at about three times the binary semi-major axis. Using the measured separation as a lower limit for the binary semi-major axis, we expect the circumbinary disc to extend to ≥175 mas, which is broadly consistent with the measured size of the *L*′-band structure. As no dedicated PSF star observations have been obtained with this filter, new observations will be required in order to confirm this finding and to better characterise the *L*′-band geometry.

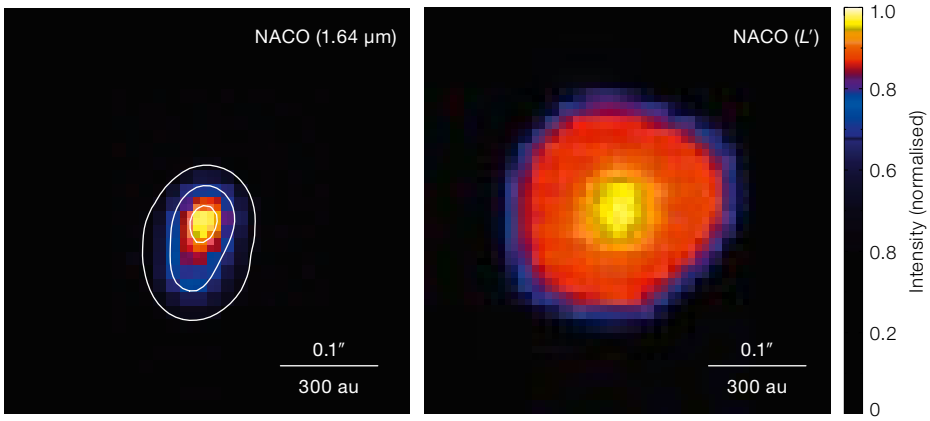

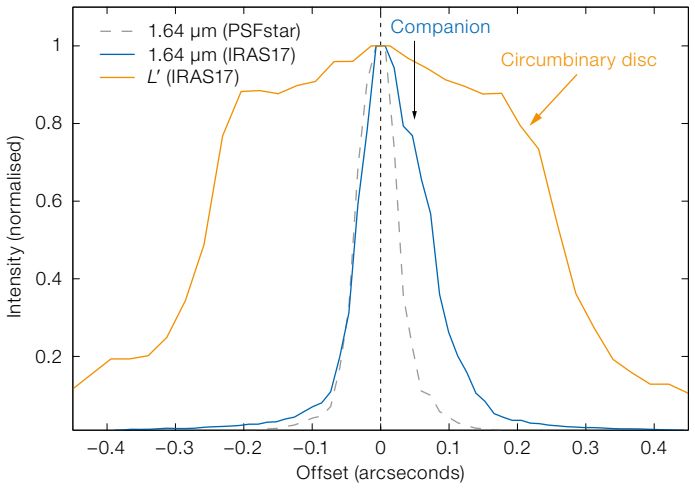

Figure 3. Top: NACO images of IRAS 17216-3801 taken with a 1.64-μm narrow-band filter and the *L*′-band filter. Left: Radial cut along the binary separation vector, overplotted with the PSF measured on a calibrator star in the 1.64-μm filter.

Insights into the dynamical history of IRAS 17216-3801

To our knowledge, this study marks the first time that the circumstellar discs of a high-mass protobinary system could be spatially resolved. We find that the circumstellar discs are strongly misaligned with respect to the binary separation vector, which provides insight into the dynamical history of the system.

Theoretical studies have uncovered various formation mechanisms that could result in misaligned discs, including the fragmentation of self-gravitating discs, perturbation by a third body, or infall of material whose angular momentum vector was misaligned to that of the gas from which the binary initially formed (Bate et al., 2010). However, once a highly misaligned system has formed, tidal interactions will work towards realigning the discs. This realignment should happen on the viscous timescale (Papaloizou & Terquem, 1995) or on the much shorter precession timescale (Bate et al., 2000). Based on our estimates of the individual stellar masses and of the outer disc radii, we derive an upper limit on the precession timescale of ~200 000 years for the circumprimary disc and ~900 000 years for the circumsecondary disc. Our observations therefore suggest that tidal realignment is still ongoing, indicating the young dynamical age of the IRAS 17216-3801 system.

Tracing accretion onto the individual components

Our GRAVITY observation also covers spectral lines corresponding to the Brγ 2.16 μm hydrogen recombination line and CO bandheads between 2.3–2.4 μm. This allows us to determine whether

these lines are associated with the primary star, secondary star, or the extended environment. We measure non-zero wavelength differential phase signals and visibility signals that are distinctly different for the Brγ line and the CO bandhead emission (Figure 4, left), indicating that they originate in different regions of the circumstellar environment.

The CO bandheads are believed to trace warm (> 10^3 K) neutral gas. We find that the CO line emission is spatially extended and comes from a region between the two stars. This suggests that the molecular emission might trace extended gas streams between the two discs, opening up the exciting prospect of imaging these gas streams with future GRAVITY observations at better uv-coverage.

The Brγ line, on the other hand, traces hot (> 10^4 K) ionised gas and reveals both mass accretion and ejection processes (for example, Kraus et al., 2008; Kurosawa et al., 2016; Caratti o Garatti et al., 2016). For IRAS 17216-3801, we find that the line emission originates from compact regions close to the individual stars, where 60 % of the Brγ emission is associated with the secondary star, while only 40 % is associated with the primary. This is also confirmed by an independent measurement we obtained in 2012 in parallel to the AMBER observations of the source using the CRyogenic InfraRed Echelle Spectrometer (CRIRES). CRIRES spectra (R = 100 000) were obtained with three different slit orientations, allowing us to constrain the spatial origin of the line emission using the spectro-astrometry technique. In the bottom panel of Figure 4 we overplot the Brγ-line photocentre offsets (measured relative to the continuum photocentre after continuum correction) with the position of the stellar components at that epoch. The Brγ photocentre offsets are located between the two stars, but are more closely clustered towards the secondary. Both stars therefore contribute to the line emission, although the secondary contributes a significantly larger fraction (62 %) to the total line flux than the primary (48 %), confirming the values that we found independently with GRAVITY.

The higher Brγ flux measured towards the lower-mass secondary star indicates that

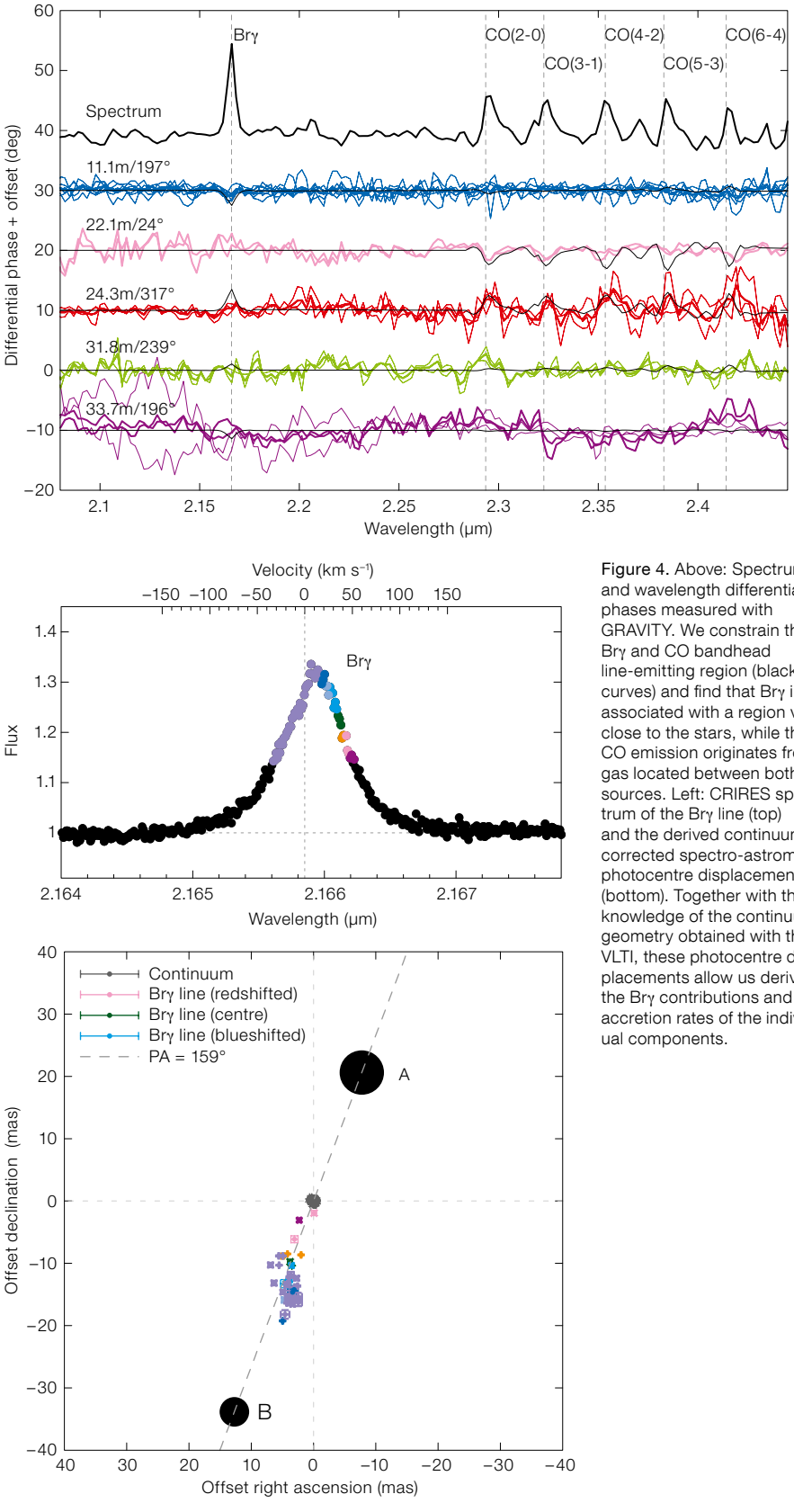

Figure 4. Above: Spectrum and wavelength differential phases measured with GRAVITY. We constrain the Brγ and CO bandhead line-emitting region (black curves) and find that Brγ is associated with a region very close to the stars, while the CO emission originates from gas located between both sources. Left: CRIRES spectrum of the Brγ line (top) and the derived continuum-corrected spectro-astrometric photocentre displacements (bottom). Together with the knowledge of the continuum geometry obtained with the VLTI, these photocentre displacements allow us derive the Brγ contributions and accretion rates of the individual components.

it accretes at a higher rate than the primary. This might seem counter-intuitive at first. However, hydrodynamic simulations predict that close companions disrupt the accretion stream onto the primary and channel most of the infalling material onto the circumsecondary disc, effectively limiting the mass that the primary can accrete (Bate & Bonnell, 1997). Our GRAVITY and CRIRES observations of IRAS 17216-3801 provide some tantalising first observational evidence of this effect.

Future outlook

The discovery of the IRAS 17216-3801 binary system and the unique capabilities of the VLTI open up exciting new opportunities to study dynamical interaction in high-mass protobinary systems and to characterise the physical conditions in circumstellar discs and circumbinary discs. There is a strong need to discover additional high-mass protobinary systems in order to build a statistically significant sample. This will allow us to explore the relation between binary properties (for example, separation and mass ratios) and the resulting disc structure, enabling a better understanding of the role of multiplicity in high-mass star formation.

Acknowledgements

This work was enabled by the tremendous advancements in the VLTI infrastructure over the last few years and the GRAVITY beam combiner (GRAVITY Collaboration, 2017). We thank the GRAVITY consortium and the Science Verification team, which is composed of ESO employees and GRAVITY consortium members.

References

Bate, M. R. & Bonnell, I. 1997, MNRAS, 285, 33
Bate, M. R. et al. 2000, MNRAS, 317, 773
Bate, M. R. et al. 2010, MNRAS, 401, 1505
Boley, P. et al. 2013, A&A, 558, 24
Caratti o Garatti, A. et al. 2016, A&A, 589, L4
Caratti o Garatti, A. et al. 2017, Nature Physics, 13, 276
Chini, R. et al. 2012, MNRAS, 424, 1925
Dale, J. E. & Davies, M. B. 2006, MNRAS, 366, 1424
GRAVITY Collaboration 2017, A&A, 602, A94
Johnston, K. et al. 2015, ApJ, 813, 19
Kratter, K. M. & Matzner, C. D. 2006, MNRAS, 373, 1563
Kraus, S. et al. 2008, A&A, 489, 1157
Kraus, S. et al. 2010, Nature, 466, 339
Kraus, S. et al. 2017, ApJL, 835, L5
Kuiper, R. et al. 2010, ApJ, 722, 1556
Kurosawa, R. et al. 2016, MNRAS, 457, 2236
Lazareff, B. et al. 2017, A&A, 599, L85
Papaloizou, J. C. B. & Terquem, C. 1995, MNRAS, 274, 987
Sridharan, T. K., Williams, S. J. & Fuller, G. A. 2005, ApJL, 631, L73

Enrico Sacchetti/ESO

The Very Large Telescope Interferometer Delay Lines.

ESO/P.Horálek

Upper: Preliminary design review of the Extremely Large Telescope instrument HARMONI involving members of the instrument consortium and the review team.

Lower: ESO press conference announcing the first discovery of a neutron star merger (Press Release: eso1733).

ESO/M. Zamani

DOI: 10.18727/0722-6691/5055

The ESO Survey of Non-Publishing Programmes

Ferdinando Patat[1]
Henri M. J. Boffin[1]
Dominic Bordelon[1]
Uta Grothkopf[1]
Silvia Meakins[1]
Steffen Mieske[1]
Marina Rejkuba[1]

[1] ESO

One of the classic ways to measure the success of a scientific facility is the publication return, which is defined as the refereed papers produced per unit of allocated resources (for example, telescope time or proposals). The recent studies by Sterzik et al. (2015, 2016) have shown that 30–50 % of the programmes allocated time at ESO do not produce a refereed publication. While this may be inherent to the scientific process, this finding prompted further investigation. For this purpose, ESO conducted a Survey of Non-Publishing Programmes (SNPP) within the activities of the Time Allocation Working Group[1,a], similar to the monitoring campaign that was recently implemented at ALMA (Stoehr et al., 2016). The SNPP targeted 1278 programmes scheduled between ESO Periods 78 and 90 (October 2006 to March 2013) that had not published a refereed paper as of April 2016. The poll was launched on 6 May 2016, remained open for four weeks, and returned 965 valid responses. This article summarises and discusses the results of this survey, the first of its kind at ESO.

Sample selection and general properties

The SNPP sample included all Normal, Guaranteed Time Observations (GTO) and Target of Opportunity (TOO) programmes that were scheduled between October 2006 and March 2013. This timeframe was selected to accommodate some delay between data acquisition and publication. To minimise ambiguity, we only considered programmes for which all runs were scheduled at the highest priority (i.e., Visitor Mode [VM] or A-ranked Service Mode [SM]). In addition, only programmes that had acquired a minimum amount of data were included in order to remove obvious cases, with a threshold of one science frame per allocated hour. In the selected period range, we identified 2716 proposals that obeyed the above criteria (90.7 % of the total A-ranked SM and VM proposals), involving 2089 Normal, 478 GTO and 149 TOO programmes.

According to the ESO bibliographic database telbib[2] (Grothkopf & Meakins, 2015), 1278 (47.1 %) of these programmes have not produced a refereed paper as of 16 April 2016. This gives an overall publication return of 52.9 % with publication fractions of 52.5 %, 52.7 % and 59.7 % for Normal, GTO and TOO programmes, respectively.

1143 Principal Investigators (PIs) were associated with the 2716 survey programmes; 755 (66.1 %) of the PIs from this group did not publish a paper associated with these programmes. 34 % of PIs published results for all programmes, 29 % published results for some programmes, and 37 % published results for none at all. 45 % of the PIs were associated with only one programme from the survey, and 55 % of these did not publish. On average, 1.1 proposals per PI have not yet produced a refereed paper.

The sample of 2716 survey programmes involves time allocated on 33 different instruments. For programmes that were allocated time on more than one instrument, we introduced the concept of a fractional proposal, attributing to a given instrument a fraction corresponding to the portion of total time assigned to it. For instance, if a programme was allocated one hour on FORS2 and four hours on UVES, this was counted as 0.2 and 0.8 proposals for the two instruments respectively. It is worth noting that 91.5 % of the survey proposals requested time on a single instrument, and 7.6 % requested two instruments. Table 1 shows the distribution of proposals per instrument for the entire survey sample, as well as for the sub-sample that did not publish. For simplicity, we grouped instruments with fewer than 50 proposals under OTHER. These correspond to 5 % of the total and involve eleven instruments, including SUSI2, TIMMI2 and VIRCAM.

Table 1. SNPP proposal distribution per instrument. The data are presented in ascending non-publishing fraction (last column). Only instruments with more than 50 programmes are listed separately. The rest is grouped under OTHER.

Instrument	No. of fractional proposals	% of total no. of proposals	No. of non-publishing pr.	% of total	Non-publishing fraction (%)
AMBER	249.6	9.2	148.6	11.6	59.5
CRIRES	132.2	4.9	82.2	6.4	62.1
EFOSC2	160.6	5.9	61.3	4.8	38.2
EMMI	58.4	2.2	25.7	2.0	44.0
FEROS	71.0	2.6	21.8	1.7	30.7
FLAMES	82.3	3.0	34.9	2.7	42.5
FORS1	55.7	2.0	24.1	1.9	43.3
FORS2	323.6	11.9	138.1	10.8	42.7
HARPS	103.4	3.8	22.9	1.8	22.1
HAWK-I	51.7	1.9	28.5	2.2	55.1
ISAAC	124.2	4.6	71.9	5.6	57.9
MIDI	96.2	3.5	34.9	2.7	36.3
NACO	256.1	9.4	130.5	10.2	51.0
OTHER	136.3	5.0	72.0	5.6	52.8
SINFONI	123.5	4.5	68.9	5.4	55.8
SOFI	132.0	4.9	53.8	4.2	40.8
UVES	148.6	5.5	56.0	4.4	37.7
VIMOS	101.1	3.7	61.3	4.8	60.7
VISIR	89.2	3.3	43.4	3.4	48.7
X-shooter	220.3	8.1	97.2	7.6	44.1
All	**2716.0**	**100.0**	**1278.0**	**100.0**	**47.1**

	Responses including option		Weighted responses	
Option	No.	%	No.	%
1. Published	124	12.8	102.5	10.6
2. Insufficient quality	202	20.9	128.7	13.3
3. Insufficient quantity	165	17.1	95.3	9.9
4. Inadequate tools	61	6.3	25.2	2.6
5. Null or inconclusive	187	19.4	117.9	12.2
6. Lack of resources	176	18.2	93.8	9.7
7. No longer interesting	38	3.9	21.9	2.3
8. Still working	352	36.5	228.3	23.7
9. Non-refereed paper	66	6.8	33.2	3.4
10. Other	188	19.5	118.2	12.2
			965	100

Table 2. Summary of the SNPP responses.

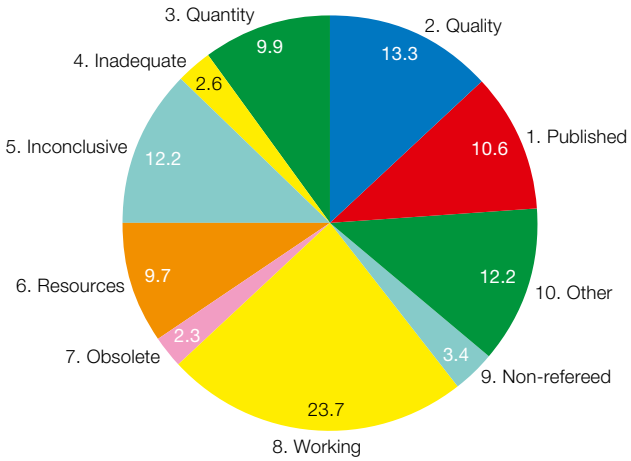

Figure 1. Results of the SNPP survey (weighted fractions of the various options; see text).

Table 1 also shows the nominal non-publishing fraction per instrument. According to this metric, which neglects instruments with low number statistics (i.e., OTHER), the most productive instrument is HARPS with a nominal publication return rate of about 78 %. At the other end of the distribution, VIMOS and CRIRES are characterised by return rates lower than 39 %. Although there is certainly a degree of instrument dependence, approximately 80 % of the proposals show a publication rate of less than 60 %, irrespective of the instrument used to produce the data.

The questionnaire

The PIs were asked the following question: "*Why were you not able to publish the results of your observations in a refereed paper?*" and were provided with ten possible options:

1. I did publish a refereed paper (provide a hyperlink in the comments).
2. Insufficient data quality (observations out of required specifications).
3. Insufficient data quantity (partially completed programme).
4. Inadequate ESO data reduction tools.
5. Null or inconclusive results.
6. Lack of resources on the PI side.
7. Science case no longer interesting.
8. I am still working on the data (provide time estimate in the comments).
9. I published a non-refereed paper (provide a hyperlink in the comments).
10. Other.

The web form included a free-text field for comments. The responses were tagged with the Programme ID, to enable the analysis of correlations between the answer and programme properties (for example, time, constraints, instruments, scientific category, etc.).

Of the 1278 targeted programmes, we received responses for 965 (75.5 %). Accounting for the fact that approximately 70 queries could not be delivered (due to out-of-date User Portal profiles), the response return was 80 %, which is much higher than expected from web-based surveys (~ 10 %; Fan & Yan, 2010). The response rate increased for more recent time allocations, with a response rate of 85 % from PIs associated with programmes from the last semester, compared to 70 % from PIs from the first semester.

PIs were allowed to select more than one option in their replies. Most selected a single option (55.5 %), with 31.1 % selecting two options and fewer than 10 % selecting three. The most popular single-option response was "8. I am still working on the data" (14 %), followed by "1. I did publish a refereed paper" (9 %). The most popular two-option response was "6. Lack of resources on the PI side" and "8. I am still working on the data" (5 %), followed by "2. Insufficient data quality" and "3. Insufficient data quantity" (3 %).

The general outcome of the survey is summarised in Table 2. Given the possible multiple options within each single response, the results are presented in two flavours. For each single option, we list the number and percentage of responses and the weighted number and percentage. The weighted values were computed by giving equal weights to the various options within the same response (Figure 1). By construction, the number of weighted responses (and percentages) adds up to 965 (100 %), whereas this is obviously not the case for the non-weighted responses. The two sets of numbers have different meanings: the latter is related to the frequency of responses associated with a given option, while the former provides information about its relative importance. The difference becomes clearer when considering the following simplified example. If a hypothetical survey includes the following four responses: (1, 1, [2, 4, 5, 6], [2, 7, 8, 9]), the non-weighted frequencies of options 1 and 2 are both 50 %. On the other hand, the weighted fractions of the two options are 50 % (1) and 25 % (2), respectively. Therefore, while options 1 and 2 were included in the same fraction of responses (50 %), option 1 is twice as significant.

The breakdown of responses by instrument shows some instrument-specific dependencies. For instance, while for X-shooter the frequency of option 8 is equal to the average (23.7 %), UVES is characterised by a significantly larger fraction (35.5 %), and AMBER shows a lower fraction (18.0 %). This may be related to the specific scientific areas covered by the instruments, the complexity of the

science cases involved, and their appeal to the community.

In the following sections, we will go into more detail for each of the options in the questionnaire.

Option 1: I did publish a refereed paper
Of the 124 responses associated with option 1, 14 provided incomplete information (for example, no link to the refereed publication or a link to a non-refereed publication). These cases were conservatively counted as non-published. The remaining 110 replies can be grouped as follows: a) the Programme ID was either wrong or absent (61; 55.5 %); b) the refereed paper appeared in print after the SNPP sample definition and was listed by telbib (25; 22.7 %); c) the paper is in the process of being accepted (21; 19.1 %); and d) the paper is missing from telbib (3; 2.7 %). 11.4 % of the responses correspond to false negatives (i.e., published programmes that were initially classified as non-publishing). This fraction, deduced from the 965 replies, can be used to compute the completeness-corrected value of the publication rate within the whole SNPP sample (*N* = 2716; 58.9 %).

In the following we use the term "completeness" to refer to the completeness of telbib. In response to the information provided by the PIs, 64 telbib records were modified. The vast majority (87.5 %) of these records were previously included in the database, but the particular Programme ID in question was missing. We updated these records accordingly. Only eight papers (12.5 %) had not previously been considered as using ESO data; these records were added to the telbib database without further verification. As a side note, the SNPP has allowed us to robustly determine that the telbib completeness is better than 96 %.

Options 2 and 3: Insufficient data quality and/or quantity
We will discuss options 2 and 3 together because there is a clear overlap, as confirmed by comments from the PIs. In total, these two options account for 23.2 % of the cases, with 8.2 % citing only option 2, and 4.9 % citing only option 3.

There is a striking difference between SM (32 %) and VM (68 %) programmes in the responses associated with option 2. This is likely due to the fact that VM observations are more adversely affected by bad weather conditions, while by definition SM is less affected by weather. We found a small correlation with requested seeing constraint and Quality Control (QC) grades in the SM programmes. Unsurprisingly, the majority of the affected SM programmes requested relatively good conditions (seeing < 1 arcsecond) and associated observations had higher fractions of B quality control (QC) grades (i.e., one of the observing constraints was violated up to 10 %) compared to the rest of the sample.

A clear dichotomy is also seen when considering responses per telescope, with the largest fractions related to the Very Large Telescope Interferometer (VLTI; 26 %), and Unit Telescope 1 (UT1; 20 %). The vast majority (90 %) of VLTI programmes involved AMBER and were associated with Guaranteed Time Observations (GTO), which are often riskier as they tend to involve new instrumentation. For UT1, most cases are related to the early years of CRIRES operations or problems with the degraded coating of the FORS2 longitudinal atmospheric dispersion corrector, which have since been resolved (Boffin et al., 2015).

A detailed analysis of the responses that only cited option 3 confirms that the corresponding programmes had been affected by weather, technical losses (in VM), or a completion fraction of lower than ~ 50 % (for SM). We conclude that most of the cases involving options 2 and 3 can be accounted for within ESO's operation model, and/or reflect the early operation of new complex systems.

Option 4: Inadequate ESO tools
This was the least selected option, with a weighted fraction below 3 %, indicating that a negligible fraction of users identify the software provided by ESO as the cause for non-publication.

Option 5: Null or inconclusive results
The fraction of cases reporting null or inconclusive results is comparable to that of option 2 (insufficient quality). Although null or inconclusive results are arguably part of the scientific process, PIs may be reluctant to admit this, potentially biasing the responses and underestimating the fraction. No correlation was found between the fraction of inconclusive results and the scientific subcategories of the programmes, indicating that all science cases are affected in similar ways.

Option 6: Lack of PI resources
The weighted frequency of this option is 9.7 %. When considered together with option 8 below, these two options account for 33.4 % and point to a significant difficulty in the community to keep up with the rate of data production.

Option 7: Science case no longer interesting
Only 2.3 % of the cases were indicated as obsolete science. These occurrences can be tentatively identified as instances in which the data delivery duty cycle and/or the time taken for the PI to make the data publishable was too long compared to the evolution in the given field.

Option 8: I am still working on the data
This was the most frequent response. Excluding the 13 cases in which options 1 and 8 were selected, a total of 339 responses included this option: 135 as single option, 49 with option 6, 26 with option 10, and 129 in other combinations. For a more quantitative approach we introduce the ratio, R, between the number of proposals for which work is still in progress and the total number of non-publishing proposals (corrected for telbib completeness). The previous numbers yield $R = 339/(965\text{-}110) = 39.6 \pm 2.5$ % for the overall SNPP sample. This ratio can be calculated individually for each semester to study its evolution with time. The completeness-corrected result is presented in Figure 2, which shows a net and steady overall decrease for older programmes. The fact that $R = 78$ and not zero for the earliest semester in the sample indicates that it takes longer than 12 semesters for all programmes that will eventually produce a refereed publication to do so.

Before we discuss this result in more detail, we will define the Publication Delay Time Distribution (PDTD), which describes the delay between the allocation and the publication time. This provides a measure of the complete duty cycle, including the time for ESO

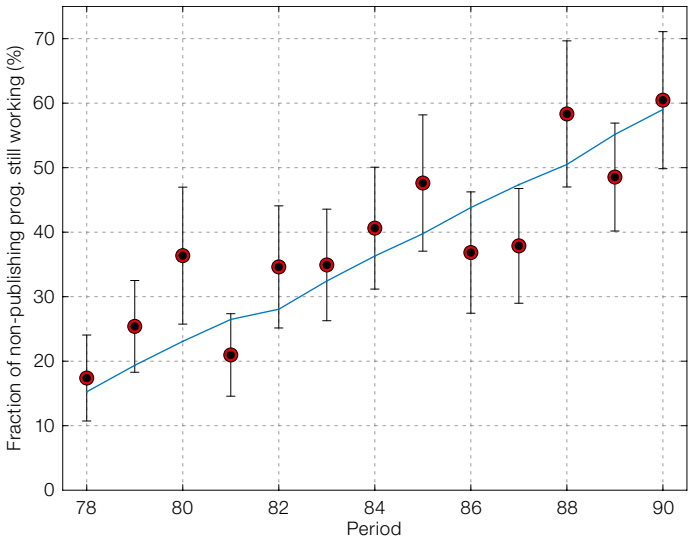

Figure 2. Completeness-corrected fraction of non-publishing programmes still working on the data as a function of allocation period (red symbols). The blue line traces the expected behaviour for $f_P{}^0 = 75.2\,\%$ (see text). The error bars indicate the Poissonian uncertainties (1-sigma level).

to deliver the data and for the user to process, analyse and publish them. We used the data provided by the ESO telbib interface to derive this function[b]. For each year from 2008–2015 we extracted the refereed publications per programme for programmes that used Paranal telescopes. Due to their nature, Large Programmes and Director Discretionary Time Proposals were excluded. Each publication in the sample of 1303 refereed papers is characterised by the publication year (t_P) and the programme's allocation period (P). A given publication year is tagged with its central semester, P_0[b]. The publication delay, in semesters, is then computed as $\Delta P = P - P_0$.

The sample data show that only 1.1 % of papers are published with a null delay using the above definition, while this grows to 11 % for $\Delta P = 6$ semesters, after which it steadily decreases for larger delays. This is illustrated in Figure 3, which also includes the cumulative distribution function, indicated as $C(t)$ (where the time t is counted from P). At face value, it takes 7 semesters to reach 50 % of the publications, and 20 semesters to reach 95 %, in agreement with Sterzik et al. (2016). The quantity $1–C(t)$ can be regarded as the probability that a programme that has not published a refereed paper after a time t, will publish it in the future. For example, a programme that has not published after 10 semesters has a 22 % residual probability of publishing in the future.

The behaviour of $R(t)$ in Figure 2 is a direct consequence of the publication delay. In fact, it is easy to show that if f_P^0 is the underlying publication fraction (i.e., the return rate one would measure for a sample of programmes at a time when $C = 1$), then the ratio $R(t)$ observed for a set of proposals all allocated in the same period and observed after a time t (i.e., the time when the survey is carried out) is given by:

$$R(t) = f_P^0 \frac{1-C(t)}{1-f_P^0\, C(t)}$$

One can also show that this expression can be applied to compute $\bar{R}$ for a whole sample, including programmes allocated in a period range, by replacing $C(t)$ with its weighted average $\bar{C}$:

$$\bar{C} = \frac{\sum_P N(P)\, C(P_S - P)}{\sum_P N(P)}$$

where $N(P)$ is the number of proposals allocated in semester P, and P_S is the period in which the survey is run. It can be readily demonstrated that the expected publication fraction at the time of the survey is simply $f_P = f_P^0\, \bar{C}$.

In the real case $\bar{C} = 0.78$, while the SNPP provided $\bar{R} = 0.396 \pm 0.025$. The above relation can be inverted to express f_P^0 as a function of $\bar{R}$, from which one can finally estimate the delay- and completeness-corrected return rate: $f_P^0 = 0.75 \pm 0.01$. This implies that after waiting a sufficiently long time, more than 20 semesters after the most recent period in the sample (see Figure 3), one would measure a publication return of approximately 75 %.

This calculation conservatively assumes that all programmes for which the users have specified option 8 will eventually publish. This assumption can be verified by comparing the real data with two predictions that descend from the above equation. The first is the overall publication fraction expected for the real SNPP case, which is given by $f_P = f_P^0\, \bar{C} = 58.5 \pm 1.0\,\%$. This can be directly compared to the completeness-corrected value derived from SNPP, 58.9 % (see above), which is fully consistent within the estimated uncertainty.

The second prediction concerns the time dependence of $R(t)$, as defined by the above relation. This is compared to the real SNPP data in Figure 2 (blue line), which illustrates how the predicted behaviour matches the data within the estimated uncertainties.

The above results indicate that the SNPP fraction of option 8 gives a realistic representation of the situation and is not the result of a "convenient answer" from PIs attempting to justify a lack of publication. In other words, the SNPP result is fully compatible with the estimated PDTD, and shows that the publication delay correction is significant, especially when the most recent periods included in the sample date back less than 10–12 semesters at the time of the survey.

Option 9: I published a non-refereed paper

The cases in which a programme did not publish a refereed paper but rather a non-refereed article account only for 3.5 % of the total. This implies that, with very few exceptions, if a project does not produce a refereed publication then it will not produce any publication at all.

Option 10: Other

This option reflected 12.3 % of the cases and the associated comments yielded a mixture of reasons, the most frequent being that the person leading the project left the field. Other recurrent explanations included: lack of ancillary data from other facilities, results not meeting expec-

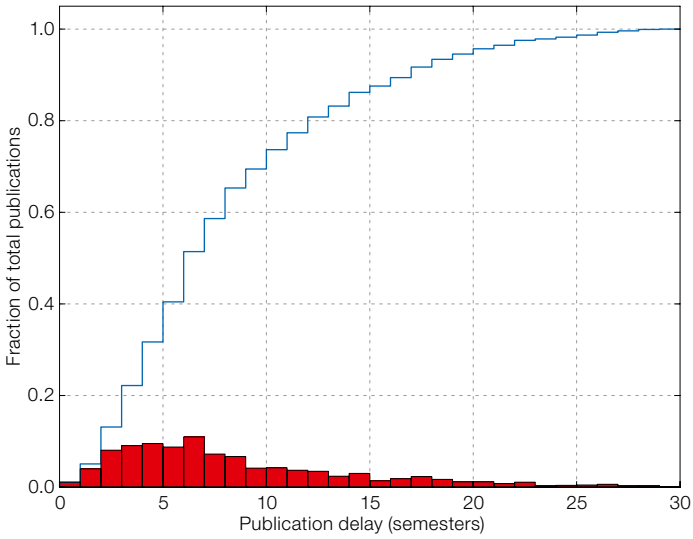

Figure 3. Publication delay time distribution. The blue line traces the cumulative distribution function $C(t)$.

	Service Mode			Visitor Mode		
	Allocated time		Publishing fraction (%)	Allocated time		Publishing fraction (%)
Quartile	Time range (nights)	Median time (nights)		Time range (nights)	Median time (nights)	
1	0.1–0.8	0.4	39.5 ± 4.3	0.1–1.2	1.0	50.5 ± 4.5
2	0.8–1.4	1.0	53.6 ± 4.7	1.2–2.1	2.0	53.0 ± 4.7
3	1.4–2.4	1.9	58.9 ± 5.9	2.1–4.0	3.0	66.0 ± 4.8
4	2.4–12.5	3.4	61.3 ± 6.1	4.0–12.5	6.0	68.9 ± 6.5

Table 3. Fraction of proposals that published at least one refereed paper for Service and Visitor Mode programmes as a function of allocated time (in nights) in the four quartiles of the respective time distributions.

tations, lowered priority of the project because of more pressing activities, quicker results obtained by other teams and/or with better-suited instruments, non-detections, etc.

Considerations on observing mode and allocated time

As a final analysis, we have derived the completeness-corrected publication fractions considering VM and SM separately, as the two observing modes were reported to behave in a different way by Sterzik et al. (2016). For this purpose, we have considered only single observing mode proposals within the SNPP initial sample, including 1089 SM programmes (40.1 %) and 1493 VM programmes (55.0 %). The remaining 134 mixed observing mode programmes (4.9 %) were excluded from the calculations. For each of the observing modes we have computed the time intervals that define the four quartiles of the respective time distributions. These differ for SM and VM, with median allocated times of 1.4 and 2.1 nights, respectively. For the time conversion, we adopted the ESO convention of 10 hours per night in odd periods and 8 hours per night in even periods.

Finally, we derived the publication fraction, f_P, within each time bin for the two observing modes separately (see Table 3). An interesting feature, common to both SM and VM, is the steady increase of the return rate for larger time allocations: the publication fractions in the fourth quartile are 60 % and 40 % larger than in the first quartile for the two modes, respectively.

Another aspect is the larger return of VM programmes when compared to SM (Sterzik et al., 2016). To some extent this is expected, as VM programmes tend to be larger than SM programmes. This becomes clearer when comparing SM and VM runs with the same median duration. For instance, the two rates are very similar for SM runs in their second quartile (53.6 %) and the VM runs in their first quartile (50.5 %), both having a median duration of one night. Although observing mode effects cannot be excluded, the amount of time allocated to the programme appears to be the dominant factor.

Figure 4 (upper panel) shows the dependence of publications on the allocated time, plotting the completeness-corrected publication fraction measured by SNPP in octiles of the overall time distribution (each time bin includes about 320 proposals). GTO programmes constitute 17.6 % of this sample, potentially biasing this result. As GTO programmes make systematic use of novel instruments designed to cover the specific science cases for which they were built, they tend to be more productive than average (Sterzik et al., 2015). For this reason, we produced a similar plot for Normal programmes (Figure 4, lower panel), which reveals a similar trend, albeit with more noise. We conclude that larger programmes tend to be more productive on average; this is in line with the results of Sterzik et al. (2015, 2016). We find the same trend within the Normal programmes, which account for the largest fraction of the allocation (both in terms of number of proposals and time).

In an attempt to understand what makes larger allotments more productive, we examined the frequency of the SNPP options as a function of allocated time, dividing the programmes into the four quartiles of the time distribution. No significant dependence was found for any of the options, suggesting that the lower observed return rate f_P for smaller time allocations was the fruit of a lower inherent return rate f_P^0, regardless of the reason for the lack of publication.

We note that two non-publishing programmes with very different allocations are counted in the same way here. However, it is obvious that they have a different impact in terms of “wasted” telescope time. To quantify this aspect, we computed the telbib completeness-corrected fraction of scheduled time that was allocated to non-publishing programmes as a function of their size (in the four quartiles of the time distribution). We did this for the entire SNPP sample, both as observed and correcting for the publication delay

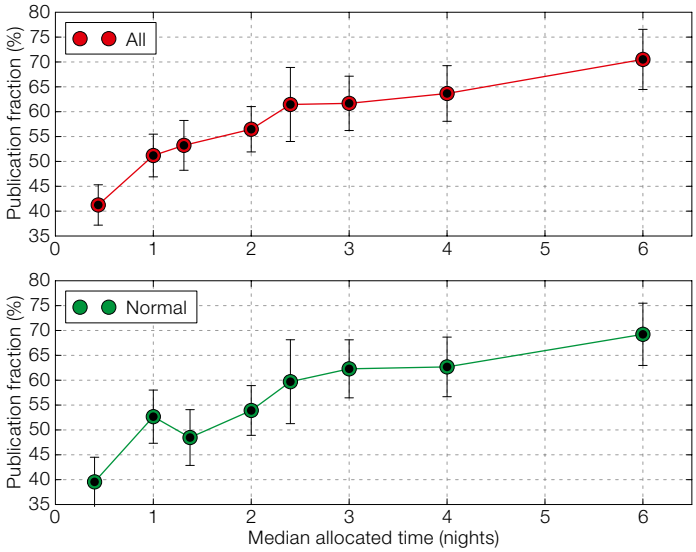

Figure 4. Fraction of proposals that publish at least one refereed paper as a function of allocated time (nights) for all programme types (upper panel) and for normal programmes only (lower panel). The ×-axis position of the points marks the median allocated time within each octile bin.

Quartile	Allocated time: Time range (nights)	Allocated time: Median time (nights)	Fraction of total time allocated to non-publishing progs. (%): Observed	Fraction of total time allocated to non-publishing progs. (%): Delay-corrected
1	0.1–1.0	0.7	4.0	3.1
2	1.0–2.0	1.7	8.5	6.1
3	2.0–3.0	3.0	8.1	5.6
4	3.0–12.5	4.5	16.2	10.5
All	0.1–12.5	2.0	36.8	25.3

Table 4. Fraction of allocated telescope time not producing a refereed paper in the four quartiles of the time distribution measured by SNPP (Observed) and extrapolated in the hypothesis that all programmes that included option 8 (still working) will eventually publish (Delay-corrected).

(Table 4), assuming that all the work from in progress cases will eventually produce a refereed paper. At the time of the SNPP survey, about 37 % of the time allocated to A-ranked SM and VM programmes had not produced a refereed publication. This fraction in time is very similar to the corresponding completeness-corrected fraction in proposals (100 % – 58.9 % = 41 %). Once corrected for the publication delay, this fraction reduces to about 25 %. Therefore, as in the case of the number of proposals, about one quarter of the telescope time allotted to A-ranked SM and VM proposals will not lead to a refereed publication.

A closer inspection of Table 4 reveals that, although larger programmes tend to be more successful in terms of producing at least one publication (Table 3 and Figure 4), the non-publishing time fraction tends to increase with their size. This finding is equivalent to the lower number of publications per programme per unit of allocated time that was reported by Sterzik et al. (2015, 2016) for proposals with sizes between the short Normal (below 20 hours) and Large Programmes (above 100 hours).

One can assume that there exists an optimal distribution of allocated times that maximises scientific return and minimises the waste of telescope time. Identifying such an ideal distribution is beyond the scope of this paper. However, Table 4 allows us to gain a first insight into the boundary conditions of such a parameter search: in both cases (observed and delay-corrected), programmes with allocations below and above ~ 2.5 nights "waste" the same amount of time. This implies that increasing the number of programmes with allocations larger than this value would effectively decrease the overall amount of time that leads to no refereed publication.

This can be understood considering two extreme cases in which the schedule is completely filled with a) only programmes shorter than one night, or b) only programmes longer than three nights. The first case would yield a much larger number of allocated programmes than in the second case (by a factor larger than 12), but the total amount of "wasted" time would also be larger. The SNPP data, once corrected for completeness and time delay, show that about 40 % of programmes shorter than one night do not publish, producing a time waste of this same magnitude in the hypothetical first case.

On the other hand, programmes longer than three nights would "waste" less time (about 20 %), but the number of published papers would be much smaller than in the first case, which would likely result in a decrease of the overall scientific return.

These simple considerations suggest that the optimal distribution of allocated times must ensure the proper level of diversity, by including a mix of programme sizes.

Conclusions

The performance of a scientific facility can be evaluated using various metrics, each of which are affected by different issues. In this study, we have focused on the binary bibliographic figure of merit, i.e., the publication or lack of publication of at least one refereed paper. This is one of the simplest bibliometric estimators, as it does not account for the publication's impact or the resources involved. The fact that a programme has not yielded a refereed publication does not necessarily imply that the observations were a complete waste of resources. Nevertheless, analysing this aspect and understanding its possible causes is certainly one of the basic steps that institutes and organisations such as ESO must undertake to characterise their overall efficiency.

The SNPP has shown that there are many reasons why a programme may not produce a refereed publication. With the notable exception of option 8 ("team still working on the data") and the combination of options 2 and 3 ("insufficient data quality and quantity"), there is not a single, dominant culprit.

The relatively large fraction of proposals for which work is still in progress (~ 40 %) is fully compatible with the Publication Delay Time Distribution deduced from an

independent set of programmes. Once corrected for the publication completeness of the telbib database — where the vast majority of the missing cases are generated by wrong or absent Programme IDs in the published papers — and for the publication delay, the estimated asymptotic publication rate is approximately 75 %. This means that, at least in the phase covered by the SNPP, about a quarter of the proposals scheduled in VM and/or in A-ranked SM will never publish a refereed paper.

Although this fraction can likely be decreased by further improving the overall workflow, part of the problem may be inherent. The non-negligible fraction of cases of insufficient resources (generally option 6 but also indicated in option 10) and the typically long publication delay may be symptoms of workload pressure in the community. The significant numbers of cases in which negative or inconclusive results do not turn into publications also support this conclusion. This reflects what may be a growing cultural problem in the community as scientists tend to concentrate on appealing results, especially if they have limited resources, and need to focus predominantly on projects that promise to increase their visibility (see Matosin et al., 2014 and Franco, Malhotra & Simonovits, 2014).

An important result that emerged from this study is the higher publication rate of programmes associated with larger allocations of telescope time. This is detected in both observing modes (SM and VM) as well as in the Normal programme type sub-sample. The SNPP did not reveal any significant dependence on allocated time in the distributions of responses for programmes with no refereed publications. This may be interpreted as an indication that a minimum amount of data is required to achieve results of a sufficient quality and quantity to warrant a publication (including the necessary effort that goes with it) across all science cases. We cannot exclude the possibility that the time distribution is skewed towards smaller requests by the general perception that this increases the chances of success rate during the selection process.

As the scientific process requires experimentation, it is necessary for an observatory to accommodate a fraction of risky proposals. When compounded with technical and weather losses, a 100 % return in publications across all programmes becomes impossible. Nevertheless, the current level of 75 % may be improved by a further 10–15 % by addressing specific factors. For example, by further optimising how observations are scheduled and executed at the telescope and re-evaluating the optimal fraction of risky observations, ESO can improve its data delivery performance. At the same time, the community can optimise the distribution of resources to ensure that data can be analysed more effectively as soon as it becomes available.

Acknowledgements

The authors are grateful to Francesca Primas, Martino Romaniello, and all of the members of the Time Allocation Working Group for their help during the formulation of the SNPP questionnaire.

References

Boffin, H. M. J. et al. 2015, The Messenger, 159, 6
Fan, W. & Yan, Z. 2010, Computers in Human Behavior, 26(2), 132
Franco, A., Malhotra, N. & Simonovits, G. 2014, Science, 345, 1502
Grothkopf, U. & Meakins, S. 2015, ASP conference series, 492, 63
Matosin, N. et al. 2014, Disease Models and Mechanisms, 7(2), 171
Sterzik, M. et al. 2015, The Messenger, 162, 2
Sterzik, M. et al. 2016, SPIE, 9910E..03S
Stoehr, F. et al. 2016, arxiv:1611.09625

Links

[1] Time Allocation Working Group Report: http://www.eso.org/public/about-eso/committees/uc/uc-41st/TAWG_REPORT.pdf
[2] ESO telbib database: http://telbib.eso.org

Notes

[a] Throughout this paper the definition of non-publishing programmes includes archival publications, i.e., articles that would be published by scientists not included in the list of co-investigators for the given proposal. Therefore, in this study, a non-publishing programme is one that has produced no refereed publication of any kind.

[b] Any given calendar year intersects with three ESO semesters, only one of which is fully contained in the given year (the one running from 1 April to 1 October). We call this the central semester P_0. The data show that for any year in our telbib sample, no publication is produced in P_0+1, while there is always at least one publication in P_0, and several in P_0–1. Therefore, P_0 can be regarded as the most recent scheduled period producing a publication in the given year. P_0 is simply given by $P_0 = 2(t_p - 2008) + 81$. Although the time delay could be defined and computed in a more accurate way, a resolution of one semester is sufficient for the purposes of this study.

ESO/B. Tafreshi (twanight.org)

The Very Large Telescope.

DOI: 10.18727/0722-6691/5056

On the Availability of ESO Data Papers on arXiv/astro-ph

Uta Grothkopf[1]
Dominic Bordelon[1]
Silvia Meakins[1]
Eric Emsellem[1]

[1] ESO

Using the ESO Telescope Bibliography database telbib, we have investigated the percentage of ESO data papers that were submitted to the arXiv/astro-ph e-print server and that are therefore free to read. Our study revealed an availability of up to 96 % of telbib papers on arXiv over the years 2010 to 2017. We also compared the citation counts of arXiv *vs.* non-arXiv papers and found that on average, papers submitted to arXiv are cited 2.8 times more often than those not on arXiv. While simulations suggest that these findings are statistically significant, we cannot yet draw firm conclusions as to the main cause of these differences.

The ESO Telescope Bibliography telbib is a database of refereed papers published by the ESO user community[1]; all telbib data papers use at least some data from ESO facilities. The telbib database is curated and further developed by the ESO librarians. Records in the database are linked to the ESO Science Archive, enabling easy access from the literature to the data used in the papers and *vice versa*. In addition, telbib entries are comprehensively tagged and annotated, allowing us to derive visualisations, statistics and reports for various parameters. The telbib content spans more than 20 years, beginning with the publication year 1996, and the database has become an essential tool in understanding publishing trends among the ESO user community. Further information about telbib is available on the web[2,3].

As of July 2017, telbib included almost 13 600 records. 95 % of these papers were published in the core astronomy journals, namely in Astronomy & Astrophysics (A&A; 49 %), the former Astronomy & Astrophysics Supplement Series (A&AS; 2 %), the Astrophysical Journal (ApJ; 20 %), the Astrophysical Journal Supplement Series (ApJS; 1 %), the Monthly Notices of the Royal Astronomical Society (MNRAS; 19 %), and the Astronomical Journal (AJ; 4 %). A more detailed distribution of ESO data papers across journals can be seen in Figure 1.

The ESO Library provides journal access to ESO staff through subscriptions. In astronomy, the most prominent journals (A&A, ApJ/ApJS, AJ and MNRAS) are community owned and operated. This enables astronomers to influence developments in journal publishing to a large extent, including changes to subscription fees and page charges. This differs across scientific disciplines. Steep increases in subscription fees to scholarly journals, along with widespread public access to the internet, led to the start of the Open Access (OA) movement in the 1990s.

Open Access publications

According to the Scholarly Publishing and Academic Resources Coalition (SPARC), Open Access in scholarly literature is defined to be the "free, immediate, online availability of research articles coupled with the rights to use these articles fully in the digital environment"[4]. This means that users can read, download, copy, distribute, and text mine articles, or use them for any other lawful purpose. Creative Commons copyright licenses define standardised ways of sharing and reusing. The most commonly-used license, called "CC BY Attribution", allows a wide range of reuses provided that credit is given to the original creators. An overview of CC licenses can be found on the Creative Commons website[5].

Different classifications exist to describe the various flavours of open access; the most common versions are as follows:

1. Green OA: Papers are typically published in subscription-based journals, but authors self-archive manuscripts on their webpages or submit them to institutional or subject-based repositories (for example, arXiv/astro-ph) where the articles are free to read for everyone. Green OA does not require a CC license.
2. Gold OA: Articles are published in OA journals. Authors, institutions, or other stakeholders pay a publication fee so that the articles become available to everyone for all permitted uses. These are governed by CC licenses. Some publishers offer the option for authors to pay an article processing charge (APC) to make individual articles available through open access in otherwise subscription-based journals; this is then called "hybrid OA".
3. Delayed and temporary OA: Responding to the mandates issued by governments and funding agencies, many journals are applying delayed OA by providing free access to their publications after a given time. Most core astronomy journals are currently available and are free to read after one year, with the exception of MNRAS, which is only free to read three years after publication. Since these articles were originally published in a subscription-based (toll-access) journal, there is no CC license. Alternatively, publishers may choose to provide free access to specific sections or articles — for

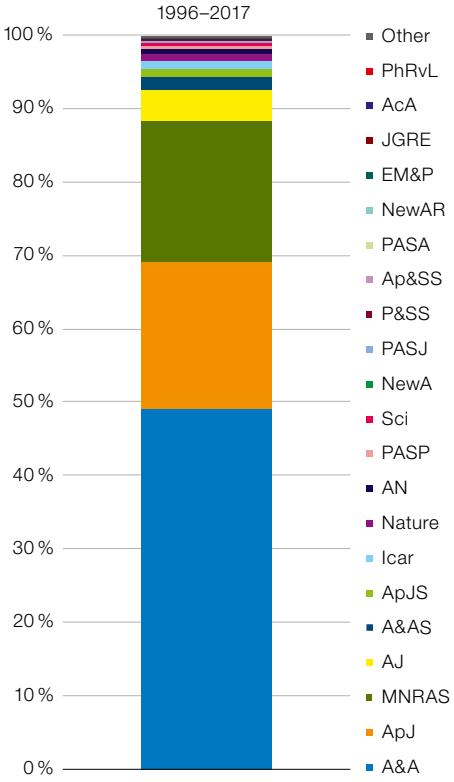

Figure 1. Journal distribution of ESO data papers published between January 1996 and July 2017 (total number: 13 569). Journals in which less than three telbib papers were published are categorised as Other.

example, the latest issue — for a specific amount of time.

In a recent article, Piwowar et al. (2017) undertook a large-scale analysis of the dissemination of OA articles in the sciences. They found that at least 28 % of the scholarly literature is OA, equivalent to 19 million articles out of the 67 million included in the study. By far the largest number falls in a category called "Bronze OA" by the authors, meaning that the articles are free to read on the publisher's website but do not have an explicit open access license (similar to the delayed/temporary OA mentioned above). In astronomy, the huge archive of historic literature pertains to this category, including core journals such as A&A, ApJ, AJ and MNRAS spanning back to the first volumes. These historic volumes were scanned by the National Aeronautics and Space Administration Astrophysics Data System (NASA ADS) Abstract Service in collaboration with the Wolbach Library at the Harvard-Smithsonian Center for Astrophysics, and are freely available to the community (Eichhorn et al., 2003).

Piwowar et al. (2017) also studied the so-called OA citation advantage in order to verify whether open access articles are actually cited more often. The authors report that on average, OA articles receive 18 % more citations. In this paper, we study the fraction of papers published between January 2010 and July 2017 that are included in the telbib database and have been submitted to arXiv/astro-ph. We also investigate whether there is any difference in impact (as measured by the number of citations) between papers that were submitted to arXiv and those that were not.

telbib papers and arXiv/astro-ph

The astronomy community has a strong culture of sharing research products, including scientific papers, observatory publications, data, presentation slides, software, code, etc. It is not surprising that astronomers were among the early adopters of the arXiv/astro-ph e-print server and continue to be one of the strongest user groups today, according to arXiv submission rate statistics[6].

Number of papers	2010	2011	2012	2013	2014	2015	2016	2017
All telbib	738	786	866	842	871	865	944	601
Posted on arXiv	653	712	793	787	822	827	909	567
Non-arXiv	85	74	73	55	49	38	35	34
Percentage arXiv	88.5 %	90.6 %	91.6 %	93.5 %	94.4 %	95.6 %	96.3 %	94.3 %

Table 1. Number of papers per year per category: all telbib papers, arXiv papers, non-arXiv papers and the percentage of telbib papers posted on arXiv.

Figure 2. Percentage of telbib papers submitted to arXiv between January 2010 and July 2017.

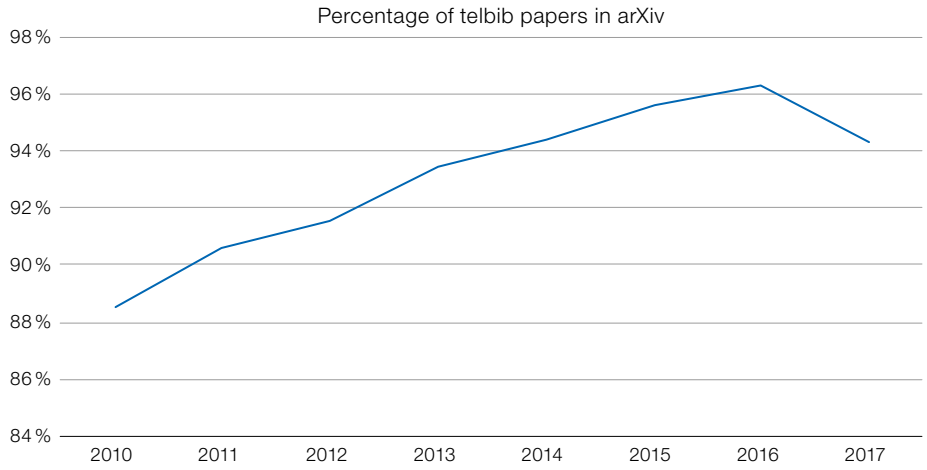

Taking this tradition into account, we investigate the extent to which papers that use ESO data are free to read. We do not include all flavours of OA, but merely study whether or not papers included in telbib have been submitted to arXiv. Articles that are available otherwise, be it through open access journals, via delayed OA, or as part of a section made available free of charge for a given time by the publisher, are not defined as free to read here unless they were also posted on arXiv.

Methodology

We used telbib to obtain a list of NASA ADS bibliographic reference codes (bibcodes) for ESO data papers for each year. This list was posted to the ADS Search application programming interface (API) requesting the bibcode, identifier and citation count fields. The identifier field is an array of identifiers that ADS stores, including bibcodes, DOIs and arXiv IDs.

In the result set, we searched each record's list of identifiers for either an arXiv bibcode (i.e., a bibcode created for an ADS preprint and replaced by a journal-based bibcode after publication) or an arXiv identifier with its own consistent pattern. We catalogued these as arXiv papers accordingly.

After querying the ADS API, we took an additional verification step of querying arXiv for the papers that seemed to be "non-arXiv". We searched by author, year and title fragments, then manually compared result records to their ADS counterparts. Using this method we found approximately 30 additional papers that were hosted on arXiv across the seven-year span. These papers were subsequently assigned to the arXiv paper category.

Fraction of ESO data papers on arXiv/astro-ph

Our study focused on refereed papers published from January 2010 to July 2017 in the ESO Telescope Bibliography. In 2010, 88.5 % of the telbib papers were submitted to arXiv. A steady increase can be seen over the following years until an impressive submission rate of 96.3 % is reached in 2016. The percentage seems to be lower in 2017, but only the first seven months of this year could be considered.

Total number of citations	2010	2011	2012	2013	2014	2015	2016	2017
All telbib	33.776	29.693	27.783	26.453	20.046	14.630	8.226	1.953
Posted on arXiv	32.251	28.409	26.516	25.909	19.534	14.408	8.138	1.939
Non-arXiv	1.525	1.284	1.267	544	512	222	88	14

Median number of citations								
All telbib	26	24	21	19	15	11	5	2
Posted on arXiv	30	26	22	21	16	11	6	2
Non-arXiv	10	12.5	11	7	6	3	2	0
Ratio arXiv *vs.* non-arXiv	3.0	2.1	2.0	3.0	2.7	3.7	3.0	

Table 2. Total and median number of citations: all telbib papers, papers posted on arXiv, and papers not posted on arXiv, along with the ratio of arXiv *vs.* non-arXiv median citations (from January 2010 to July 2017; citations as of 28 August 2017).

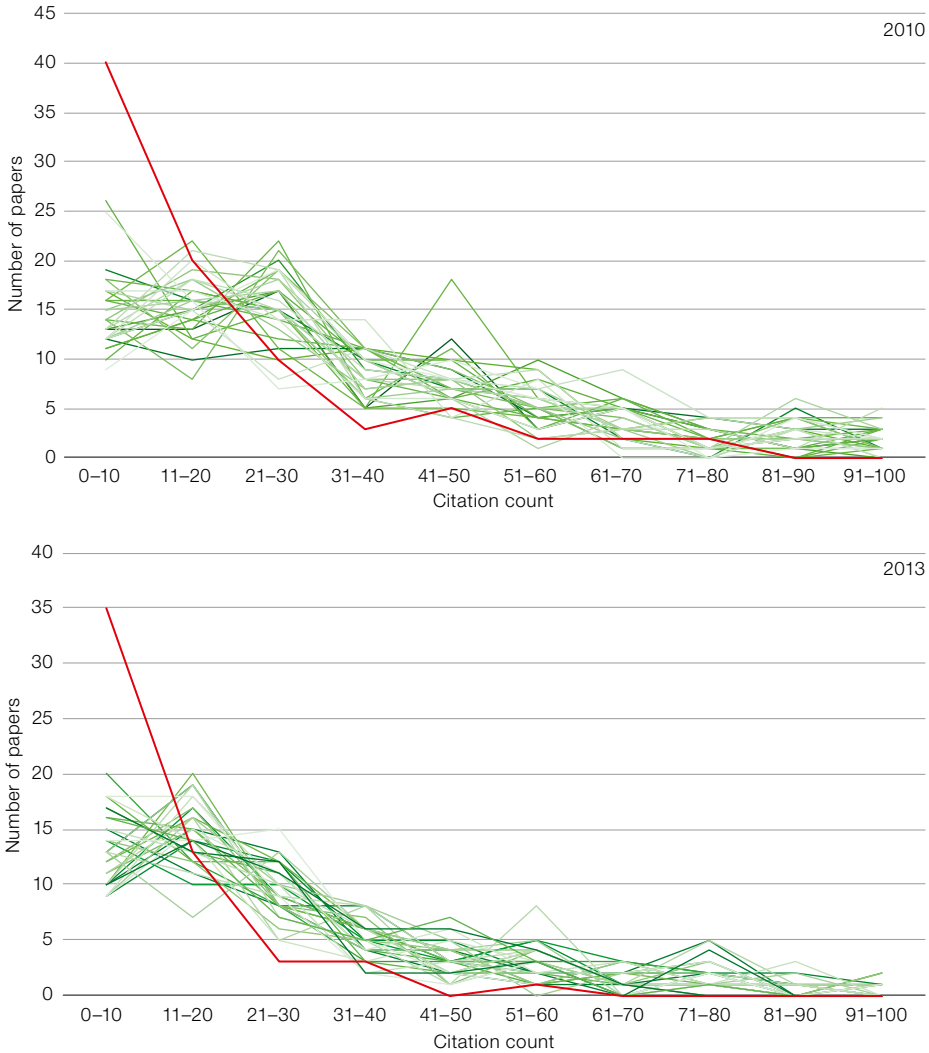

Figure 3. The distribution of citations for non-arXiv papers published in 2010 and 2013 (red line) *vs.* realisations of the same number of randomly selected papers from the entire set of telbib papers published in that year (green lines) for 2010 (top: 85 papers) and 2013 (bottom: 55 papers).

The detailed results are given in Table 1, while Figure 2 shows the percentage of telbib papers in arXiv by year.

Looking in more detail at the non-arXiv papers, we found a wide variety of author affiliations and ESO facilities that provided the observations for these papers. In addition, non-arXiv manuscripts were published in all the major astronomy journals. We also investigated the impact of these non-arXiv papers, where impact is defined as the number of citations relative to the median AJ citation (Bordelon et al., 2016). The most cited non-arXiv papers have an impact of approximately 7–10 for the publication years 2010–2016, with one paper reaching an impact of greater than 17. This means that these specific papers have been cited considerably more often than the median AJ paper of the same year. However, such high-impact papers appear to be outliers. In summary, no obvious pattern can be identified at first glance that would explain why some papers were not submitted to arXiv.

In order to further investigate possible reasons for not submitting a paper to arXiv, we conducted an (unrepresentative) survey among some of the authors of non-arXiv papers (~ 20 % of the 2016 and 2017 papers), asking them about their motivation. While we only received a response rate of about 60 %, we found that there are various reasons for non-submission. Most frequently, authors were too busy for the submission process and had other priorities. One author stated that arXiv was not considered essential for the publishing process.

Differences in citation counts of ESO data papers posted on arXiv *vs.* non-arXiv

In a second step, we investigated whether arXiv papers are indeed cited more often. For the same set of papers as before (telbib papers published between January 2010 and July 2017), we obtained the citations from the ADS and calculated the total and median citations for the two groups (Table 2).

Comparing the median citations for the years 2010–2016, we found that

manuscripts submitted to arXiv received on average 2.8 times more citations than the non-arXiv papers, despite the few high-impact non-arXiv papers mentioned above. Naturally, the most recent papers have not gathered enough citations to achieve a meaningful result. Kolmogorov-Smirnov tests have been conducted to verify our findings. The results suggest that the differences between arXiv and non-arXiv papers are very significant.

We also compared the citation counts of non-arXiv papers with realisations of the same number of randomly selected telbib papers from the same year. For the years of our study, the non-arXiv sets show particularly high fractions of papers with low citations (0–10), followed by only a few papers with higher citations (> 30 citations for publication years 2010–2012; > 20 for publication years 2013–2014; and > 10 for publication years 2015–2017). Two examples from publication years 2010 and 2013 are shown in Figure 3.

Conclusion

Using the ESO Telescope Bibliography (telbib) as a testbed, we investigated the fraction of refereed papers published between January 2010 and July 2017 that were submitted to arXiv/astro-ph and are therefore free to read. Our study revealed an increasing fraction of papers posted on arXiv, from 88.5 % in 2010 to 96.3 % in 2016. The percentage for 2017 (94.3 %) should be treated with caution as the year is not yet complete and the fraction may change. Why some papers are not posted on arXiv is unclear, as there are no significant trends among this group in terms of ESO facilities used, author affiliations or journals involved. A survey among these authors suggested various motivations for non-submission, with the top reason being a lack of time for the submission process.

A comparison of the average citation counts of arXiv *vs.* non-arXiv papers revealed that on average, papers published between 2010 and 2016 that were made available on the e-print server receive a factor of 2.8 more citations. Simulations suggested that these findings are statistically significant. While the differences in citations seem striking at first glance, we note that the sample of non-arXiv papers investigated is small (on average, 55 papers per year). Posting manuscripts on arXiv certainly enhances their visibility among the community, but we cannot draw a definitive conclusion as to whether these differences in citations are solely caused by submission to arXiv or whether other factors are at play.

Based on this study of telbib papers, we conclude that an almost complete availability of the core literature in astronomy through green OA puts the community in an advantageous situation regarding both literature access and dissemination.

Acknowledgements

We thank Wolfgang Kerzendorf and Jason Spyromilio for inspiring discussions (and a constant supply of chocolate). This research has made use of NASA's Astrophysics Data System; thank you so much ADS team for your excellent service to the community!

References

Bordelon, D. et al. 2016, Proc. SPIE., 9910, 99102B
Eichhorn, G. et al. 2003, LISA IV, ed. Corbin, B. G., Bryson, E. P. & Wolf, M., (Washington, DC: U. S. Naval Observatory), 145
Piwowar, H. et al. 2017, PeerJ Preprints, 5, e3119v1

Links

[1] telbib database: telbib.eso.org
[2] telbib methodology: www.eso.org/sci/libraries/telbib_methodology.html
[3] ESO Libraries publications: www.eso.org/sci/libraries/useful_links/publications.html
[4] SPARC Open Access: https://sparcopen.org/open-access
[5] Creative Commons licensing: https://creativecommons.org/share-your-work/licensing-types-examples
[6] arXiv submission rate statistics: https://arxiv.org/help/stats/2016_by_area/index

DOI: 10.18727/0722-6691/5057

Report on the ESO and Excellence Cluster Universe Workshop

Galaxy Ecosystem: Flow of Baryons through Galaxies

held at ESO Headquarters, Garching, Germany, 24 –28 July 2017

Vincenzo Mainieri[1]
Paola Popesso[2]

[1] ESO
[2] Technical University of Munich, Germany

This conference focussed on the "baryon cycle", namely the flow of baryons through galaxies. The following aspects were discussed: a) the gas inflow into systems through streams of pristine gas or as drizzles of recycled material; b) the conversion of this gas into stars; and c) the ejection of gas enriched with heavy elements through powerful outflows. Understanding these different but mutually connected phases is of fundamental importance when studying the details of galaxy formation and evolution through cosmic time. This conference was held following the month-long workshop of the Munich Institute for Astro- and Particle Physics (MIAPP)[1] entitled: "In & out: What rules the galaxy baryon cycle?" It therefore provided an opportunity to share the main outcomes of the MIAPP workshop with a larger audience, including many young outstanding scientists who could not attend the MIAPP workshop.

In total, the conference attracted 132 participants who attended 67 talks over the

Figure 1. Participants of the workshop in front of ESO headquarters.

course of one week[2]. The first day was dedicated to the observational and theoretical constraints of gas inflow into galaxies. The need for gas replenishment in galaxies has been established for a long time in order to explain the constant star formation activity of star-forming galaxies over the past 10 Gyrs. The volume of the observed cold gas reservoir is only sufficient to sustain star formation on relatively short timescales of approximately one Gyr, which implies that a galaxy’s gas must constantly be replenished.

Simon White opened the conference by highlighting many unresolved questions regarding the nature of gas infall and the possible role of outflows in regulating galaxy star formation activity. A review by Christopher Martin presented the potential of using the recently commissioned Keck Cosmic Web Imager (KCWI) instrument to map Lyα nebulae around distant quasars and streams of pristine gas infalling into galaxies at very high redshifts. Similarly, Fabrizio Arrigoni Battaia emphasised the role of the Multi Unit Spectroscopic Explorer (MUSE) instrument on the Very Large Telescope (VLT) by discussing a survey of ~60 quasars at $z \sim 3$, which aimed to study extended ultraviolet emission tracing the inflow of cool gas from the circumgalactic medium (CGM) into the galaxy.

Joop Shaye showed how mock spectra generated by the EAGLE (Evolution and Assembly of GaLaxies and their Environments) project, a cosmological hydrodynamical simulation, can be used to analyse the Keck Baryonic Structure Survey Data. This analysis suggests that the prominent redshift-space distortions observed in the H I, C IV and Si IV absorption features around galaxies at redshift $z \sim 2$ are predominantly caused by gas infall rather than outflows. Dusan Keres discussed the interconnection of gas inflows and outflows in regulating galaxy star formation activity in numerical simulations. In low-mass galaxies, the inflow of gas triggers star formation and consequently supernovae outflows. The fate of the outflowing gas is either to leave the galaxy, if its velocity exceeds the escape velocity of the system, or to lead to gas circulation by falling back into the galaxy in a so-called “galaxy fountain”.

The second day of the conference was dedicated to reviewing our current understanding of the evolution of the gas content of galaxies though cosmic time and the efficiency in converting it into stars. Claudia Lagos showed how semi-analytical models with very different predictions about galaxy gas content can reproduce the evolution of the galaxy stellar mass function and the cosmic star formation history remarkably well. This points to the need for the next generation of models to focus on correctly reproducing the neutral and molecular gas content of galaxies through cosmic time.

Eva Schinnerer presented several highlights of the Physics at High Angular Resolution in Nearby GalaxieS (PHANGS) project, which is mapping a sample of local star-forming galaxies at high angular resolution. MUSE and ALMA high-resolution observations show that: a) the star formation efficiency is not uniform, with significant variations inside the galaxy; b) the molecular gas structure depends on the local environment within the system; and c) active galactic nuclei (AGN) feedback might alter the velocity and chemistry of the gas. Moving to higher redshifts, Reinhard Genzel reviewed our current understanding of the evolution of the gas content of galaxies though cosmic time, using a sample of more than 600 galaxies with CO detections from the Institut de Radioastronomie Millimétrique (IRAM) and the Atacama Large Millimeter/submillimeter Array (ALMA), and infrared detections from the Herschel Space Observatory. Several scaling relations were discussed, including the evolution of the cold gas depletion time *versus* specific star formation, which show consistent results in different tracers of the cold gas mass.

The last two days of the conference were dedicated to discussing whether gas outflows were due to either AGN or stellar feedback. The aim was to understand the

following aspects: a) the multi-phase nature of a gas outflow; b) its connection to the inflow; c) its effect on the galaxy cold gas content and thus star formation activity; and d) its effect as preventive feedback in massive halos. As a first step, several speakers presented both observations and simulations, trying to clarify the occurrence of outflows and galactic winds in AGN and star forming galaxies. David Rupke reviewed the demographics of AGN outflows in the local Universe, and showed that most nearby quasars host galactic scale outflows in ionised gas, most likely powered by the quasar itself.

Ongoing surveys such as KASH*z* (KMOS AGN Survey at High redshift) and SUPER (SINFONI Survey for Unveiling the Physics and the Effect of Radiative feedback) will extend studies to much higher redshifts and link the properties of large-scale outflows with those of the galaxies' central black holes (for example, through measurements of the Eddington ratio, luminosity, black hole mass).

Thorsten Naab gave a review, from a theoretical perspective, of the galactic winds due to stellar outflows in several gas phases (molecular, neutral and ionised). While the simulations suggest that in most cases the gas should escape the galaxy, the observed outflow velocities for both AGN and stellar feedback outflows are well below the galaxy escape velocity. This could point to the circulation of gas that falls back into the system after outflowing from the disc to a small distance away, leading to accretion of recycled material.

The potential impact of outflows on the gas content of a galaxy and therefore its star formation activity was the subject of much discussion. Roberto Maiolino showed observational evidence for outflows to remove gas locally within the galaxy without affecting the global galaxy properties. As also pointed out by Romeel Dave during his review, AGN-driven outflows may provide preventive feedback by dumping energy into the galaxy halo and therefore preventing further gas accretion. However, the uncertainties in the current estimates of the mass-loading factor and wind geometry are still large, and the observational evidence for clear gas inflow into galaxies is elusive. Integral field spectroscopy with MUSE and ALMA will reveal much more about the nature of galaxies as "gas factories" in the near future.

Links

[1] MIAPP workshop: http://www.munich-iapp.de/programmes-topical-workshops/2017/galaxy-baryon-cycle
[2] ESO Excellence Cluster workshop: http://galaxyecosystem.wixsite.com/ecog

DOI: 10.18727/0722-6691/5058

Report on the ESO Workshop

Early Stages of Galaxy Cluster Formation 2017 (GCF2017)

held at ESO Headquarters, Garching, Germany, 17–21 July 2017

Tony Mroczkowski[1]
Andra Stroe[1]
Paola Andreani[1]
Monique Arnaud[2]
Fabrizio Arrigoni Battaia[1]
Carlos De Breuck[1]
David Sobral[3]

[1] ESO
[2] Service d'Astrophysique/DAPNIA/DSM, CEA Saclay, Gif-sur-Yvette, France
[3] Lancaster University, United Kingdom

The formation of the largest gravitationally bound structures in the Universe, clusters of galaxies, and how these environments affect the galaxies within them are major themes in cosmology and galaxy evolution. The high-redshift progenitors of clusters, called "protoclusters", are still in the process of hierarchical assembly. The transition from protocluster to cluster is gradual, driven by accretion and spectacular mergers that are expected to last roughly one billion years. This workshop aimed to address open questions in protocluster and cluster formation, to define the similarities and distinctions between the two, and to evaluate the best tools and methods for their detection and study.

Protoclusters, high-redshift galaxy clusters and merging clusters represent the first stages in the formation of the most massive known bound objects in the local Universe. The accepted view in hierarchical structure formation is that protoclusters and galaxy clusters form via mergers, the most energetic events since the Big Bang, and via the accretion of material along intercluster filaments. Merging cluster environments represent the only astrophysical laboratories where we can study a relatively short (< 1 Gyr) but decisive period in the evolution of clusters: a period that impacts the formation and evolution of both the intracluster plasma and the member galaxies of the cluster.

This workshop brought together experts who study the evolution of protoclusters and clusters across the entire electromagnetic spectrum. This workshop was unique due to the equal mix of scientists studying galaxy clusters and protoclusters (the precursors to galaxy clusters typically located at redshifts $z > 2$, i.e., the first 3 Gyr since the formation of the Universe), and also due to the goal of precisely defining what links and dis-

tinguishes protoclusters and clusters. Surprisingly, this workshop may have been the first of its kind, as protocluster experts tend to meet separately from their lower-redshift counterparts.

The workshop sought to place the evolution of protoclusters and clusters within a larger context, and to explore how they impact their constituent galaxies. The specific questions addressed during this workshop include:

– How do we define a protocluster, and how do we distinguish it from a cluster that is not yet virialised? How do we detect disturbed (proto)clusters in upcoming surveys? How can we optimise our observing strategies?
– How far back in time can protoclusters be found, and how reliably can they be identified? Are the high-z overdensities and galaxy associations really the progenitors of galaxy clusters in the local Universe? How do we differentiate between, for example, filaments, chance superpositions and true protoclusters? How do merging clusters in the local Universe ($z < 1$) compare to their high-z counterparts?
– At what stage does the intracluster medium (ICM) form? Do protoclusters have hot (> 1 keV) X-ray emitting atmospheres? How important are the non-thermal components (such as shocks, turbulence and cold fronts) to the properties of the intracluster medium of merging or forming clusters?
– How is the formation of protoclusters related to the peak of star formation and black hole activity? What is the nature of the galaxies within protoclusters and merging clusters? Do cluster member galaxies form and evolve in the (proto)cluster environment, or are the intermediate environments much more important than previously thought? What physical processes dominate the quenching of infalling satellite and member galaxies? How do shocks, turbulence and cold fronts affect star formation and active galactic nuclei (AGN) activity?
– When and how do the central AGN engines begin to interact with the ICM?
– What facilities will be required to address these questions in the future?

Outcomes

The programme and presentations from GCF2017 are available as an online archive[1]. Here, we highlight the invited review talks that introduced the topic of each section. Monique Arnaud gave the opening address, summarising the field and placing structure formation in context. Gabriella de Lucia summarised the state-of-the-art hierarchical structure simulations. Nina Hatch provided the observers' perspective on protocluster assembly and placed it in theoretical context. Marcus Brueggen shifted the discussion to more local cluster studies, where clusters are used as laboratories for fundamental plasma interactions. Dominique Eckert then discussed the chemical enrichment histories of the ICM. Nick Battaglia opened the discussion of how and why we could measure the masses of forming protoclusters, focusing on their relevance as cosmological probes, while Adam Muzzin moved the discussion back to the difficult but crucial work necessary to understand protocluster environments and their evolution into clusters. Finally, Megan Donahue outlined what we have learned about nearby ($z < 0.2$) clusters in the last two decades and how this knowledge can be applied in future work.

Overall, the evolution of a protocluster into a cluster is a continuous process, marked by dramatic merger events along the way. As such, the definitions of each will always include a few ambiguous cases, but the workshop facilitated useful discussions between theorists, observers, and instrumentation experts. Rather than simply hearing the latest results from one's own field, many — including the organisers — felt the workshop had taught them something beyond their area of expertise.

With an increasing number of cluster-like objects being found beyond $z > 1$ and with protoclusters now found at lower redshifts (as low as $z \sim 1.6$, rather than $z > 3$), it is clear that the distinction between protoclusters and clusters is mainly a matter of the median density reached by the object. Large objects that exceed galaxy scales at overdensities greater than 200 times the critical density of the Universe, typically within a Mpc radius, qualify as bona fide clusters or groups of galaxies. Protoclusters, on the other hand, are looser associations that are on their way to becoming clusters, and often span ~ 10 Mpc. A third grouping

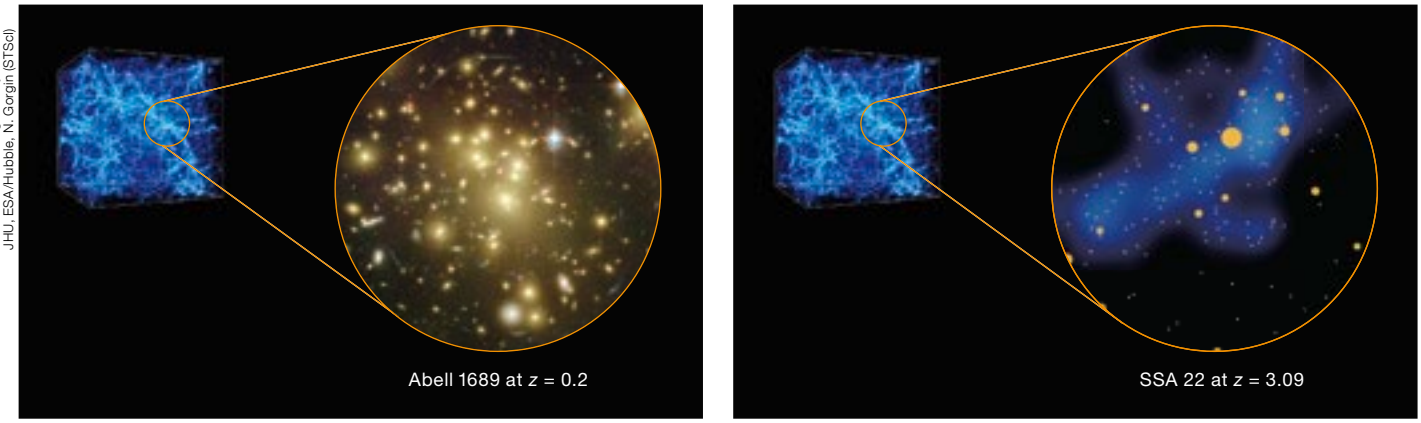

Figure 1. The left panel shows a cosmological volume simulation at $z = 3$, and the massive protocluster SSA22 at $z = 3.09$. The right panel shows the simulation at local redshifts, when the density contrast of the largest objects has dramatically grown, alongside a Hubble Space Telescope (HST) observation of the massive cluster Abell 1689 at the local redshift of $z = 0.23$.

Center for Cosmological Physics, NASA, JHU, ESA/Hubble, N. Gorgin (STScI)

Center for Cosmological Physics/Tamura et al. (2009)

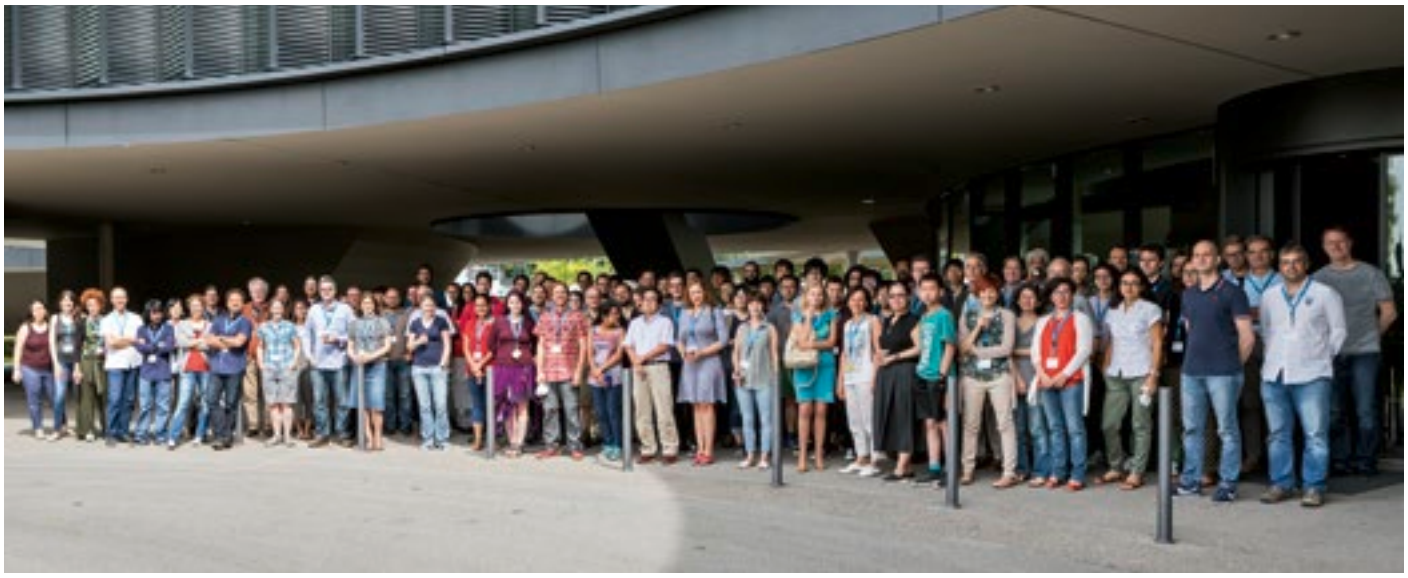

Figure 2. Workshop participants.

includes unbound structures — often superpositions thought to be protoclusters — that have not and will not exceed the overdensity threshold critical to collapse gravitationally.

Many of the questions we set out to address remain unanswered. However, it is clear the field is making substantial progress with the tools available, and will benefit greatly from the next generation of tools. More detailed gas physics, including star formation and AGN feedback at all epochs, is necessary for progress to be made with the simulations. From an observational perspective, it is clear the community is looking forward to the Extremely Large Telescope for improved imaging and spectroscopy at visible wavelengths. However, there is an equally high demand to improve the mapping speeds at millimetre and submillimetre wavelengths through projects such as the Atacama Large Aperture Submillimeter/millimeter Telescope (AtLAST[2]), particularly for high-redshift clusters and protoclusters, and through X-ray surveyors for their lower redshift counterparts ($z < 1.3$).

Workshop demographics

Like many workshops, the Science Organising Committee sought fair representation from the community. To this end, we voted on eight invited speakers, using the sole criterion of who would give the best review of each topic. The end result was a 50:50 ratio of male to female speakers.

Attendees came from five continents (all but Africa and Antarctica), with the following percentages:
– 54 % Europe (Germany, Italy, France, UK, Switzerland, Turkey, Spain, The Netherlands);
– 23 % North America (US, Canada);
– 15 % Asia (Japan, South Korea, India, China);
– 5 % South America (Chile, Brazil);
– 3 % Australia.

We find that 35 % of the abstract submissions were from women, which matched the 35 % of talk allocations to women. The talk selection was made blindly (one member of the Science Organising Committee removed names and identifying information about the authors and then abstained from voting), so we conclude that the method likely worked to address gender biases. We also had a decent level of participation from young researchers, with the following breakdown according to seniority: ~ 25 % students, ~ 30 % postdoctoral researchers, and 45 % tenure-track or tenured faculty. Each of these groups was well-represented in the talks.

The workshop had a high level of participation, with approximately 100 participants. We attribute this to both the compelling nature of the subject matter, which draws researchers at all career stages, and to the generous support that kept the cost of attendance relatively low (see acknowledgements).

Acknowledgements

We are grateful for the financial and logistical support of several parties that made this workshop possible. Several junior scientists received support from the European Union's Horizon 2020 Research and Innovation programme under grant agreement No. 730562 (RadioNet). The workshop itself received generous financial support from ESO's Directorate for Science, and logistical and venue support from ESO.

We especially thank Stella Chasiotis-Klingner for her efforts in organising the conference logistics, Ariadna Manilla Robles, Christian Peest, and Fabrizio Arrigoni Battaia for support before and during the conference, ESO catering for providing coffee breaks, and the Scientific Organising Committee for bringing together a compelling programme.

References

Tamura, Y. et al. 2009, Nature, 459, 61

Links

[1] GCF2017 Programme: https://www.eso.org/sci/meetings/2017/GCF2017/program.html
[2] The upcoming AtLAST workshop: https://www.eso.org/sci/meetings/2018/AtLAST2018.html
[3] HST image of Abell 1689: http://hubblesite.org/image/1276/news_release/2003-01

DOI: 10.18727/0722-6691/5059

Fellows at ESO

Hugo Messias

Hugo Messias

It was difficult to begin writing this article because I don't see myself as a conventional astronomer who was into science from a young age. So I wonder — why would you be interested? You're likely reading this because you're a curious person, and you either already know me and want to improve that knowledge, or you just wonder what induces a person to work in astronomy. We are curious beings and fiercely seek answers and patterns everywhere, and this is in fact one of the reasons why I work in astronomy.

First let me give you a bit of a background: my parents are both electrical engineers, and one of my grandparents owned a grocery shop and thus wanted to make sure his grandchildren knew maths. Being an active kid, my parents tried to keep me occupied and so I developed a lot of different interests. But in Portugal, students need to decide in high school — starting from the tenth grade — which future career to pursue. I still feel that this decision is forced on kids too soon, but I was lucky to be allowed to take a mix of arts and physics classes until I went to college. I liked drawing, especially the geometry exercises requiring 3D mental-rendering, but I ended up going into physics — likely influenced by the telescope my parents bought me, and the fact that the first two bright objects I pointed it at were Jupiter and Saturn. I still wonder if that tender present was a way for my parents to tell me that I couldn't draw. In their defence, there is some supporting evidence for this.

My physics degree, obtained in Lisbon (at the Faculdade de Ciências da Universidade de Lisboa [FCUL]), went by fast, or at least it seems like that now. At first I didn't feel like I was in the correct place — there were too many physics jokes that I didn't get, and people knew way more than I did even before we started classes. But I can't forget the history of physics class that I took. At high school, history didn't seem interesting as it involved too much memorisation and was too focussed on conquering and fighting without addressing the underlying reasons. In this class, however, the history behind the history was highlighted. I learned with Ana Simões and Henrique Leitão that the giants of physics, upon whom our knowledge now stands, were funnier than anyone thought. We would learn how and why technology and society kept pushing each other further and further into what we are and know today. My experimental physics class also helped me to make sense of the world around me and I realised that I was in the right place after all!

With João Yun, a very helpful and trustworthy person, I made my first contact with college-level astronomy and the research group at the Lisbon Astronomical Observatory. I met Rui Agostinho (who possesses an awesome level of physics knowledge), from whom I learned a lot about the impressive nineteenth century observatory and the people who worked there, as well as a number of fun and smart ways to approach science outreach. I started working with José Afonso, who later became my PhD supervisor together with Bahram Mobasher. The thesis has a really long title and it involves dusty galaxies. Part of my PhD work could be applied to the James Webb Space Telescope galaxy surveys, which first introduced me to the Atacama Large Millimeter/submillimeter Array (ALMA).

Right after I finished my PhD thesis, the first ALMA call for proposals went out. Thanks to Carlos De Breuck, I was fortunate enough to see the antennae being built and was able to go up to the Chajnantor plateau together with some other astronomers to see the first stages of the array. On top of that, I was about to fly to the Universidad de Concepción (UdeC) in Chile for my first postdoctoral position under an ALMA-CONICyT (Comisión Nacional de Investigación Científica y Tecnológica) project. ALMA was everywhere! At UdeC, I got my hands on ALMA data targeting an impressive lensed major merger. It was my first contact with a large project (the Herschel-Astrophysical Terahertz Large Area Survey [H-ATLAS]), and it made me realise that astronomy is still a field that can unite clearly distinct cultures from around the world in a common goal. ALMA is probably the best example in existence, and being part of it is priceless!

I returned to Portugal to work with José Afonso at the Portuguese ALMA Centre of Expertise as its lead scientist. This project was aimed at instructing the Portuguese community — and ourselves — about ALMA and its science. During these three intense years, I learned a lot about project management and about ALMA, and I also significantly broadened my research interests. By chance, I noticed the call for ALMA Fellowships. I felt that I needed to learn more if I wanted to help the Portuguese community more, and I applied.

So here I am now, writing this in the ALMA control room while waiting for observations to finish. After one year as an ALMA Fellow, I still feel great. I'm able to visit the telescope from time to time and be involved in amazing projects such

as the ALMA Phasing Project, which once again shows what ALMA is about: a diverse group of people from different cultures and backgrounds, coming together to make a ground-breaking facility a reality. Together we're enabling a giant leap forward in knowledge in a number of areas, from solar physics to the first galaxies in the Universe. For me, astronomy is simply this: satisfying your curiosity and mixing cultures in so many ways.

Allison Man

Allison Man

Ever since I was young, I have been a curious person and have always liked to pose questions about the sky and everything beneath it: Why does the Moon change its shape? Why is there life on Earth and not other places? What is the definition of life? I was therefore happy to discover a profession where the entire purpose is to pose questions and seek answers in science.

This was an unusual choice of profession among fellow students in Hong Kong, a financial hub, where young people aspire to be bankers and corporate managers. I always knew I wanted to study astrophysics, but the subject was not offered at my home university so I did my bachelor studies in physics. Somehow I managed to find people who encouraged me to pursue my dreams. With the help of my mentor Kinwah Wu, I won a summer research studentship and spent a month at the Mullard Space Science Laboratory in the UK to work on my first research projects. Later that year, I was fortunate enough to be supported by my family to spend a year abroad in Denmark as an exchange student. The choice to study in Denmark was encouraged by a serendipitous encounter with Ole Strömgren, the son of Bengt Strömgren — a Danish stellar astrophysicist who played a key role in the early years of ESO.

Living in Denmark was an eye-opening experience for me. It was fascinating to learn that the life cycles of stars can be described by mathematical equations with simple assumptions. The egalitarian values of Danish society also appealed to me and I realised that I could choose to live my life differently. I decided to pursue a MSc degree in astrophysics at the University of Copenhagen. This was not an easy choice, as it meant that I had to live far from my family, and I also had no means to afford the hefty tuition fees because of my status as a foreign student. Thankfully, the professors at the Dark Cosmology Centre convinced the Faculty of Science to award me a stipend and waive my tuition so I could pursue my studies. I went on to learn cosmology, galaxy evolution and astrobiology, which deepened my fascination with the Universe and how humans came to be.

While searching for a thesis project, I spoke to astrophysicists in Copenhagen about their research. I was particularly impressed when Sune Toft, a Lundbeck research group leader who had returned to Copenhagen upon completing an ESO Fellowship in Garching, described how "dead" massive galaxies puff up in size to become the largest elliptical galaxies in the Universe. I was excited to embark on an MSc project with him to measure the sizes of massive galaxies with archival Hubble Space Telescope data.

I quickly discovered that many of the galaxies were in pairs and appeared to be interacting. This was interesting because in concordance cosmology, massive galaxies are thought to assemble from merging smaller ones. However, whether massive galaxies merged more frequently in the past was a disputed topic, as observations provided contradictory evidence. I therefore changed my research direction and measured galaxy merger rates instead of sizes, work that expanded into my PhD project.

Using deep field galaxy surveys taken with the Visible and Infrared Survey Telescope for Astronomy (VISTA) and the Hubble Space Telescope, I gathered a large sample of more than 1000 galaxy mergers and inferred that the discrepancy across observations is due to selection effects. My results implied that, to properly measure the galaxy merger rate, it is important to obtain galaxy gas mass measurements with the Atacama Large Millimeter/submillimeter Array (ALMA). As part of my PhD studies, I spent half a year visiting the Institute for Astronomy at the University of Hawaii, collaborating with Dave Sanders and Josh Barnes. It was a memorable experience for me on all fronts: learning about far-infrared astronomy and merger simulations, observing on Mauna Kea, and of course enjoying the mountains and the ocean in my free time!

After my PhD, I was happy to be awarded an ESO Fellowship to develop my research in a broader context, asking questions such as "Do galaxy mergers trigger starburst activity and active black holes?" and "How do massive galaxies shut down their star formation?" ESO and Munich in general provide a stimulating research environment, where I can bring my ideas to fruition and find experts in any field of interest. My functional work

for ALMA has enabled me to exploit my newly acquired knowledge in radio interferometry to address my science questions. Since coming to ESO I have been awarded 100 hours of observations with ALMA and the Very Large Array (VLA) to study cold gas in early galaxies. By combining radio interferometry with optical and near-infrared observations at the Very Large Telescope, I plan to investigate how star formation proceeds in the early Universe.

As much as I enjoy the intellectual stimulation of my job, I draw satisfaction from bringing people together with science. ESO is a prime example of the success and value of international collaborations. This summer, I taught at the West African International Summer School for Young Astronomers[1] held in Ghana. The students were remarkably motivated and "code-savvy", at least compared to myself as a bachelor student! Since returning from Ghana, I have launched a mentorship programme to connect these students with astrophysicists across the world, and have begun to develop a research-training programme for them with other ESO astronomers. My own mentors have been crucial to my journey to becoming a professional astrophysicist, so I hope that I can engage more colleagues to support and encourage these bright students to pursue science as a career.

Links

[1] West African International Summer School for Young Astronomers: http://www.astrowestafrica.org

DOI: 10.18727/0722-6691/5060

External Fellows at ESO

In addition to the ESO fellowships, a number of external fellows are hosted at ESO. A profile of one of these fellows is presented here.

Iván Oteo

Iván Oteo

Perhaps contrary to most astronomers, my love-hate relationship with astronomy did not start when I was a child. In fact, until I was about 16 I was really passionate about medicine and was convinced I would become a surgeon. However, everything changed when I started my last year of high school, when I had a great physics teacher whose lessons made me change my mind. The decision to pursue a degree in physics was not easy, and I still sometimes wonder what could have happened if I had studied medicine instead. I have the impression that it would have been a job that I would have enjoyed as much as being a researcher in astronomy. I studied in Sevilla, a beautiful city about 120 km away from Cádiz, the city where I was born and where I lived until I was eight years old, and Chiclana de la Frontera, the place where I spent most of my adolescence.

When I started my physics degree I was not thinking of specialising in astronomy, but rather in quantum or nuclear physics. My passion for these topics increased over the course of my five-year degree, and in my final year I even received an offer to start a PhD in quantum physics with one of my teachers beginning in 2008. I really wanted to take that career path, but in June 2008 I had the opportunity to complete a three-month summer studentship at the Instituto de Astrofísica de Canarias (IAC) in Tenerife. I could choose from a list of projects and I selected the one on solar physics, but a couple of weeks before starting I was informed that the project had been cancelled and I had to choose another one. This time, I chose one on high-redshift quasars amplified by gravitational lensing.

Those three months were quite intense, both in terms of work and my social life. I made many friends; there were 14 summer students in total and most of us came from outside Tenerife so it was easy to form a close-knit group. I enjoyed living on that amazing island and, most importantly, I also realised that I wanted to keep working on astronomy. Unfortunately for my degree teacher back in Sevilla (or perhaps fortunately), I decided to stay in Tenerife and start a master's degree in astrophysics. At the time, it was possible to start a PhD at the same time as a master's degree, but most deadlines for PhD positions in Tenerife had already passed so I decided to stay there, begin the two-year master's, and then start the PhD one year later. The plan worked. A year later I received an offer to complete a PhD at the Instituto de Astrofísica de Canarias, working on the multi-wavelength characterisation of star-forming galaxies at different redshifts, with a focus on the galaxies detected in the deep extragalactic surveys taken with the Herschel Space Observatory.

I had a great time during my PhD and enjoyed doing research in astronomy. For this reason, I decided to apply for a postdoctoral position to keep working on high-redshift dusty star-forming galaxies, specifically on the properties of their dust and molecular gas using submillimetre, millimetre and radio interferometric observations. I moved from Tenerife to Edinburgh to work at the Royal Observatory and am currently based at ESO. I had not done any submillimetre, millimetre or radio interferometry work before, so this was a challenge, but also a lot of fun. I worked with interferometers such as the Atacama Large Millimeter/submillimeter Array (ALMA), the Very Large Array (VLA), the NOrthern Extended Millimeter Array (NOEMA), the Submillimeter Array (SMA) and the Australia Compact Telescope Array (ATCA), as well as with single-dish submillimetre/millimetre telescopes such as the James Clerk Maxwell Telescope (JCMT), the Atacama Pathfinder EXperiment (APEX) and the Institut de Radioastronomie Millimétrique (IRAM) 30-metre telescope; the latter being my favourite! Interestingly, despite working at ESO I have never observed directly with any ESO telescope, although I did get some data from the Very Large Telescope (VLT) and Visible and Infrared Survey Telescope for Astronomy (VISTA) in service mode. I wish I could visit Paranal and La Silla soon — as well as ALMA and APEX, of course!

One of my main research areas is the study of ultra-luminous dusty galaxies in the early Universe. I first try to find them using far-infrared, submillimetre and millimetre bands to sample the dusty emission peak, then confirm their distances (i.e., their redshifts), and finally study their gas, dust and stars to investigate their properties and evolution. This requires the use of multi-wavelength observations, which is the reason why I use so many telescopes around the world and why I spend a significant amount of my working time in observatories as well as writing telescope proposals. In fact, the latter is one of my most enjoyable activities: it's exciting to write proposals to discover new galaxies and study them in detail!

I am also involved in ALMACAL, a wide and deep submillimetre/millimetre survey being carried out by gathering publicly-available ALMA calibration observations. This is a huge project; so far, it has collected more than 700 hours of ALMA observations in more than 500 calibrator fields. This represents a much larger dataset than any other ALMA project — larger than all the current ALMA Large Programmes combined. Working with such a huge dataset is not easy, but discovering galaxies that no one has seen before is awesome. I am also the Principal Investigator of a VISTA Public Survey called SHARKS (Southern Herschel-Atlas Regions *K*-band Survey), which is completing relatively deep *K*-band imaging over the Herschel-Astrophysical Terahertz Large Area Survey (H-ATLAS) equatorial and southern fields. It aims to characterise the stellar emission of all H-ATLAS galaxies, among other goals such as completing a cosmographic study of lensed galaxies and looking for the most massive high-redshift galaxies and extreme structures.

Acknowledgements

I would like to acknowledge the support received from the University of Edinburgh through the European Research Commission Advanced Grant COSMICISM, 321302 (Principal Investigator: Rob Ivison).

D. Kordan/ESO

The Atacama Large Millimeter/submillimeter Array.

Personnel Movements

Arrivals (1 October–31 December 2017)

Europe	
Barna, Barnabás (HU)	Student
Burger, Claudia (DE)	Director of Administration
Cerpa Urra, Nelly Natalia (CL)	Student
Escate Giribaldi, Riano (PE)	Student
Fensch, Jérémy (FR)	Fellow
Hashiba, Natsuki (JP)	Student
Jethwa, Prashin (UK)	Fellow
Löbling, Lisa (DE)	Student
Miotello, Anna (IT)	Fellow
van der Burg, Remco (NL)	Fellow
Wylezalek, Dominika (DE)	Fellow

Chile	
Agliozzo, Claudia (IT)	Fellow
Eftekhari, Sara (IR)	Student
Kakkad, Darshan (IN)	Fellow
Meilland, Anthony (FR)	User Support Astronomer
Sanchez, Joel (MX)	Fellow
Silva, Karleyne (BR)	Operation Staff Astronomer
Villenave, Marion (FR)	Student
Yang, Chentao (CN)	Fellow

Departures (1 October–31 December 2017)

Europe	
Falkendal, Theresa Maria (SE)	Student
Nedelchev, Borislav (BG)	Student
Nogueras Lara, Francisco (ES)	Student
Verzichelli, Gianluca (IT)	Quality Assurance Manager

Chile	
Bellhouse, Callum (UK)	Student
Dumke, Michael (DE)	Operation Staff Astronomer
Guieu, Sylvain (FR)	Physicist
Muñoz, César (CL)	Student

Message from the Editor

Gaitee A. J. Hussain[1]

[1] ESO

As the new editor I am looking forward to the challenge of maintaining the high standards established by my predecessor, Jeremy Walsh, and ensuring that The Messenger remains an effective means to inform the astronomical user community of exciting results and developments at ESO. I take this opportunity to remind you that The Messenger welcomes topical contributions showcasing your own use of ESO's facilities and programmes.

I will be investigating new ways to disseminate highlights from each issue using electronic means, including social media. However, rest assured that there will be no compromise to the excellent quality of the print edition — as ensured by the impressive efforts and talents of the ESO graphics and layout experts, Jutta Boxheimer and Mafalda Martins.

I would like to warmly thank Jeremy Walsh for showing me the ropes with such generosity and patience, and for ten years of stewarding the Messenger — bringing his vast experience and talents to bear. A composite of all the cover images of the journal from this period is shown on p. 71. I know our readers will join me in wishing Jeremy an excellent and well-deserved retirement!

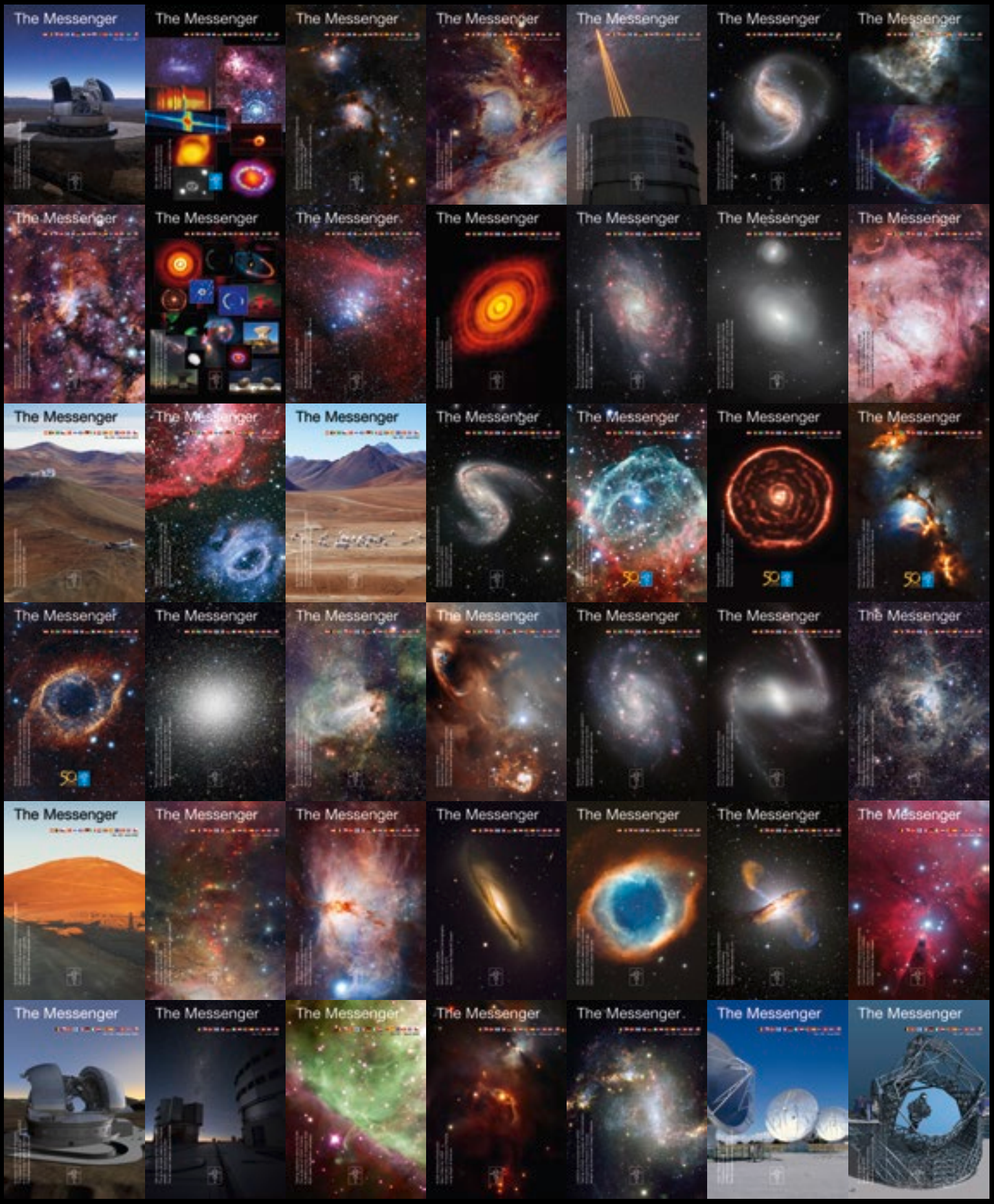

The Messenger over Jeremy Walsh's tenure. These covers are arranged in chronological order, from March 2007 (bottom right) to June 2017 (top left).

ESO, the European Southern Observatory, is the foremost intergovernmental astronomy organisation in Europe. It is supported by 16 countries: Austria, Belgium, Brazil, the Czech Republic, Denmark, France, Finland, Germany, Italy, the Netherlands, Poland, Portugal, Spain, Sweden, Switzerland and the United Kingdom. ESO's programme is focused on the design, construction and operation of powerful ground-based observing facilities. ESO operates three observatories in Chile: at La Silla, at Paranal, site of the Very Large Telescope, and at Llano de Chajnantor. ESO is the European partner in the Atacama Large Millimeter/submillimeter Array (ALMA). Currently ESO is engaged in the construction of the Extremely Large Telescope.

The Messenger is published, in hardcopy and electronic form, four times a year: in March, June, September and December. ESO produces and distributes a wide variety of media connected to its activities. For further information, including postal subscription to The Messenger, contact the ESO education and Public Outreach Department at:

ESO Headquarters
Karl-Schwarzschild-Straße 2
85748 Garching bei München, Germany
Phone +49 89 320 06-0
information@eso.org

The Messenger:
Editors: Gaitee A. J. Hussain
Graphics: Mafalda Martins
Layout, Typesetting: Mafalda Martins
Design, Production: Jutta Boxheimer
Proofreading: Lauren Fuge
www.eso.org/messenger/

Printed by G. Peschke Druckerei GmbH
Taxetstraße 4,
85599 Parsdorf, Germany

ISSN 0722-6691

Contents

Front cover: Composite image (using *g*, *r*, *i*, & Hα narrow-band filters) of the star forming region, Sharpless 29, from the VLT Survey Telescope. This shows how hot young stars can shape the environment in which they are born, heating up the surrounding dust and driving strong stellar winds that carve out cavities. See Release eso1740 for details. Credits: ESO/M. Kornmesser